INJECTABLE DELIVERY SYSTEM BASED ON 5-ETHYLENE KETAL-ε - CAPROLACTONE FOR THE DELIVERY OF VEGF AND HGF FOR TREATING CRITICAL LIMB ISCHEMIA

by

Iyabo Oladunni Babasola

A thesis submitted to the Department of Chemical Engineering

In conformity with the requirements for

the degree of Doctor of Philosophy

Queen's University

Kingston, Ontario, Canada

(May, 2012)

Abstract

The aim of this thesis is to determine the feasibility of an injectable delivery system based on 5-ethylene ketal ε-caprolactone for localized delivery of vascular endothelial growth factor (VEGF) and hepatocyte growth factor (HGF) for treating critical limb ischemia. HGF and VEGF were chosen because of their ability to simultaneously stimulate the proliferation and migration of endothelial cells, to initiate the formation of blood vessels and the recruitment of pericytes to stabilize the blood vessels. Homopolymer of 5-ethylene ketal ε-caprolactone and its copolymer with D,L-Lactide were synthesized by ring opening polymerization using hydrophobic initiator (octan-1-ol) or an hydrophilic initiator (MPEG), and stannous octanoate as a co-initiator/catalyst. The resulting polymers were amorphous and viscous liquids at room temperature. The viscosity, biodegradation rate, and release rate were varied by copolymerizing with D,L-lactide and/or initiating with MPEG or octan-1-ol. *In vitro*, the polymers degraded with surface erosion characterized by a nearly linear mass loss with time with no significant change in number average molecular weight and glass transition temperature. The ratio of EKC to DLLA in the copolymer remained the same throughout the degradation studies. A similar degradation mechanism was observed *in vivo* when the copolymer initiated with octan-1-ol was implanted subcutaneously in rats. *In vivo*, the polymer exhibited a moderate chronic inflammatory response, characterized by the presence of neutrophils, macrophages, fibroblasts and fibrous capsule formation. The inflammatory response decreased with time but was still on going after 18 weeks of subcutaneous implantation. Protein release from the polymer was transported by convection through the hydrated polymer region, at a rate determined by the osmotic pressure generated and the hydraulic conductivity of the polymer. Highly bioactive VEGF and HGF were released in a sustained manner, without burst effect for over 41 days when delivered simultaneously, using the osmotic release mechanism. VEGF was released at the rate of 36 ± 7 ng/day for 41 days, while HGF was released at the rate of 16 ± 2 ng/day for 70 days. Factors that influenced release of

proteins were their solubility in the concentrated trehalose solution and hydraulic permeability of the polymer. This delivery system can serve as a potential vehicle for controlled release of VEGF and HGF for treating critical limb ischemia or the controlled release of other proteins for other clinical applications.

Acknowledgements

I am forever grateful to God Almighty, the source of all wisdom and understanding; to you alone be all the glory.

I would like to thank my supervisor Dr Brian Amsden for his remarkable supervision, encouragement and financial support during my studies. Your outstanding devotion to your student's success is noted by all and is much appreciated.

Special thanks to my husband, Adegboyega Babasola for your exceptional patience, help and encouragement during my studies, you are a rare treasure. I would like to thank my children: Favour, Flourish and Faith for your patience during my studies, you are the best. I would like to appreciate the immeasurable love and support of my parents and parents-in-law especially with making out time to help with my children during this busy period, your sacrifices are priceless and can never be forgotten.

I appreciate the financial support provided by the Canadian Institute of Health Research, School of Graduate Studies, the Department of Chemical Engineering at Queens University and the Ban Righ Centre.

I would like to thank Dr Ju Bianco of the human mobility and research center for your invaluable input in the animal studies and histology.

I would like to thank all my friends; Ade and Veronica Adetola, Pastor Ade and Pastor Seun Sobanjo, Tola and Yinka Agbelese, Babatunji and Lola Farinloye, Olu and Lydia Bamidele, Ufoma and Omoyeni Ugolo, James and Bola Oni, Patrick and Cynthia Egbunonu and Pastor Bode and Debbie Olutunda, for all your support and prayers.

Finally, I would like to thank my lab mates; Abby Sukarto, Denver Surrao, James Hayami, Nicholas Hadjiev, Moira Vyner, Julian Chesterman and Dale Marecak for all your support and friendship.

Table of Contents

List of Figures

List of Tables

List of Abbreviations

VEGF: Vascular endothelial growth factor

HGF: Hepatocyte growth factor

bFGF: Basic fibroblast growth factor

UPA: Urokinase-plasminogen activator

MMPs: Matrix metalloproteinases

HIF-1α: Hypoxia-inducible factor

ECs: Endothelial cells

SMCs: Smooth muscle cells

Ang: Angiopoietins

TGF-β: Transforming growth factor

PDGF: Platelet derived growth factor

FGF: Fibroblast growth factor

EGF: Epithelial growth factor

Tie2: Receptor tyrosine kinase expressed on angiopoietins

VE Cadherin: Vascular endothelial cadherin

TNF-α: Tumour necrosis factor –α

PMNs: Polymorphonuclear leukocytes

PF4: Platelet factor

IL-1: Interleukin-1

IL-3: Interleukin-3

IL-4: Interleukin-4

IL-6: Interleukin-6

IL-8: Interleukin-8

IFN-γ: Interferon-gamma

LTB4: Leukotriene

MCP-1: Monocyte Chemoattractant Protein

G-CSF: Granulocyte-colony stimulating factor

GM-CSF: Granulocyte macrophage-colony stimulating factor

FBGCs: Foreign body giant cells

FBR: Foreign body reaction

CCL2: C-C chemokine ligand-2

CCL3: C-C chemokine ligand-3

EKC: 5-ethylene ketal ε-caprolactone monomer

DLLA: D, L lactide monomer

MPEG: Methoxy poly(ethylene glycol)

PTMC: Poly (trimethylene carbonate)

PLA: Poly(lactic caid)

T_g: Glass transition temperature

M_n: Number average molecular weight

PDI: polydispersity index

E: Activation energy

η: Viscosity

DCM: dichloromethane

Chapter 1

GENERAL INTRODUCTION

1.1 Introduction

Peripheral vascular occlusive disease is a progressive illness that results in occlusion of arteries to the limb, due to atherosclerosis of large and medium sized arteries [1]. As the condition progresses, blood flow to the distal tissues is severely impeded, depriving these tissues of oxygen and nutrients, which leads to critical limb ischemia (CLI) in tissues fed by the diseased artery [2]. These patients experience chronic ischemic rest pain, ulcers, or gangrene in the lower limb, and have a poor prognosis [3]. This condition afflicts 27 million people in the western world [2, 4], and it is estimated that there are 500 new cases of critical limb ischemia per million individuals in the USA and Europe each year [3]. The number of patients in this group is expected to increase with the continued aging of the general population and increased incidence of concomitant diseases such as obesity and diabetes mellitus [2, 5, 6].

Currently, peripheral perfusion for short occlusions of the iliac arteries can only be improved by angioplasty, and long segments of occlusions, especially those distal to the common femoral artery, are best treated by bypass surgery[2, 4]. These treatment options are highly invasive and lead to eventual amputation in more than 50,000 patients each year in the United States [2]. The need for amputation is due to inadequate autologous vein material to use as a bypass conduit, the anatomic extent and the distribution of arterial occlusive disease, occlusion of distal downstream target arteries for bypass, micro-vascular disease that prevents healing despite a successful bypass, and other co-morbid conditions that make major surgeries hazardous [2, 7]. For 10-30% of these patients, revascularization is not a suitable option; greater than 40% of this patient population will require major amputation, and 20% will die within 6 months [3, 4, 8]. The body is capable of developing new collateral blood vessels to mediate ischemia by producing endogenous angiogenic growth factors, but this spontaneous biologic response, termed angiogenesis,

typically occurs very slowly in the body, and is often unable to replace the lost blood flow completely [9]. As a result, the exogenous administration of these angiogenic growth factors is required. This treatment process is called therapeutic angiogenesis.

In this work, the angiogenic growth factors considered for treating critical limb ischemia were vascular endothelial growth factor (VEGF) and hepatocyte growth factor (HGF), due to their ability to synergistically induce the proliferation and migration of endothelial cells to form blood vessels and the recruitment of pericytes to stabilize the formed blood vessels. These growth factors were formulated with trehalose and BSA, lyophilized and incorporated into a liquid injectable polymer based on 5-ethylene ketal ε-caprolactone by simple mixing and released via an osmotic pressure release mechanism. The reason for this formulation approach will be developed throughout the following literature review.

Chapter 2

LITERATURE REVIEW

2.1 Blood Vessels

Blood vessels include arteries, arterioles, capillaries, venules, and veins[10-12]. These vessels are distinguished from one another by the difference in their physical dimensions, morphological characteristics, and function [11]. As the arteries get further away from the heart, they branch into smaller vessels (lumen diameter of 30 μm) known as the arterioles [12]. The arterioles further branch into smaller diameter vessels known as the capillaries. Capillaries have a diameter of 6 μm [12, 13] and consist of one layer of endothelial cells. From the capillaries, oxygen and nutrients are transferred to the tissues in exchange for carbon dioxide and waste from the tissues [10-12]. The capillaries merge together to form vessels with larger diameter (lumen diameter of 20 μm) called the venules which transport deoxygenated blood and waste to the veins (lumen diameter of 0.5 cm) and finally to the vena cava (lumen diameter of 3.0 cm), from where deoxygenated blood is transported to the thin walled chamber of the heart (right atrium) and then to the right ventricle [10-12]. Figure 2-1 shows the structure of an arteriole. The intima is the inner (blood contacting) layer of all the blood vessels and consists mainly of endothelial cells supported by an internal elastic lamina [14]. All the other blood vessels apart from the capillaries have a second layer known as the media, which consist of pericytes, smooth muscle cells and their extracellular matrix (elastin fibres) [14, 15]. The media is thicker in the arteries and arterioles compared to the veins and venules[12]. Larger vessels such as arteries and veins, contain a third, outer layer, called the adventitia, which is composed principally of nerve endings, a few resident inflammatory cells, fibroblasts, and their extracellular matrix (collagen fibres) [15, 16].

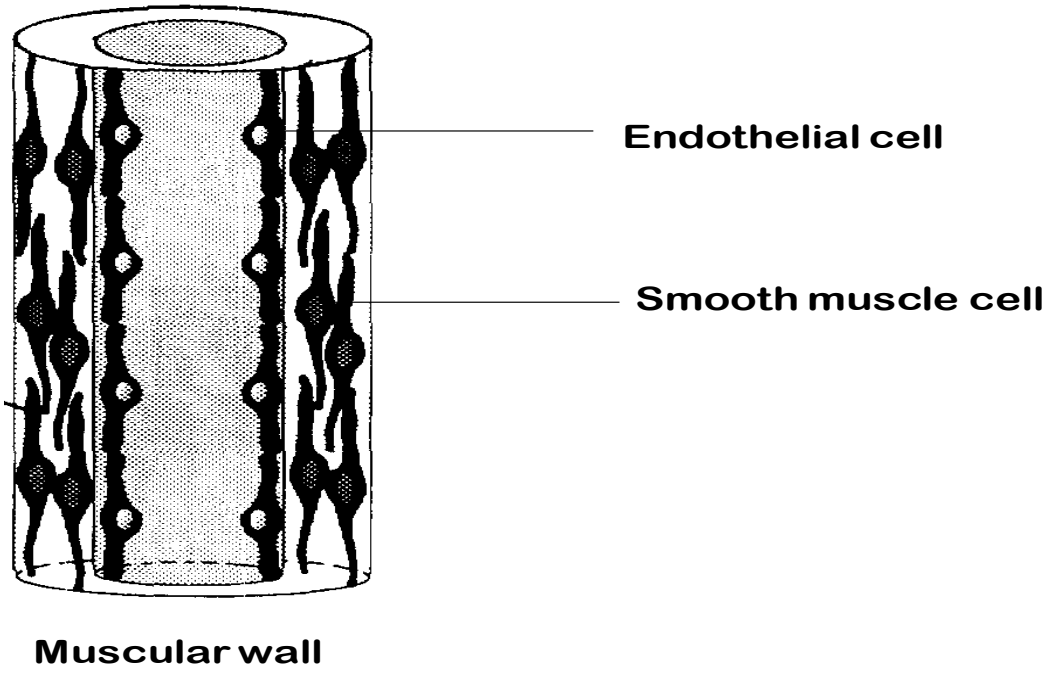

Figure 2-1: Structure of an arteriole showing the endothelium ensheathed with two layers of smooth muscle cells (Used with permission from [17])

The endothelium, which consists of a thin layer of endothelial cells, regulates vascular tone, hemostasis and vascular permeability [18]. Pericytes have close contact with endothelial cells via pores in the basal lamina and thus influence the proliferation of endothelial cells [19, 20]. Pericytes, like smooth muscles cells, respond to factors secreted by endothelial cells and regulate blood vessel diameter by contraction and relaxation[20]. The elasticity of the elastin fibers in the media ensures the delivery of blood to the tissues and provides the elasticity and resilience required to generate continuous blood flow[18]. The adventitia acts as a biological processing centre for the retrieval, integration, storage, and release of key regulators of the vessel wall function [16]. In response to hormonal, inflammatory and environmental stresses such as hypoxia or ischemia, resident adventitial cells (fibroblasts, progenitor cells) are activated to increase cell proliferation, expression of contractile and extracellular matrix protein, secretion of chemokines, cytokines and growth factor that contribute significantly to vascular remodeling[21].

2.2 New blood vessel formation process

The formation of new blood vessels is a complex process and can occur via a number of different processes, which include vasculogenesis, angiogenesis, and angiogenic remodeling or arteriogenesis [22-24]. However, the relevant processes of blood vessel formation in this study are angiogenesis and arteriogenesis.

2.2.1 Vasculogenesis

Vasculogensis, which occurs only in the embryo, is the process whereby hematopoietic stem cells and endothelial progenitor cells differentiate, proliferate *in situ* within a previously avascular tissue and then coalesce to form a primitive tubular network [23, 25].

2.2.2 Angiogenesis

Angiogenesis involves the sprouting of new blood vessels from pre-existing blood vessels to form new capillary networks [26]. Each step in angiogenesis is mediated and controlled by a variety of growth factors and these growth factors are secreted in a spatial and temporal manner in a tightly controlled fashion. The driving force for angiogenesis is hypoxia in the surrounding tissue [17], which stimulates endothelial cells to secrete proteinases, such as urokinase-plasminogen activator (UPA) and the matrix metalloproteinases (MMPs), which cause rapid degradation of the nearby extracellular matrix. Upon degradation of the extracellular matrix, hypoxia-inducible factor (HIF-1α) stimulates the transcription of soluble factors such as VEGF and other angiogenic cytokines to stimulate endothelial cells (ECs) to migrate and proliferate [5, 17]. The migration and proliferation of endothelial cells lead to the formation of a capillary lumen via cell-cell and cell-matrix interaction [17, 22, 23]. These new capillary networks are small with a diameter of 10 – 20 μm [13], consisting of endothelial cell tubes lacking additional wall structures [13, 26]. Figure 2-2 is a schematic representation of the process of angiogenesis, indicating the roles and timings of the multiple signaling factors involved, including angiopoietins (Ang), vascular endothelial growth

factor (VEGF), hepatocyte growth factor (HGF), transforming growth factor (TGF-β), platelet derived growth factor (PDGF), fibroblast growth factor (FGF), epithelial growth factor (EGF), receptor tyrosine kinase expressed on angiopoietins (Tie2), vascular endothelial cadherin (VE cadherin), Ephrin B2 and tumour necrosis factor -α (TNF-α) in each step of angiogenesis.

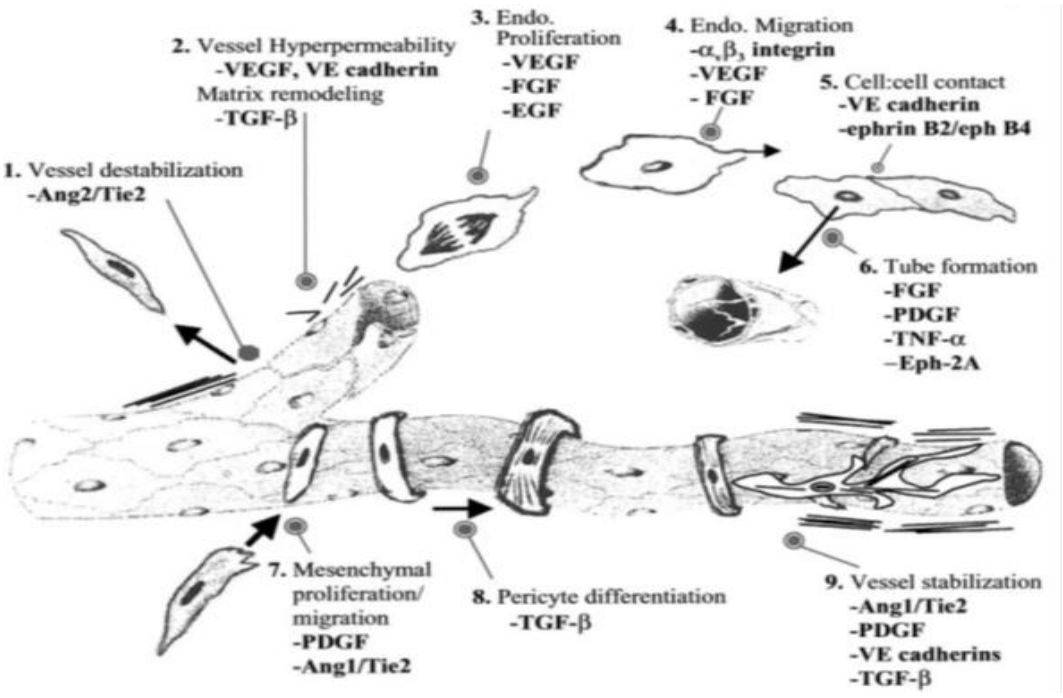

Figure 2-2: The process of angiogenesis and the soluble signaling factors involved in each stage. Used with permission from[27].

2.2.3 Arteriogenesis

Arteriogenesis is the process of remodeling a pre-existing interconnecting arteriole to increase its luminal diameter to form matured blood vessels [24, 28]. Arteriogenesis is triggered by physical forces such as increased shear forces, which appear within the collateral arteriole as a result of the vessel occlusion [17, 26]. The increased shear force upregulates cell adhesion molecules for circulating monocytes to accumulate around the proliferating artery to release required growth factors such as platelet derived growth factor (PDGB-BB) [15], basic fibroblast derived growth factor (bFGF) [15] and hepatocyte growth factor (HGF)[13].

The released growth factors act in an autocrine or paracrine manner to initiate the proliferation and migration of pericytes and smooth muscle cells (SMCs) [15]. The endothelial cells integrate tightly with the recruited smooth muscle cells (SMCs), pericytes and the surrounding matrix to form mature vessels [22, 29]. This remodeling event, which leads to an increase in luminal diameter, is necessary to accept increased blood flow and thereby provide a means to bypass the occluded vessel [24].

2.3 Therapeutic Angiogenesis

Therapeutic angiogenesis can be accomplished through the local administration of various growth factors, such as vascular endothelial growth factor (VEGF)[30-33], hepatocyte growth factor (HGF) [31, 34-36] and basic fibroblast growth factor [34, 37]. VEGF and HGF were utilized for this research as stated in chapter 1, therefore their structures and functions are provided below.

2.3.1 Vascular Endothelial Growth Factor (VEGF)

The VEGF family consists of seven members: VEGF-A, VEGF-B, VEGF-C, VEGF-D, VEGF-E, VEGF-F and placental growth factor (PIGF) [38]. VEGF-A is a key molecule in the induction of angiogenenesis and vasculogensis as it causes proliferation and migration of endothelial cells leading to sprouting and tube formation [38, 39]. VEGF-A is distinguished from other heparin-binding angiogenic growth factors by several features. First, VEGF-A is secreted by keratinocytes, pericytes, smooth muscle cells, macrophages, mast cells and adipose tissue derived cells which are in close proximity with endothelial cells. This mode of secretion suggests that VEGF-A functions in a paracrine manner to form blood vessels [17, 40, 41]. Secondly, VEGF-A binds to two tyrosine-kinase receptors present on endothelial cells, but not on other cell types: Flt or VEGF receptor 1 (VEGFR-1) and KDR or VEGFR-2. This selective binding makes the action of VEGF-A specific to endothelial cells [42]. KDR dominates the angiogenic response and is therefore of greater therapeutic interest [42]. Under appropriate dosage, VEGF-A

binds to KDR to stimulate the proliferation and migration of endothelial cells, to initiate the formation of immature vessels by vasculogenesis and angiogenic sprouting [17].

There are four isoforms of VEGF-A containing 121, 165, 189 and 209 amino acids which differ in mitogenic potency, affinity for extracellular matrix protein or cellular receptor and temporal pattern of expression [17]. However, VEGF-A_{165} is the most common and biologically active form of VEGF-A [5, 22]. For this reason VEGF-A_{165} was utilized in this research. For simplicity, VEGF-A_{165} will be referred to as VEGF henceforth. VEGF exists in both glycosylated and non-glycosylated forms, with molecular weights of 46 and 38.3 kDa respectively [43, 44]. The VEGF used in this study is the non-glycosylated form. VEGF has an isolectric point (pI) of 8.5 – 8.9 [45, 46], and it exists as a dimer covalently linked by two symmetrical disulfide bonds between cys 51 and cys 60. Each monomer is stabilized with a cysteine knot made of three disulfide bonds [47]. Each monomer consists of two domains; a receptor binding domain (pI of 5.6), and a heparin binding domain (pI of 11.6) [46]. Figure 2-3 shows the receptor binding domain of VEGF.

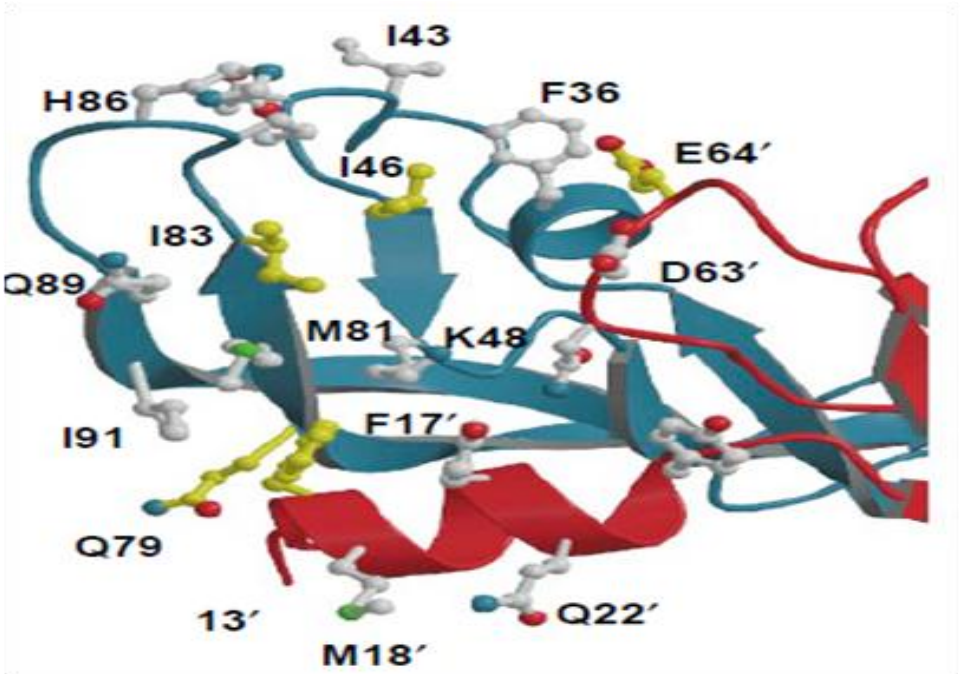

Figure 2-3:The receptor binding site of VEGF. The receptor binding site is built from strand β2, β5 and β6 from one subunit (blue) along with the N-terminal α helix from the other subunit (red). The most important binding determinants for KDR receptor are phe17', Gln79, Ile46, Glu64' and Ile83 (shown in yellow) Used with permission from [47].

The critical residues responsible for KDR binding are Phe17', Ile46, Glu64', Gln79 and Ile83. These residues span the dimer interface with short three-stranded antiparallel β sheets (β2, β5 and β6) from one subunit along with the N-terminal α helix from the other subunit [47]. The binding of VEGF to the Flt-1 receptor is mediated by residues Asp63', Glu64' and Glu67' [47]. Glu67' is part of the loop containing Asp63' and Glu64'. The half-life for VEGF in serum is 50 minutes [37]. This could be because, in the free form, there is rapid diffusion of VEGF to the surrounding tissue [33]. In addition, there is the possibility of protein degradation due to the hostile ischemic environment created by the extensive protein degradation that takes place as part of inflammation and extracellular matrix (ECM) remodeling-induced enzymatic responses [48] The N-terminal residues of recombinant human VEGF (rh-VEGF) that participate in receptor binding are prone to deamidation (Asn 10), oxidation (Met-3), and diketopiperazine reactions (Ala1-Pro2-Met3) that occur 7.4, 2.5, and 5.2 times faster, respectively, at pH 5 compared to pH 8 [43].

2.3.2 Hepatocyte Growth Factor (HGF)

Unlike VEGF, the receptor of HGF, c-met, is expressed on multiple cell types including hepatocytes, myeloid precursor cells, pericytes, smooth muscle cells and various epithelial and endothelial cells[40, 42]. HGF, following binding to the c-met receptor, stimulates proliferation, migration, and/or morphological differentiation of a wide variety of cellular targets, including hepatocytes and epithelial cells, melanocytes, endothelial cells, and hematopoietic cells [42]. HGF also induces the production of VEGF by human keratinocytes [49, 50]and endothelial cells [50]and acts as a chemoattractant for pericytes [51]. The synthesis of HGF by mesenchymal cells such as fibroblasts and SMCs coupled with effects on epithelial and endothelial cells suggest a paracrine mode of action [52]. HGF has a pI of 9.5 and a half-life of 3-5 minutes in plasma [53, 54]. The short half-life could be as a result of the same reason suspected for VEGF. HGF is part of the plasminogen related growth factors synthesized as a 90 kDa

biologically inactive precursor, mostly found in a matrix-associated form [55]. This is converted in the extracellular matrix to a biologically active heterodimer consisting of a 60 kDa α chain, and a 30 kDa β chain by proteolytic cleavage using pure urokinase [55, 56]. The α chain contains a well-defined N-terminal hydrophobic domain and an hairpin-loop region (N; residues 31-127), followed by four 'kringle' domains (K1-K4) while the β chain resembles a serine protease in sequence, with no protease activity [57].

Figure 2-4 shows the hairpin-loop region and the N-terminal domain of HGF. The N domain of HGF plays an essential role in interactions with the c-met receptor and heparin. This domain resides primarily in the N and K1 domains, which contain a hairpin-loop region (residues 70-96), characterized by two disulfide bonds [57]. HGF is a heat labile protein; it loses activity significantly when heated at 56°C for 30 minutes or completely by boiling for 1.5 minutes [58]. Activity is also partially lost when treated with 1M acetic acid or completely by trypsin digestion [58]. HGF is also known to lose activity by electrostatic interaction with gelatin made using the alkaline process of hydrolysis [59].

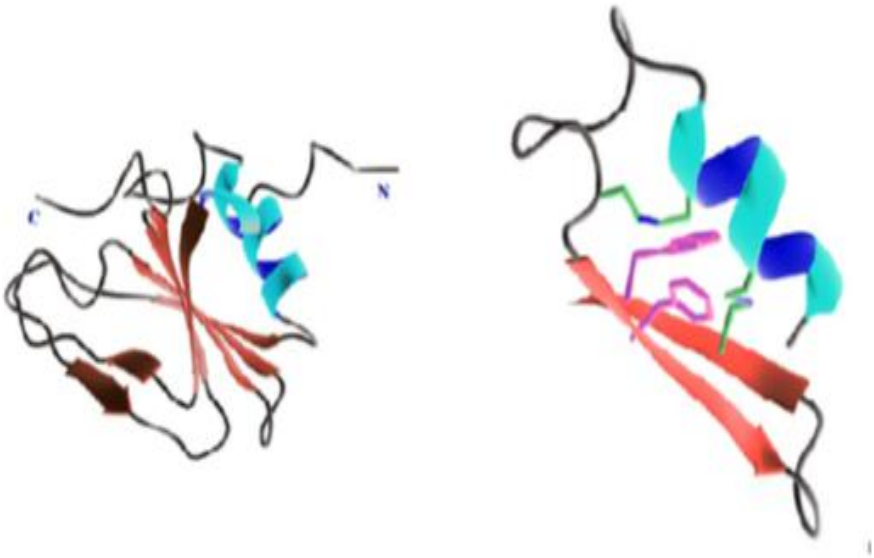

Figure 2-4: The structure of the N domain of HGF (left) [57]. The structure of the hairloop region in the N domain of HGF (right). Used with permission from [57].

The co-release of VEGF with HGF approach was chosen for our studies because several studies have shown that the administration of a single growth factor is not sufficient for the formation of stable and functional blood vessels. As discussed above, the formation of new blood vessels is a complex process, which requires multiple growth factors to work together in an ordered sequence to induce endothelial cell activation, proliferation, migration and tube formation, as well as attract pericytes and smooth muscle cells to complete the angiogenic cascade [40, 60-63]. VEGF was chosen because it promotes the initial stages of angiogenesis by stimulating the proliferation and migration of endothelial cells, which is an essential rate limiting step in physiological angiogenesis [40, 42, 61, 64]. HGF stimulates endothelial cells to proliferate and migrate and induces blood vessel formation *in vivo* in a dose dependent manner [42, 52, 65]. HGF also induces the production of VEGF by human keratinocytes [49, 50]and endothelial cells [50]and acts as a chemoattractant for pericytes [51]. The combination of VEGF and HGF has been shown to produce a synergistic effect on endothelial cell proliferation and migration [42, 52, 66].

2.4 Growth Factor Delivery Strategies

The typical experimental approach of administering growth factors involves either bolus injection into the ischemic site, or systemic administration using intra-venous and intra-peritoneal injection of a growth factor solution. Although therapeutic benefit was reported with bolus and systemic injection of vascular endothelial growth factors in rabbits [41, 67], pigs [68] and dogs [37], no significant improvement in the quality of life of patients that are not suitable candidates for standard revascularization was achieved in phase 2 clinical trials [69]. These growth factors are quickly cleared or metabolized in the tissue, because of the hostile ischemic environment created by the extensive protein degradation that takes place as part of inflammation and extracellular matrix (ECM) remodeling-induced enzymatic responses [2, 33, 48, 70]. As a result, these growth factors have short elimination half-lives after injection. Like other therapeutic proteins, growth factors are readily susceptible to enzymatic degradation, oxidation, aggregation, denaturation and adsorption at interfaces, isomerization, deamidation and diketopiperazine formation in a

physiological environment [43, 71]. In deamidation, the side chain linkage in a glutamine or asparagine residue is hydrolyzed to form a free carboxylic acid [72]. In isomerization, the peptide backbone is transferred from the α-carboxyl of an asparagine or glutamine residue to the side chain β or γ carboxyl [72] . Oxidation is the modification of the methionine residue to either a metsulfoxide or metsulfone derivative [73]. Adsorption at the interface occurs when there is hydrophobic contact between a protein and a hydrophobic polymer in the presence of water/organic solvent interfaces [46]. The dketopiperazine reaction occurs in peptides and proteins that possess the N-terminal sequence in which proline in the second to the last residue undergoes a non-enzymatic aminolysis [74] . All these degradation pathways could lead to unfolding, precipitation and aggregation of proteins.

Preliminary experiments and preclinical trials have indicated that a continuous, local administration of these angiogenic growth factors at the ischemic site is necessary to induce neovascularization [62, 75]. This continuous release is needed because angiogenic factors act as survival factors for endothelial cells, and exposure to the growth factor needs to be sustained to prevent early apoptosis of the migrating endothelial cells. For example, application of VEGF [33, 60, 64] or of VEGF and PDGF-BB [60, 76] at the ischemic site for 4 weeks resulted in elevated vascularity and improved blood flow in a hind limb ischemic mouse and rat model. This result suggests that the co-release of VEGF and HGF may be required for at least four weeks to generate stable and functional blood vessels[60, 76]. To attain therapeutically relevant local concentrations via systemic injection, multiple large doses must be injected, which is inefficient and may result in unwanted blood vessel growth [6, 33, 77]. To achieve effective local low dose and sustained delivery, three alternative strategies have been examined: gene therapy, cell therapy, and polymeric delivery.

2.4.1 Gene Therapy

Gene therapy is a sophisticated form of sustained delivery system. It involves the insertion of a new gene that encodes the expression for the production of a specific growth factor into a cell. The new

gene is usually inserted *in vivo* using different vectors, but sometimes *ex vivo,* and then the cells implanted. Once transfected, the target cells express the required growth factor for days, weeks or even longer, depending on the specific tissue transfected and the vector used. Figure 2-5 shows the gene therapy approach to therapeutic angiogenesis using viral vectors.

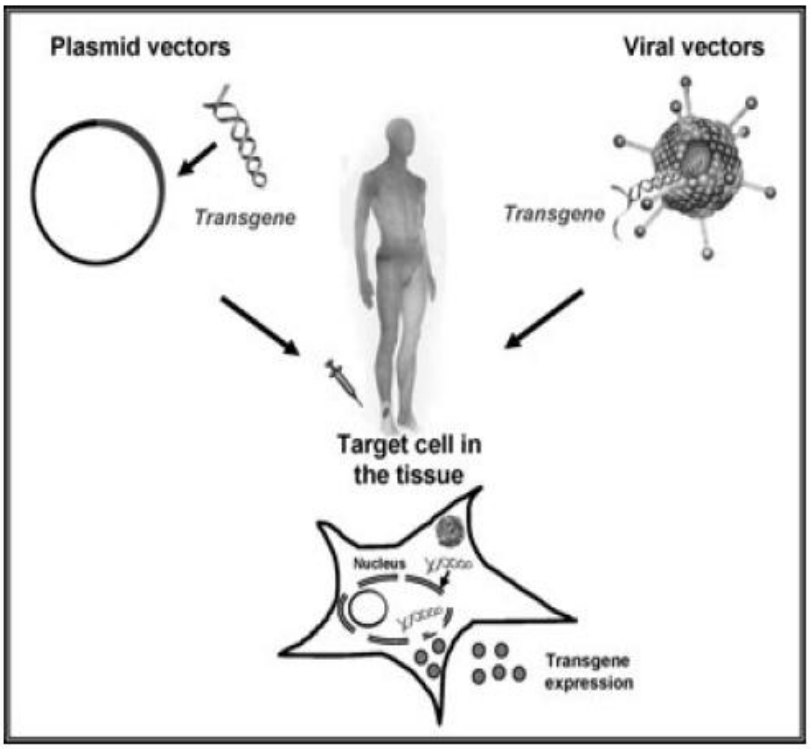

Figure 2-5 : The gene therapy approach to therapeutic angiogenesis using viral vectors. Used with permission from [78].

Viral vectors are currently the most efficient gene delivery method, taking advantage of the natural ability of viruses to penetrate into the host cells and transfer their genetic material to the nucleus. However, viral vectors such as the retrovirus and adenovirus have serious safety concerns such as oncogenicity, toxicity and immunogenicity [79]. The effectiveness of gene therapy in reduction of amputation rate, improvement of skin ulcer and hemodynamic improvement has been investigated in clinical trials in humans, but the results have been disappointing [3, 80]. The disappointing results can be

attributed to inconsistent levels of growth factor expression achieved with the same administered dose of gene vector in different individuals, variability due to differences in transfection efficiencies, and low transfection rates producing variable intra-individual doses [5].

2.4.2 Cell Therapy

Another strategy of achieving new blood vessel formation is by delivery of stem or progenitor cells to the ischemic site. The stem cells are either transplanted locally [81, 82] or via intravenous transfusion [83]. However local transplantation is more advantageous as it will increase cell density at the target site and may reduce systemic side effects. The endothelial progenitor cells used have been derived from such sources as bone marrow mononuclear cells (BM-MNCs) [82, 84], human adipose tissue derived stromal cells (ASC)[85] and human umbilical cord blood endothelial progenitor cells (EPC)[83]. The fate of stem and progenitor cells at the site of angiogenesis remains controversial. Initially, reports indicated engraftment and differentiation of epithelial progenitor stem cells to matured endothelial cells within the growing capillary network [81, 82]. Recent studies indicate that the implanted stem progenitor cells function in a paracrine mode of action by secreting angiogenic and antiapoptotic factors such as VEGF and HGF to stimulate the proliferation and migration of existing endothelial cells and pericytes, forming new blood vessels [85, 86]. The secreted antiapoptotic factor may reduce or prevent the apoptosis of endothelial cells and pericytes.

There has been some evidence of stem or progenitor cell therapy in experimental models of hind limb or myocardial ischemia achieving success [81, 83]. In a recent review of clinical studies done using stem cells, [87] 18 of the 25 clinical studies that reported on the use of mononuclear cells or progenitor cells for the treatment of patients with critical limb ischemia were analyzed. This analysis indicated that progenitor cell-based therapies are safe, feasible and promote vascularization in ischemic tissues with improved clinical outcomes but the low therapeutic efficacy due to poor survival of cells transplanted into ischemic tissues remains the largest obstacle. In addition, the clinical studies thus far have been small and lacked

double-blinded controls, as a result, larger, randomized and blinded studies still need to be done to illustrate the efficacy of this therapy. Furthermore, there are still questions about cell populations to be used, optimal doses, and routes of administration that need to be addressed [87]. Inconsistencies in these parameters could lead to variability in results obtained.

2.4.3 Polymeric Delivery

In comparison to gene and cell therapy, polymeric delivery systems have a number of advantages, including a precise knowledge of the delivered dose, the ability to achieve prolonged delivery, and the ability to combine several proteins in a single formulation. The desired controlled release devise should deliver the encapsulated protein in its active form. The main issue of polymeric delivery systems for protein therapeutics is possible degradation of the protein within the device during manufacture, storage or upon implantation and release from the device [31, 88, 89]. As a result, the presence of moisture and use of high temperature must be avoided during device fabrication [51]. In addition, the chosen controlled release device should be easily introduced to the affected site, delivering an effective, local, therapeutically relevant concentrations, at a sustained rate, with little biodistribution outside the ischemic region, and with minimal initial burst release. For example, a high burst release of VEGF could lead to the formation of abnormal and short-lived blood vessels [64, 90]. Furthermore, the delivery device should be made from biocompatible and biodegradable materials with non-toxic degradation products [33]. A review of a variety of approaches that have been examined for polymeric growth factor delivery has been recently published [51]. These approaches include hydrogels, matrices, microparticles, polymeric monoliths and liquid injectable hydrophobic polymer devices, made using natural and synthetic materials such as gelatin, collagen, alginate, poly(N-isopropylacrylamide), chitosan, poly(trimethylene carbonate), poly(orthoesters) and poly(lactic-co-glycolic acid) (PLGA).

2.4.3.1 Hydrogels

Hydrogels are polymer networks that are physically or chemically crosslinked, and which absorb large amounts of water while retaining their three dimensional form [60, 61, 91]. The mechanical properties of hydrogels can be similar to that of the extracellular matrix; therefore, inflammation as a result of mechanical irritation can be avoided. Although hydrogels can be introduced into the body with minimally invasive procedures, a potential problem with hydrogels as protein delivery systems is the possibility of protein hydrolysis and aggregation while storing the delivery system with the large amount of water [71]. Moreover, release durations *in vitro* and *in vivo* are generally too short to provide effective neovascularization, being on the order of days [35, 36, 61, 92]. A number of different hydrogels have been examined as potential angiogenic growth factor delivery systems, including chitosan, gelatin, collagen and alginate; however, alginate has been the most commonly used.

Alginate is a random copolymer of D-mannuronic acid and L-guluronic acid residues [33, 93], and has been widely investigated as a delivery system for various growth factors. Alginate gels in the presence of divalent cations, such as calcium, which ionically crosslink the negatively charged carboxylate groups in the L-guluronic blocks of alginate. This gentle gelling property makes it an attractive polymer for this application [93]. Highly purified alginates are biocompatible; however, alginate itself degrades very slowly [33], and its gels degrade in an uncontrollable manner, releasing high molecular weight chains that may have difficulty being cleared from the body [94]. Drug release from non-degradable alginate hydrogels is predominantly driven by diffusion [33]. Alginates can be rendered degradable by partial oxidation of the uronate residue to an open chain adduct to make it more susceptible to hydrolysis using sodium periodate [33, 93]. Another strategy of controlling degradation is by using a binary molecular weight formulation by incorporating low molecular weight chains, which more readily disassociate from the gel, and can be subsequently excreted from the body [33, 35, 44]. In contrast to non-degradable alginate hydrogels, where diffusion is the predominant mechanism of growth factor release, growth factor release from degradable gels could be tuned by controlling both diffusion and alginate degradation [33, 35].

Silva and co-worker [33] investigated the release of VEGF from gels formed from binary molecular weight alginate that was either partially oxidized with sodium periodate or non-oxidized. VEGF release from the partially oxidized form was faster with a high initial burst of 40% and total fraction released of about 80% after 30 days, while VEGF release from the non-oxidized form was sustained with 15% initial burst and 50% released after 30 days. The released VEGF was biologically active for 4 days with little distribution outside the ischemic region. However, fully normal limb perfusion was not achieved after 42 days and bioactivity data for the released VEGF after 4 days were not shown [33]. Considering the water content of the hydrogel (98 % (w/v)), there is the possibility of protein hydrolysis and aggregation while storing the delivery system with the large amount of water. Recently, Ruvinov and co-workers formed a complex between HGF and sulfated alginate via electrostatic interaction [35]. The growth factor was released at a rate determined by its binding constant to the hydrogel [35, 36]. However, after *in vivo* injection into ischemic myocardial tissue, 75% of the incorporated HGF was released after 6 hours followed by a slow release for 5 days, after which only 85% of the incorporated HGF was released [35]. Though the released growth factor was bioactive, the high burst release of 75% after 6 hours might lead to significant undesirable side effects.

Collagen type 1 is the most abundant protein present in the body of mammals with a long history of clinical use and has been explored as a delivery vehicle for bFGF[70] and HGF[70, 95]. Impregnation of HGF into freeze-dried collagen sheets/microspheres was carried out by use of phosphate buffered saline solution (PBS, pH 7.4) containing various concentrations of HGF [70, 95]. At this pH, HGF was electrostatically bound to the collagen matrix and was released *in vivo* at a rate similar to the degradation rate of the collagen matrix[70, 95]. Release occurred for about 30 days at a decreasing rate with time. Though this approach led to increased number of blood vessels and promotion of vascular maturation compared to control [70], no attempt was made to determine the bioactivity of the released HGF. With the high water

content of the collagen gel (83 % (w/v)), there is the possibility of protein hydrolysis and aggregation while storing the delivery system.

Gelatin is a denatured collagen commercially available as a bioabsorbable polymer. It is enzymatically degradable and has a long history of clinical use due to its biocompatibility and biodegradability in the physiological environment [96, 97]. To enhance its use as a controlled release device, it is crosslinked using chemical crosslinkers such as glutaraldehyde [59, 97]. The degradation rate and hence the release of growth factors is determined by the extent of crosslinking of the gelatin matrix [59]. Depending on its processing procedure, gelatin can be positively or negatively charged at physiological pH, and the charge can be utilized in the electrostatic binding of oppositely charged protein, providing an additional means of controlling release[59, 97]. The alkaline process hydrolyses the amide groups of asparagines and glutamine into carboxylic groups, thus converting these residues to aspartate and glutamate while the acidic pre-treatment does not affect the amide groups present. As a result, the gelatin processed with an alkaline process possesses a greater proportion of carboxyl groups, rendering it negatively charged and lowering its isoelectric point (pI) to 5 compared to acidic-processed gelatin which possesses a pI of 9 which is similar to that of collagen [96].

Gelatin can be readily prepared into sheets, foams and microspheres by simple techniques. Growth factors incorporated within these gelatin forms were released at a rate determined by their affinity for gelatin[97] and or the extent of crosslinking [59, 98]. Gelatin has been used for the delivery of VEGF[98], bFGF[97] and TGF-β1 [97] and HGF[59] both *in vitro* and *in vivo*. With the gelatin crosslinked with 10 mM glutaraldehyde, containing 60 ng of VEGF /mg of gelatin microparticles, a high burst release of 61% was observed on the first day followed by 1.5%/day from day 1 to 3, 0.8% /day from day 3 to 16 and 1.3%/day from day 16-28[98]. Though the released VEGF maintained 90% bioactivity for over 14 days, the high burst release of 61% on the first day could lead to significant side effects[98]. Though the released HGF was capable of increasing capillary density and enhance blood flow in a hind limb ischemic model[59],

the disadvantage of this approach is the decreased bioactivity of HGF as a result of electrostatic complexation [59], the resulting complex between the positively charged growth factor and the negatively charged gelatin formed may be immunogenic, and the rate of gelatin degradation would vary from individual to individual which would affect release kinetics.

Chitosan is a linear copolymer of linked β-(1→4) glucosamine (2-amino-2-deoxy-D-glucose) and N-acetyl-D-glucosamine (2-acetamido-2-deoxy-D-glucose), obtained by purifying deacetylated chitin[99]. It has been shown to be biocompatible, biodegradable[100], to accelerate wound healing [99] and to have antimicrobial properties[101]. However, chitosan is insoluble at neutral pH. A water soluble and photo-crosslinkable derivative of chitosan was prepared by grafting 4-azidobenzoic acid to the available free amine groups of lactose modified chitosan [102]. When exposed to UV irradiation, the azide group is converted to nitrene which is highly reactive with amino groups, inducing reaction with the amine group of chitosan. A disadvantage of this approach is the possibility of non-specific interaction of these nitrenes with amino groups on the incorporated protein itself, resulting in protein denaturation. This polymer has been used for the release of bFGF [103] and VEGF[103, 104]. Using this approach, a burst release of about 10-25% was observed on the first day with no substantial release afterwards, by the end of the release studies, approximately 80% of the incorporated growth factors were still retained in the photopolymerized polymer[92, 103, 104]. The incomplete release of bFGF and VEGF observed could be due to the aggregation of the protein within the device possibly due to the interaction of nitrene with the amino acid of the protein or hydrolysis of the protein due to the high water content of the gel[103, 104]. This approach was used to deliver bFGF to ischemic regions in rabbit hearts, and the released bFGF induced angiogenesis in the ischemic myocardium [92]. However, the extent of release and in *vivo* release rate were not assessed.

2.4.3.2 Microparticles

Polymeric microparticles in the form of microspheres, microcapsules, and nanoparticles capable of delivering a prolonged and constant amount of growth factors have been developed [46, 105-107]. Potential

advantages of this approach are the possibility of injection at the site of action and long term release [108]. Microspheres made from poly(lactic acid) (PLA), poly (glycolic acid) (PGA) and their copolymer (PLGA) for prolonged and sustained delivery of therapeutic proteins have been developed using various emulsion methods[46, 105, 106]. Generally, depending on polymer formulation and encapsulated drug, the drug release profile from PLGA microspheres is characterized by an initial burst, followed by a diffusion and/or erosion release phase [89, 107]. The initial burst release is due to the surface resident protein particles, while the diffusion controlled release is a result of dissolved protein diffusing through the water filled pores and channels within the microspheres [89, 107, 109]. The erosion release mechanism depends on the polymer degradation rate, the size of the system, and the process used to obtain the particles [107]. However, major issues with this delivery system are low protein encapsulation efficiency [89]and possible protein instability induced during manufacture, storage and release resulting in incomplete release and loss of protein activity [46, 89, 110]. The presence of water/organic solvent interfaces and hydrophobic contact between protein and hydrophobic polymer results in interfacial adsorption followed by unfolding and aggregation during microsphere preparation [88, 109]. Incomplete protein release occurs as a result of hydrophobic interactions between protein and polymer leading to aggregation and precipitation, while loss of protein activity during release occurs due to hydrolytic degradation of the polymer, which generates acidic oligomers and monomers lowering the pH within the microsphere to as low as 1.5[111]. Therefore, protein denaturation may be much more pronounced inside the microparticles than on the surface [89]. The pH reduction within the microsphere has been linked to aggregation and hydrolysis of ovalbumin [89] and VEGF [46, 106] over time. Denatured or aggregated protein species will not only be therapeutically inactive, but may cause unpredictable side effects such as immunogenicity or toxicity [112]. Effective control over protein stability during microsphere processing can be generally exerted by selecting suitable techniques and using stabilizers, whereas protein stability during the release stage is much more difficult to attain [88]. Despite these limitations, PLGA microspheres have been explored for the delivery of VEGF [46, 105-107, 110, 113] and HGF [107].

Cleland and coworkers [46] prepared microspheres with an initial VEGF loading of 9% (w/w) using a spray drying technique. With formulations containing 10 mg/mL of VEGF and 1 mg/mL of trehalose, a low initial release of less than 10% followed by a lag phase of 5 days and sustained release phase was observed, with over 90% of the incorporated VEGF released in 35 days. However, the released VEGF aggregated and hydrolyzed over time and lost 15% of its heparin affinity after 8 days. However, the released VEGF did not lose its ability to bind the KDR receptor that stimulates endothelial cell proliferation after 8 days of release from the microspheres, producing a dose dependent angiogenic response. Kim and Burgess [110]examined the release of VEGF from PLGA microspheres *in vitro* and *in vivo* after subcutaneous injection in rats. Their study showed that VEGF was released as the polymer degraded both *in vivo* and *in vitro*. About 25% of the VEGF activity was lost and this loss was attributed to the acidic microenvironment within the PLGA microsphere. In a more recent study, Formiga and coworkers [106] prepared microspheres with an initial VEGF loading of 0.06% w/w using a solvent/extraction evaporation method. A low initial release of 10% in the first 6 hours was observed, with about 60% released from day 1 to 7, and a much slower release rate from day 7 to 28 when about 75 % of the incorporated VEGF had been released, and about 25% of the incorporated protein appears to be non-releasable. VEGF released increased angiogenesis and arteriogenesis in an acute ischemia-reperfusion rat model. Using two cell based assays, the released growth factors on day 3 and day 7 were bioactive, but the bioactivity of the VEGF released (15% of incorporated VEGF) from day 7 to day 28 was not assessed. With 25% of non-releasable VEGF, there is the possibility that the released growth factor beyond 7 days may have been denatured.

Zhu and coworkers [107] prepared microspheres made from a blend of PLGA and poly(hydroxyalkanoate) for HGF delivery. HGF was loaded into the polymer at 0.002% (w/w) using the water-in-oil-in-water technique. With formulations containing 0.002 % w/w of HGF and 5% w/w of BSA, two phases of release were observed, a low initial release in the first two weeks as a result of diffusion from areas near the surface and a subsequent accelerated release that was consistent with the accelerated

mass degradation of the polymer. Over 90% of the incorporated HGF was released after 70 days. Using cell-based assays, the HGF released was highly bioactive for over 40 days when about 65% of the incorporated HGF has been released. The bioactivity of the remaining HGF released after 40 days was not determined, and there is the possibility of HGF aggregation and hydrolysis due to pH reduction within the PLGA microsphere.

2.4.3.3 Porous Matrices/Scaffolds

Matrices are polymers fabricated into porous or non-porous three-dimensional structures with dispersed solid growth factor particles. Porous scaffolds can provide a large surface area for cell infiltration, which will elicit the ingrowth of blood vessels and reduce fibrous encapsulation or fibrosis when implanted [114]. Fibrous encapsulation is disadvantageous especially in drug delivery, as it may create a barrier to growth factor transport into the surrounding tissue, thereby reducing growth factor release rate [51]. Growth factors can be either adsorbed to the scaffolds[115, 116], mixed in the lyophilized form into the polymer before processing the polymer into a porous scaffold, or by pre-encapsulating the growth factor in microspheres and then fabricating scaffolds from these particles[46, 62, 107, 108]. Adsorbing growth factors onto the scaffold is an inefficient process, and results in low encapsulation efficiency and a high burst effect [115, 116]. Pre-encapsulating the growth factor into microspheres using the emulsion technique has been attributed to loss of protein bioactivity [110].

Cleland and co-workers [46] encapsulated VEGF with different ratios of trehalose into PLGA microspheres and compressed them into a dense and non-porous disk by compression molding. On the first day, less than 10% of the incorporated VEGF was released, followed by a lag of 10 days, after which two phases of release were observed: from 10 – 21 days when about 40% was released, and a much rapid release from 21 – 40 days when almost complete release was achieved. However, no effort was made to determine the bioactivity of the released VEGF. Sheridan and co-workers [117] also prepared VEGF loaded scaffolds made from PLGA. A large burst effect of 20% was observed on the first 2 days, with a total of

about 40% of VEGF released after 44 days. The released VEGF was bioactive over the first 7 days when about 25% was released, after which bioactivity was not measured. The ability of this delivery system to stimulate angiogenesis in a lower hind limb model was reported by Sun and co-workers [32]. In their study, a burst release of about 30% of VEGF was observed on the first day, after which VEGF was released at 30-90 ng/day with a total of 80% of the incorporated VEGF released after 30 days. The released VEGF induced tissue perfusion, greater capillary density, and more mature-appearing vasculature compared to the controls [32]. Considering the rather low level of VEGF released after 44 days from PLGA which may have low pH within the device, there is the possibility of VEGF aggregation within the device.

To improve the encapsulation efficiency and release profile of VEGF from PLGA scaffolds, Ennett and coworkers [118] pre-encapsulated VEGF in PLGA microspheres and distributed the microspheres in PLGA scaffolds that were made using the gas foaming/particulate leaching method. When implanted *in vivo*, a burst release of 26% was observed within the first day, followed by a sustained release reaching 75% by day 15, and 80% by day 35. Using this approach, a greater number of blood vessels were found surrounding the implant when compared to control after *in vivo* implantation. The overall percentage of VEGF released that was bioactive was not assessed, and it is possible that the VEGF remaining underwent aggregation and hydrolysis due to pH reduction within the PLGA microsphere.

Smith and co-workers [119] incorporated HGF in PLGA porous scaffolds by immersing PLGA microspheres in alginate/HGF solution. This suspension was then lyophilized to obtain a powder, which was pressed in the presence of NaCl to form disks, and the disks were subjected to 800 psi of CO_2 for 24 hours. The NaCl was leached out from the disk by immersing in 0.1M $CaCl_2$ for 16 hours. In the first 24 hours, 35% of the incorporated HGF was released, 55% was released on the 4^{th} day and 63% on the 10^{th} day. By the 35^{th} day, about 70% of the incorporated HGF was released and about 80% of the released HGF was bioactive over time. However, this procedure is inefficient as only 55% of the incorporated HGF was successfully encapsulated into the disk.

The degradation of growth factors released from matrices made from PLGA is likely a result of the same issues reported for microspheres. In addition, matrices can only be delivered to the ischemic site via implantation, and this is a major setback.

2.4.3.6 Multiple Growth Factor Delivery

The need for the co-administration of two or more growth factors to achieve stable blood vessel formation has motivated the investigation of multiple growth factor delivery systems. Richardson and co-workers made porous scaffolds by compressing particulate PLGA that was mixed with VEGF that had been co-lyophilized with alginate and NaCl, with microspheres pre-encapsulated with platelet derived growth factor BB (PDGF-BB) to provide multiple growth factor delivery with a distinct release rate for each factor. PDGF-BB stabilizes primitive blood vessels by inducing the migration and proliferation of smooth muscle cells [17]. VEGF and PDGF-BB were co-released at the rates of 79 and 1.5 - 60 ng/day respectively for the first 7 days followed by a slower release rate that was sustained for up to 35 days with no burst effect. After two weeks of implantation, this release pattern generated larger and more matured blood vessels than delivery of either factor alone when implanted in a mouse hind limb ischemia model [62]. However, the long-term stability of the blood vessels was not assessed and the encapsulation efficiency of VEGF and PDGF-BB were not determined. Despite the fact that the released growth factors were reported to be bioactive over the first 3 weeks, the bioactivity data was not reported. There is the chance of reduction in bioactivity of the released growth factors as a result of the acidic degradation products formed when PLGA is hydrolyzed, especially at the latter stages of release.

Using a similar approach, Chen and coworkers [113] pre-encapsulated PDGF-BB in PLGA microspheres, and then the PLGA microspheres were lyophilized with or without VEGF in an alginate solution. Each layer of the scaffold was mixed separately, and manually compacted in a scaffold die. Layers were compacted on top of each other and then finally compressed at 1,500 psi in a Carver press for

1 minute to form a single scaffold. Samples were exposed to high pressure CO_2 gas to saturate the polymer with gas. A thermodynamic instability was created by decreasing the gas pressure to ambient pressure. This led to nucleation and growth of gas pores within the polymer matrices. The NaCl particles were leached out by immersing the matrices in double distilled water to form matrices with open pores. Total protein loading after fabrication was 1.5 μg of VEGF and/or 3 μg of PDGF in layer 1 and 3 μg VEGF alone in layer 2. The release profile of VEGF determined by its radioactivity was similar in layer 1 and layer 2; a quick burst and a sustained release was observed. On the first day, there was a burst release of about 27% for VEGF but only about 8% for PDGF-BB. In the compartment delivering a high dose of VEGF alone, a high density of small, immature blood vessels was observed at 2 weeks. Sequential delivery of VEGF and PDGF-BB led to slightly lower blood vessel density, but vessel size and maturity were significantly enhanced. However, only about 80-85% of the incorporated VEGF was released depending on initial loading while about 50% of the incorporated PDGF-BB was released after about 42 days. Even though the biological activity of the growth factors released were not measured, there is the risk of loss of biological activity as a result of the acidic degradation products formed when PLGA is hydrolyzed , this is more prominent at the latter stages of release.

Hao and co-workers combined VEGF and PDGF-BB in an alginate solution prior to gelling[76]. Following an initial burst on the first day, VEGF and PDGF-BB were co-released in a sustained manner; VEGF was released at a rate of 75 ng/day from days 1–12, and 10 ng/day from days 12– 30, while PDGF-BB was released at the rate of 70 ng/day from days 1–30. Using the same approach, Sun and co-workers combined an alginate solution with VEGF and mixed it with PDGF-BB pre-encapsulated in PLGA microspheres prior to gelling[60]. VEGF and PDGF-BB were released in a sequential manner. A high burst of 50% of VEGF (1500 ng) was released within 2 days, which reached more than 70% (60 ng/day) by day 12, and more than 80% (12 ng/day) by day 36. In contrast to VEGF, about 10% (300 ng) of PDGF-BB was released within 2 days, and reached more than 40% (90 ng/day) by day 12 and more than 70% (25 ng/day) by day 36. In both cases, the dual delivery system generated larger and more matured blood

vessels that were superior to the delivery of either factor alone in a mouse hind limb ischemic model after four weeks of implantation. However, the large burst of VEGF in the first two days is inefficient and could lead to potential side effects. Though the level of bioactivity of the released growth factors was not studied, there is the potential of growth factor denaturation due to the large amount of water in the gel.

Recently, dextran based hydrogels immobilized with VEGF, stromal cell-derived growth factor -1 (SDF-1), insulin growth factor (IGF-1) and angiopoetins-1 (Ang-1) have been shown to induce more tissue in-growth with more and larger blood vessels within 3 weeks in rats compared to hydrogels immobilized with VEGF alone, which was able to induce tissue in-growth only after 5 weeks of implantation[61]. The rate of delivery and the delivery sequence using this approach was not mentioned. Though the bioactivities of the released growth factors were not determined, there is the potential of growth factor denaturation due to the high water content of the gel. More recently, Layman and co-workers examined the co-release of bFGF and G-CSF incorporated into a fibrin hydrogel. About 93% of the incorporated bFGF was released within the first 5 days with a burst release of approximately 35% on the first day while about 88% of G-CSF was released within the first 5 days with a burst release of approximately 30% on the first day. The released growth factors led to a significant increase in the reperfusion of the hind limb ischemic model in comparison to the single factor delivery, with only 80% of normal reperfusion recovered after 8 weeks [63].

Chapanian and Amsden utilized an osmotic pressure release mechanism to achieve both co- and sequential release of VEGF and HGF from cylindrical geometries, made from a biodegradable elastomer composed of photo-cross-linked, terminally acrylated star-poly(trimethylene carbonate-co-DL-lactide-co-ε-caprolactone) [31]. Co-release was achieved by co-lyophilizing both growth factors with albumin, trehalose and NaCl to generate enough osmotic pressure to drive the release. The particles were distributed throughout the polymer, poured into a mold and photocrosslinked with UV light. By using this approach, VEGF and HGF were released at similar rates, with 20% burst release on the first day followed

by a sustained release for over 14 days, with 65% of the embedded VEGF released by day 20. To achieve sequential release, the inner core of the cylinder consisted of HGF particles covered with an outer polymer layer that contained VEGF particles. The HGF particles in the inner layer contained a greater amount of NaCl to drive its release. By using this approach, VEGF and HGF were released sequentially in a sustained manner for over 30 days, with VEGF released faster than HGF. The released growth factors were highly bioactive as assessed from cell-based assays. This was the first attempt to release VEGF and HGF from the same delivery vehicle *in vitro*. However, the efficacy of this delivery system has not been tested *in vivo*. The setbacks of this approach are that there is need for surgery to implant the device and the polymer degrades at a relatively slow rate, with 9.6 ± 0.4 % mass loss after 28 weeks.

Marui and co-workers [70]combined bFGF and HGF in a collagen sheet, by rehydrating a lyophilized collagen sheet with a 20 µL PBS solution containing 5 µg of bFGF and 20 µg of HGF. HGF and bFGF were released as the collagen matrix degraded *in vivo* with a burst release of 30% on the first day and almost complete release by 28 days. This formulation induced increased number of blood vessels and promoted vascular maturity in severe murine hind limb ischemic model in a synergistic manner which was equivalent to that observed with 80 µg of bFGF or HGF alone. Though no attempt was made to determine the bioactivity of the released growth factors, there is a high likelihood of growth factor hydrolysis and denaturation due to the large water content on the gel (98 % (w/v)).

More recently, Ruvinov and coworkers [36]fabricated an injectable alginate with affinity-bound growth factors, by incubating insulin-like growth factor 1 (IGF-1) or HGF (1 mg/mL each) with alginate-sulfate solution (0.83% w/v) for about 1.5 hours at 37°C. The resulting solution was mixed with the solution of the partially calcium-cross-linked alginate to provide multiple growth factor delivery with a distinct release rate for each factor. IGF-1 was released faster than HGF; IGF-1 was released with a burst release of greater than 50 % while HGF was released with a burst release of about 5% in the first 6 hours, followed by a much lower rate of growth factor release. IGF-1 was released at a faster rate compared to

HGF, and this led to the formation of mature and larger blood vessels. The difference in release kinetics of the growth factors was attributed to their different affinity for alginate sulfate. The high burst release of IGF-1 within the first 6 hours may lead to significant side effects; furthermore, the growth factors are prone to hydrolysis and aggregation as a result of the large water content of the alginate hydrogel.

2.4.3.4 Osmotically-driven release

The protein degradation associated with acidic degradation products of the polymer vehicle can be overcome provided the proteins are completely released from the device long before the polymer degrades significantly. This type of release behavior has been shown to be possible by employing an osmotic pressure release mechanism[31]. For solid matrices, the osmotic pressure driven mechanism is determined by the osmotic activity of the embedded particles, the particle loading in the polymer and the mechanical properties of the polymer. The osmotic pressure release mechanism from solid monolith matrices proceeds as follows. Upon immersion in an aqueous environment, water molecules penetrate the polymer until they reach a polymer-encapsulated particle, hereafter called a capsule. The water dissolves the solid particle at the polymer-drug interface to form a saturated solution, generating a water activity gradient between the saturated solution formed and the surrounding aqueous media [120, 121]. The activity gradient draws water into the capsule to generate an internal osmotic pressure equal to the osmotic pressure of the saturated solution. The generated pressure is resisted by the viscoelastic nature of the polymer [122]. The outcome of this resistance is as follows: (1) when the polymer is unable to resist the pressure generated by the capsule, polymer bonds are broken, and cracks are formed in the polymer bulk, which connects the contents of the capsule to the pore network, and the dissolved contents are forced through these cracks towards the surface as a result of the pressure gradient, (2) when the generated pressure is unable to initiate bond breakage in the polymer, a thermodynamic equilibrium is established and the encapsulated drug is not released until the polymer degrades [122].

Complete release via the osmotic pressure release mechanism is achieved as the excipient osmotic activity increases [123], or the particle size [124] and tensile strength decreases [125], and reaches a maximum value at or near the percolation threshold [123]. This technique can provide many of the requirements for a successful polymer-based growth factor delivery system. It provides a sustained release of bioactive growth factors, with a near zero order release profile and with very minimal initial burst release [126]. For the osmotic pressure release mechanism to dominate and for almost complete release of protein, the protein and osmolyte particles are loaded into the polymer at a volumetric loading of less than 30% [123]. The osmotic release mechanism has been investigated for the release of VEGF and HGF from solid monoliths [31,127, 128], and for VEGF from liquid injectable polymers, [129, 130] discussed in the next section.

Solid monoliths used in osmotic release have been elastomeric matrices with dispersed particles containing a highly osmotically active compound. Gu and coworkers [125] utilized the osmotic release mechanism to release VEGF from a biodegradable elastomeric device made by photo-cross-linking an acrylated star copolymer macromer of ε-caprolactone and D, L-lactide. The photoencapsulation technique did not denature the encapsulated VEGF. In this approach, the protein was lyophilized along with trehalose, which acts as the osmotic agent, and the solid particles were distributed throughout the polymer matrix at less than 10% w/w. VEGF was released in a linear fashion for over 18 days; however, the bioactivity of the released VEGF decreased significantly after 8 days. This decrease was attributed to a decrease in the local microenvironment pH within the matrix. To eliminate the limitation of loss of bioactivity as a result of acidic degradation by-product formation, a terpolymer of trimethylene carbonate with DLLA and ε-caprolactone at a ratio of 50:25:25 was used. Poly(trimethylene carbonate) undergoes hydrolysis slowly and does not generate acidic degradation by-products, as do poly(esters). Highly bioactive VEGF and HGF were released sequentially or simultaneously from the terpolymer at a sustained rate for more than 10 days [31].

2.4.3.5 Liquid Injectable Polymers

Liquid injectable polymers are polymers with a low glass transition temperature, a low melting point and low viscosity. As a result, the growth factors can be easily incorporated throughout the polymers by physical mixing. The first of such polymer formulations examined for protein delivery was based on a semi-solid, self-catalyzed poly(ortho ester) (POEs) for VEGF delivery[131, 132] . Protein release from semi-solid, self-catalyzed POEs depended on pH, the buffering capacity of the protein solution [132], and protein molecular charge [132]. However, protein release duration was very short, ranging from 6 to 15 days [131, 132] and there was a high burst release of 20% in the first 24 hours [131, 132]. In addition, the accumulation of acidic degradation products within the polymer resulted in a drop in pH to less than 5.2 within the polymer, and this drop in pH has been cited as the cause of both protein aggregation and VEGF denaturation through hydrolysis when released from these polymers [133]. However, protein aggregation was minimized by the addition of trehalose into the formulation.

More recently, Amsden and coworkers utilized an osmotic release mechanism to release VEGF from liquid, injectable poly(trimethylene carbonate) with a molecular weight of 1600 Da. VEGF was lyophilized along with trehalose (95% w/w) and BSA (4.9% w/w), sieved to less than 45 μm, and the solid particles were distributed throughout the polymer matrix at a total loading of 1% w/w. The mass fraction of VEGF released was independent of the polymer's viscosity and the amount of VEGF in the particles.[30]. VEGF was released in a sustained manner at a rate of 15 – 20 ng/day for over 40 days, followed by a decreasing rate with time. An endothelial cell based assay indicated that the released VEGF retained about 90% of its bioactivity over 40 days. Injection of the VEGF-loaded polymer subcutaneously in the backs of rats elicited the formation of blood vessels, which regressed with time due to the low concentration of VEGF released and moreover, one single growth factor cannot complete the angiogenic cascade. Furthermore, the polymer degraded slowly *in vivo* with only 55% weight loss after 40 weeks of degradation. This slow degradation rate implies that the polymer would remain at the implantation site long after the growth factor has been released, eliciting a prolonged immunological response.

2.5 Summary

The sustained and local delivery of angiogenic growth factors is a clinically appealing strategy for treating critical limb ischemia. Reviewing the growth factors that are involved in angiogenesis, it has been identified that each step in angiogenesis is mediated and controlled by a variety of growth factors and these growth factors are secreted in a spatial and temporal manner in a tightly controlled fashion. Therefore, one single growth factor cannot complete the angiogenic cascade. For effective vascularization, two or more growth factors have to be delivered together or sequentially. Reviewing the delivery strategies of therapeutic growth factors using polymeric delivery systems, key issues associated with the bioactivity of the incorporated growth factor, the delivery mechanism, and hence revascularization to induce collateral blood vessel formation were identified. Though hydrogels can be easily injected to the affected site, one major problem with this delivery approach is that while storing the delivery system in water, there is the possibility of growth factor denaturation. Though microspheres made from hydrolysable polyesters such as PLA, PGA and PLGA could be injected directly to the affected site, they are not a suitable drug delivery system for acid sensitive growth factors that require multi-week delivery. This is because of the complex manufacturing procedure and the accumulation of acidic degradation products within the polymer that may denature the growth factor. Most of the matrices that have been investigated to date are made from polyesters such as PLA, PGA and PLGA and are subject to similar drawbacks as for microspheres. In addition, matrices have to be delivered via implantation, which requires surgery, and this is a major limitation. For most of the studies using hydrogels, microspheres and matrices, the release of growth factors is not sustained; there is incomplete release and a large initial burst of growth factors, which might be problematic as the large burst release of these factors may produce undesired side effects. It is essential that the growth factors are released in their bioactive form because denatured or aggregated growth factors will not only be therapeutically inactive, but may cause unpredictable side effects such as immunogenicity or toxicity [112]. Unfortunately, most of

the studies to date did not included bioactivity data of the growth factors after being incorporated into the delivery device; however some studies indicate a reduction in bioactivity over time.

2.6 Tissue Response to biomaterial implantation

Since the growth factors would be incorporated in a polymeric delivery device, it is essential to understand the release mechanism of the incorporated growth factors when implanted *in vivo* and most importantly the effect of the polymer and its degradation products on the surrounding tissue. The tissue response to biomaterial implantation is characterized by blood-material interactions, provisional matrix formation, acute inflammation, chronic inflammation, granulation tissue development, foreign body reaction, fibrosis/fibrous capsule formation and subsequent resolution of the inflammatory response [134-136]. This section describes the formation of the blood clot, adsorption of proteins on implanted biomaterials, and the subsequent inflammatory response.

Figure 2-6 shows the cascades of events that occur when a polymer device is implanted *in vivo*.

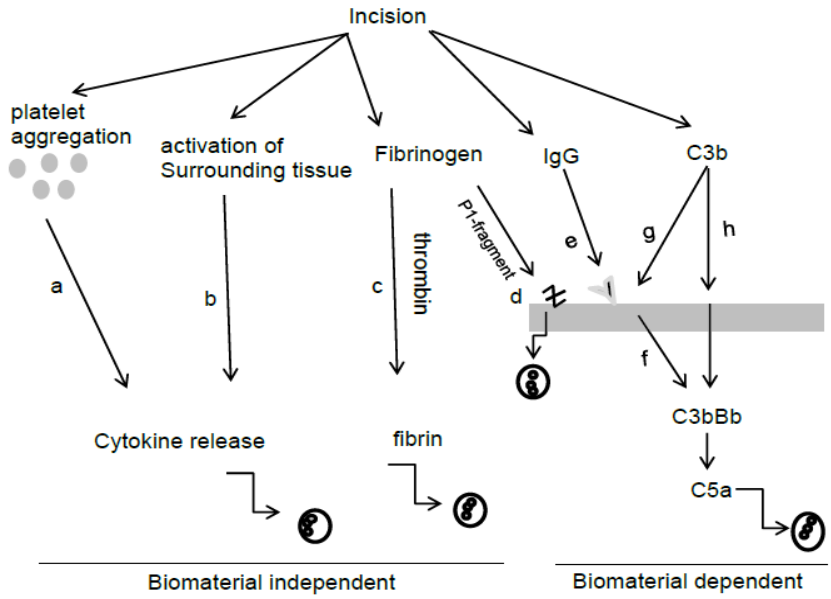

Figure 2-6: Events that occur when biomaterial is implanted *in vivo*. Adapted from [134]

As a result of the injury to the blood vessels, circulating blood platelets are exposed to proteins such as collagen in the basal lamina and extracellular matrix underneath the endothelium, which triggers platelet aggregation to form a platelet clot via the intrinsic coagulation pathway[137]. The damaged endothelium and the platelet clot provide the phospholipid surface on which prothrombin is converted to thrombin by tissue factor (thromboplastin)[12]. Fibrinogen is hydrolyzed to a dense fibrin network by thrombin which also activates fibrin stabilizing factor (factor XIII) to catalyze the formation of crosslinks within the deposited fibrin network[134]. The fibrin network forms a clot, which traps the blood cells and eventually seals off the damaged area of the endothelium to stop bleeding [12]. The coagulation enables platelets to disintegrate and shed their contents, among which are several inflammatory mediators such as VEGF, interleukin -8 (IL-8), transforming growth factor (TGF), platelet factor (PF4), interleukin – 1 (IL-1) and tissue necrosis factor (TNF-α) which recruits inflammatory cells to the site of implantation[134]. The fibrin clot formed at the tissue/polymer interface serves as a sticky provisional matrix that functions as a scaffold on which the recruited neutrophils, monocytes and macrophages interact via surface receptors[136, 138].

The adsorption of fibrinogen, complement, antibodies and other plasma proteins on the implanted biomaterial further activates the inflammatory process that was initiated by tissue damage. The adsorption of complement protein C3b on the implanted material can activate the alternate complement pathway while the specific binding of antibodies on the implanted material can activate the classical complement pathway[134]. The Fc domain of the bound antibodies is recognized by the C1q complement factor which induces the deposition of C3b on the implanted material[134]. The infiltrated phagocytes can recognize the adsorbed C3b through binding to the CR1 receptor[134]. The binding of complement factor Bb to C3b forms C3 convertase C3bBb, which splices C3 molecules to C3a and C3b to initiate the opsonisation process[134]. The opsonization initiates the release of C5a which contributes to leukocyte infiltration to the implantation site[134]. Both C3a and C5a increase the permeability of the vascular bed to induce the release

of histamine and interleukin -13 (IL-13) by mast cells in the surrounding tissues which further mediates the recruitment of phagocytic cells, including macrophages, to the site of implantation[138].[134]. Fibrinogen can adsorb onto the polymer surface and change its conformation to expose its P1 fragments, which are recognized by the phagocyte integrin complement receptor 3 (CR3), thereby activating the adhesion of tissue phagocytes to the implant [134, 135, 139, 140, 140].

The acute inflammation phase usually lasts for less than one week depending on the extent of injury, site of injury, protein adsorption on the implant and extent of provisional matrix formation[136]. This phase is characterized by the presence of neutrophils (polymorphonuclear leukocytes, PMNs), which contain a nucleus divided into 2 to 5 lobes [136]. Neutrophils are the first set of phagocytic cells to migrate toward the site of inflammation or infection, and they are attracted to the implant site by the secretion of transforming growth factor (TGF-β), platelet factor (PF4), interleukin – 1 (IL-1) and tissue necrosis factor (TNF-α) by platelets [137]. Neutrophils produce lysosomal agents and oxygen free radicals to kill any bacteria around the site of implantation [137].

The chronic inflammation phase follows the acute inflammation phase, and can extend for 2 to 3 weeks in the presence of a biocompatible biomaterial. This phase is characterized by the presence of monocytes, fibroblasts, lymphocytes, macrophages and foreign body giant cells at the tissue-implant interface [136]. These inflammatory cells are attracted to the tissue-polymer interface by the secretion of more chemoattractants such as platelet derived growth factor (PDGF), leukotriene (LTB4), monocyte chemoattractant protein (MCP-1) and interleukin 8 (IL-8) secreted by the platelets. These are in addition to chemoattractants already secreted during the acute inflammation stage, which direct the migration of macrophages to the wound site [134, 136, 137]. Interferon-gamma (IFN-γ) secreted by fibroblasts cells and IL-3 secreted by mast cells initiate the differentiation of monocytes to macrophages [136, 137, 141].

The assembled macrophages at the site of implantation further secrete chemokines and cytokines such as PDGF, tissue necrosis factor (TNF-α), interleukin 6 (IL-6), granulocyte-colony stimulating factor (G-CSF) and granulocyte macrophage-colony stimulating factor (GM-CSF), attracting more macrophages and fibroblasts to the site of implantation [134, 135]. The secreted chemokines such as of IL-1 and TNF-α activate macrophages to synthesize nitric oxide which kills pathogens and prevents further infection. Macrophages phagocytose foreign and debris material; however, due to the large size of the implanted material, macrophages undergo "frustrated phagocytosis" and fuse together to form larger foreign body giant cells (FBGCs) composed of a few dozen of individual macrophages under the influence of secreted cytokines such as interleukin-4 (IL-4) [134, 135]. The formed giant cells secrete degradative agents such as superoxides and free radicals, causing localized damage to implants and other foreign bodies [134, 135].

The secreted cytokines in the acute and chronic inflammatory phase initiate the formation of granulation tissue, which is characterized by the presence of macrophages and their derivatives, foreign body giant cells, myofibroblasts, endothelial cells, provisional extracellular matrix, fibroblasts with evidence of vascularization [135, 136]. Furthermore, the lysosomal agents and the chemical mediators secreted during the acute and chronic inflammation process activate and trigger the up-regulation of growth factors such as VEGF by fibroblasts and endothelial cells to initiate the formation of new blood vessels. When TGF-β is produced in abundance, it stimulates the extensive production of collagen I, and III, fibronectin, and proteoglycans around the implant by fibroblast like cells (myofibroblasts) and inhibits the production of matrix-degrading proteases, and subsequently activates the formation of fibrotic scar tissue around the implant [134, 136]. The thickness of the capsule formed would influence the kinetics of growth factor release from the polymer to the ischemic tissue as the released growth factors need to diffuse through the formed collagenous layer to initiate a biological function near the device [140]. The presence of macrophages and FBGCs with the components of the granulation tissue is called foreign body reaction (FBR). If the polymer becomes a source of irritation to the surrounding tissue due to the release of degradation products or leachables from the polymer [142, 143], macrophages and FBGCs will persist in an attempt to phagocytose

the polymer's degradation products by attracting more macrophages and forming more FBGCs at the implant site. As a result, the foreign body reaction may persist until the polymer fully degrades and the degradation products are removed from the body [135, 136].

The resolution of the foreign body reaction occurs when the polymer fully degrades. During this phase, low levels of TNFα-1β and TGF-β are produced by macrophages. TGF-β plays an anti-inflammatory role, by inhibiting the production and secretion of C-C chemokine ligand-2 (CCL2) and C-C chemokine ligand-3 (CCL3) by macrophages, which eventually halts the influx of phagocytic cells and most of the macrophages migrate towards the draining lymph nodes[134]. TGF-β initiates the differentiation of fibroblast-like cells to myofibroblast cells which are critical to wound healing and they actuate the shrinking of fibrotic tissue around the implant[134]. TNFα-1β and TGF-β stimulate fibroblast cells to produce collagenase that degrade the extracellular matrix and help to rearrange and re-organize a structured extracellular matrix, thus initiating repair [134].

Chapter 3

PROPOSAL AND OBJECTIVES

3.1 Proposal

Any controlled release device for treating critical limb ischemia should be easily introduced to the affected site, deliver an effective local dose of applicable growth factors in their bioactive form, with a minimal burst effect, at a sustained rate, and with little biodistribution outside the ischemic region[33, 46]. To overcome the issue of denaturation of growth factors during device fabrication and release [46, 59, 110, 144], osmotic delivery of VEGF and/or HGF from a viscous liquid, biodegradable polymer vehicle was proposed. Low molecular weight polymers based on 5-ethylene ketal ε-caprolactone were proposed as the delivery vehicle, within which growth factors would be incorporated as a lyophilized powder by simple mixing.

The rationale for this approach was as follows. 5-ethylene ketal ε-caprolactone was chosen because its homopolymer has a T_g of -35°C to -14°C [145] depending on its molecular weight, and it is amorphous. The low T_g and lack of crystallinity indicates that low molecular weight polymers prepared from this monomer would have a low viscosity and thus would be easily injected into the afflicted tissue at body temperature. Other advantages of the polymer being amorphous are that incomplete release as a result of polymer crystallinity and latter term inflammation caused by exposing polymer crystals to tissue would be avoided [143, 146, 147]. Moreover, this polymer undergoes hydrolytic degradation *in vivo*; removing the need for device explantation after the growth factor is released. 5-ethylene ketal ε-caprolactone can be readily copolymerized with other cyclic lactone monomers [148], therefore there was the possibility of adjusting the physical properties of the polymer to obtain a favorable release profile and polymer degradation rate by copolymerization with monomers such as D,L-lactide (DLLA). The osmotic release mechanism can provide a zero order release profile with no initial burst for a minimum period of two

weeks[31, 129], and the possibility of complete release of incorporated acid sensitive protein drugs before ester hydrolysis of the polymer begins.

VEGF was chosen because it promotes the initial stages of angiogenesis by stimulating the proliferation and migration of endothelial cells, which is an essential rate limiting step in physiological angiogenesis [40, 42, 61, 64]. HGF stimulates endothelial cells to proliferate and migrate and induces blood vessel formation *in vivo* in a dose dependent manner [42, 52, 65]. HGF also induces the production of VEGF by human keratinocytes [49, 50]and endothelial cells [50]and acts as a chemoattractant for pericytes [51]. The combination of VEGF and HGF has been shown to produce a synergistic effect on endothelial cell proliferation and migration, and pericyte recruitment, leading to the formation of stable blood vessels [42, 52, 66]. This delivery strategy would provide a minimally invasive means of delivering VEGF and HGF for the purpose of initiating the formation of stable and functional blood vessels for treating critical limb ischemia.

3.2 Objectives

The main objective of this work was to determine the feasibility of an injectable polymeric delivery device made from low viscosity poly(5-ethylene ketal ε-caprolactone) or its copolymer with DLLA for localized and sustained delivery of bioactive VEGF and HGF to treat critical limb ischemia.

The specific objectives were:

1. To develop and characterize an injectable delivery vehicle made from 5-ethylene ketal ε-caprolactone and its copolymer with DLLA.

2. To explore the potential of an injectable delivery vehicle consisting of low molecular weight poly(5-ethylene ketal ε-caprolactone) (PEKC) or its copolymer with DLLA for the delivery of proteins using an osmotic pressure mechanism.

3. To more clearly explain the mechanism of osmotic release of proteins from viscous liquid polymers, and in particular, the means by which the dissolved solute is transported through the polymer phase.

4. To investigate the *in vivo* biodegradation rate and tissue response to subcutaneously injected octan-1-ol initiated poly(5-ethylene ketal ε-caprolactone-co-D,L-lactide) (OCT-PEKCDLLA) in rats.

5. To investigate the ability of low molecular weight, OCT-PEKCDLLA to serve as a single, or dual, delivery system for the release of VEGF and/or HGF in a sustained manner and in their active form for a period of 4 to 6 weeks utilizing the osmotic pressure release mechanism.

Chapter 4

SURFACE ERODING LIQUID INJECTABLE POLYMERS BASED ON 5-ETHYLENE KETAL ε-CAPROLACTONE

Manuscript published in Biomacromolecules. October 2011

Iyabo Oladunni Babasola and Brian G. Amsden [†]

Department of Chemical Engineering, Queen's University, Kingston, ON, Canada

[†]Human Mobility Research Centre, Kingston General Hospital, Kingston, ON, Canada

This chapter relates to the first specific objective of this thesis, which is to develop and characterize an injectable delivery vehicle made from 5-ethylene ketal ε-caprolactone and its copolymer with D,L lactide (DLLA). The polymers were made by ring opening polymerization, initiated with hydrophobic (octan-1-ol) or hydrophilic methoxy poly (ethylene glycol) (MPEG) initiator, using stannous octanoate as co-initiator/catalyst. This paper describes the polymerization and the effect of the initiator used in the ring opening polymerization on viscosity, glass transition temperature and *in vitro* biodegradation rate. The *in vitro* cytotoxicity of the monomer's degradation product to 3T3 fibroblast cells was also investigated.

Abstract

Liquid, injectable hydrophobic polymers are potentially useful as depot systems for localized drug delivery. Low molecular weight polymers of 5-ethylene ketal ***ε***-caprolactone and copolymers of this monomer with D,L-lactide were prepared and their properties assessed with respect to their suitability for this purpose. The polymers were amorphous, of low viscosity, and the viscosity was adjustable by choice of initiator and/or by copolymerizing with D,L-lactide. Lower viscosity polymers were attained by using 350 Da methoxy poly(ethylene glycol) as an initiator in comparison to octan-1-ol, while copolymerization with D,L-lactide increased viscosity. The initiator used had no significant effect on the rate of mass loss *in vitro* and copolymers with D,L-lactide (DLLA) degraded faster than 5-ethylene ketal ε-caprolactone (EKC) homopolymers. For the EKC based polymers, a nearly constant degradation rate was observed. This finding was attributed to the hydrolytic susceptibility of the EKC-EKC ester linkage, which was comparable to that of DLLA-DLLA, coupled with a higher molecular weight of the water-soluble degradation product and the low initial molecular weight of the EKC based polymers. Cytotoxicity of the hydrolyzed EKC monomer to 3T3 fibroblast cells was comparable to that of ε-caprolactone, suggesting that polymers prepared from EKC may be well tolerated upon *in vivo* implantation.

4.0. Introduction

Recent biotechnology and drug developments have resulted in an increased demand for loco-regional administration combined with sustained and controlled release of therapeutic proteins in the treatment of conditions such as ischemia and cancer[149, 149-151]. To meet these demands, a number of different polymer formulations have been investigated that can be injected directly into the required site without the need for surgical implantation and retrieval and once injected, form a depot. One approach to achieving this aim is to utilize low molecular weight, biodegradable polymers that possess melting points below body temperature. A number of polymers have been explored for this purpose, including poly(ortho esters),[132, 152-155] low molecular weight poly(α-hydroxy acids),[156-158] hexyl-substituted poly(lactide),[159] poly(trimethylene carbonate)[160] and branched, ester linked, fatty acid polymers from the reaction of glyceryl monolinoleate with succinic anhydride[161, 162].

This formulation approach is advantageous as it allows facile incorporation of thermally sensitive drugs such as proteins and peptides by simple mixing, and injectability through standard gauge needles and thus administration via minimally invasive means. In addition, there is no need for device retrieval and there is restricted water penetration, which may provide enhanced stability for drugs such as proteins incorporated as solid particles[30]. Moreover, the viscosity and thus the injectability of the polymers can be controlled by appropriate selection of monomers and initiator[163, 164].

In this work, the development of a new polymer for use as an injectable delivery vehicle, made from low viscosity poly(5-ethylene ketal ε-caprolactone) (PEKC) or its copolymer with D,L-lactide (DLLA), is presented. PEKC was chosen because it is amorphous and has a low glass transition temperature (-35ºC at molecular weight of 2600 Da[165]). The low glass transition temperature ensures that the polymer will have a low viscosity and be easy to inject, and the lack of crystallinity will not impede degradation [147] and may prevent latter term inflammation caused by exposing polymer crystals to tissue[142,

[143]. Moreover, it was reasoned that the hydrophillic pendant ketal group would confer enhanced hydrophilicity to the polymer, modifying its hydrolytic degradation. The polymerization kinetics, physical characteristics, and *in vitro* degradation rates of these polymers were measured and are discussed in terms of the intended application as an injectable drug delivery vehicle. The polymers were synthesized by ring-opening polymerization initiated with either octan-1-ol or 350 Da methoxy poly(ethylene glycol) and copolymerized with D,L-lactide to control the viscosity, glass transition temperature, biodegradability and overall hydrophobicity. The cytotoxicity of the EKC monomer degradation products to 3T3 fibroblast cells was also assessed and compared to those of ε-caprolactone.

4.1 Materials

Unless stated otherwise, all materials were used as received from the manufacturer. 1,4-cyclohexanedione monoethylene ketal (97% purity), meta-chloroperoxybenzoic acid (MCPBA), octan-1-ol (anhydrous, purity 99%), dichloromethane (CH_2Cl_2), hexane, methanol, tetrahydrofuran (THF), ethyl acetate (EtOAc), stannous 2-ethylhexanoate (95% purity), Dulbecco's phosphate buffered saline (PBS), magnesium sulphate ($MgSO_4$), sodium bicarbonate, methoxy poly(ethylene glycol) with an average molecular weight of 350 Da (MPEG 350) and chloroform-d ($CDCl_3$) were obtained from Sigma-Aldrich, ON, Canada. Dimethyl sulfoxide-d6 (DMSO-d6, 99% purity), was obtained from Cambridge Isotope Laboratories Inc., MA, USA, D,L-lactide was obtained from Purac, the Netherlands and purified by recrystallization from dried toluene and WST-1 reagent was obtained from Roche Canada.

4.2 Methods

4.2.1 Synthesis of 5-ethylene ketal ε-caprolactone

The 5-ethylene ketal ε-caprolactone monomer was prepared by the Baeyer-Villiger oxidation of 1, 4-cyclohexanedione monoethylene ketal by meta-chloroperoxybenzoic acid (MCPBA), as described by Tian and co-workers[166] with some modifications. In a representative procedure, 50 g of MCPBA was

dissolved in 400 mL of CH_2Cl_2 and about 15 g of $MgSO_4$ and 7.5 g of sodium bicarbonate were added. This mixture was stirred until all the MCPBA had dissolved. After which, 25 g of 1,4-cyclohexanedione monoethylene ketal were dissolved in 50 mL of CH_2Cl_2, added drop-wise into the dissolved MCPBA and left to stir overnight. The stirred solution was chilled to -20ºC for 1-2 h and filtered to eliminate $MgSO_4$ and 3-chlorobenzoic acid. The solvent was evaporated and the resulting product purified by silica gel column chromatography using 5%, 10%, 15%, 20%, 25%, 30% and 35% EtOAc/hexane gradient as eluent. Following solvent removal, the final product was analysed via ^{1}H-NMR in $CDCl_3$ for composition and purity on a Bruker Avance 400 MHz spectrometer.

4.2.2 Polymer Synthesis

PEKC and its copolymer with DLLA (PEKCDLLA) were prepared through ring-opening polymerization at 110ºC for 24 hours. The reaction was catalyzed by stannous 2-ethylhexanoate and initiated by octan-1-ol (OCT-PEKC, OCT-PEKCDLLA) or MPEG 350 (PEG-PEKC, PEG-PEKCDLLA) in a vacuum-sealed glass ampoule under argon. The catalyst to initiator ratio was 3×10^{-3}:1. The monomers and initiator were added into a flame-dried glass ampoule, the required amount of stannous 2-ethylhexanoate dissolved in toluene was added, and the mixture was vortexed, purged with dry nitrogen gas for 5 minutes and placed under vacuum before heat sealing and transferring to pre-heated oil at 110ºC for 24 hours. The resulting polymers were dissolved in CH_2Cl_2 and precipitated sequentially in hexane and methanol cooled using dry ice. The molar ratio of EKC to DLLA in PEKCDLLA was designed to be 3:1 to obtain a polymer with a low glass transition temperature. For comparison, polymers of similar molecular weight were also prepared from ε-caprolactone copolymerized with DLLA and initiated with octan-1-ol (OCT-PCLDLLA) or MPEG 350 (PEG-PCLDLLA). Polymer yields ranged from 70 to 80%.

4.2.3 Polymer Characterization

To confirm the structure and purity of the polymers and to provide preliminary measurements of number average molecular weight, ^{1}H-NMR spectra of the polymers and co-polymers were recorded in

DMSO-d6 at 400 MHz. The resulting peaks were compared to the solvent peaks relative to tetramethylsilane as reference. The polymer number average molecular weights were calculated by end group analysis from the signal intensity of the methyl group of octan-1-ol at $\delta = 0.85$ ppm and MPEG 350 at $\delta = 3.23$ ppm, and the methylene group at $\delta = 2.3$ ppm for EKC and methine group at $\delta = 5.1$ ppm for DLLA. The number average molecular weight (M_n), the weight average molecular weight (M_w) and polydispersity index (PDI) were measured using a gel permeation chromatography (GPC) system consisting of a Waters 2960 separation module equipped with four Styragel HR columns (HR4.0, HR3.0, HR1.0, HR0.5 packed with 5 µm particles) in series. This was coupled with a Waters 410 differential refractometer detector and a Wyatt Technology DAWN EOS photometer multi-angle light scattering (LS) detector. Samples were prepared in anhydrous THF at concentrations of 30 mg/mL. The samples were filtered with a 0.45 µm syringe and 100 µL were injected into a column at 1.0 mL/min and 40ºC. The data were processed using Astra (version 4.90.08) software. The increments of refractive index (dn/dc) used in the molecular weight calculations were determined using a Wyatt Optilab rEX. For this purpose, samples were prepared in anhydrous THF at concentrations ranging from 3 mg/mL - 22 mg/mL.

The thermal properties of the polymers were measured with a DSC 1 STARe system (Mettler Toledo). The samples were run at a heating and cooling rate of 10 ºC/min using the following temperature program. The sample was first cooled from 25ºC to -90ºC and held for 3 minutes at that temperature. This cycle was followed by heating from -90ºC to 105ºC with a hold time of 3 minutes at 105ºC. It was further cooled from 105ºC to -90ºC with a hold time of 3 minutes at -90ºC. Finally, the sample was heated from -90ºC to 105ºC. The glass transition temperature (T_g) was obtained from the inflection point of the second heating cycle. The zero shear viscosity (η) of the polymers at temperatures ranging from 25ºC to 50ºC was measured using a TA Instruments AR 2000 rheometer ((TA Instruments, New Castle, DE). A parallel plate apparatus with cone stainless steel (0.5 DEG) attachment and 40 mm diameter was used in the steady-shear mode.

4.2.4 Polymer Degradation

In vitro degradation of the polymers was studied using about 150 mg of the polymer in 1 mL of 0.1M pH 7.4 phosphate buffer saline (PBS) at a temperature of 37ºC for 24 weeks without any agitation[147]. The buffer was replaced weekly and samples were washed with distilled water to remove residual salt and dried to a constant weight in an oven at 50ºC. Samples were assessed at each time point for weight loss, changes in molecular weight, composition and glass transition temperature. The glass transition temperatures of both the first and second heating cycle were reported. The changes in molecular weight were determined using GPC as described above.

4.2.5 Assessment of Monomer Cytotoxicity

Cytotoxicity of the EKC monomer was assessed towards 3T3 fibroblasts (CCL 92)[167]. 20 mg of monomer were degraded in 2 mL of 8X Dulbecco's modified Eagle's medium (DMEM) pH 7.4 in an incubator maintained at 37ºC for 24 hours. The resulting solution was diluted 8 times with deionised water to make the solution isotonic and the pH adjusted to 7.4 with sodium hydroxide solution. This solution was diluted with DMEM and added to passage 7 3T3 fibroblasts at concentrations of 0 to 1.2 mg/ml. 100 µL of the DMEM + degradation products solution supplemented with 5% fetal calf serum (FCS) was added to each well of a 96 well plate (n = 4). After 24 hours of culturing the cells, 10µL of cell proliferation reagent (WST-1) was added and allowed to incubate for 4 hours. The mitochondria conversion of the cells to a yellow metabolite was determined by measuring the absorbance at 440 nm (n = 4). The cytotoxicity of ε-caprolactone monomer degraded in the same fashion was also measured as a control. The results are reported as a percent of cells remaining metabolically active as compared to controls that did not receive an aliquot of monomer degradation products.

4.2 Statistics

All polymer property measurements were done on triplicate samples and are reported as the average ± the standard deviation about the average. Pair-wise evaluations of significant difference were assessed using a Student t test with a p value of less than 0.05 considered significant.

4. 3 Results and Discussion

4.3.1 Synthesis of 5-ethylene ketal ε- caprolactone

5-ethylene ketal ε-caprolactone (3) (EKC) was synthesized by the Baeyer-Villiger oxidation of 1,4-cyclohexane monoethylene acetal (1) by meta-chloroperoxybenzoic acid (2) (Figure 4-1). The reaction was complete with an average recovery of 67 % after column separation. The structure of the monomer was confirmed using ^{1}H-NMR spectroscopy in $CDCl_3$ (Figure 4-2).

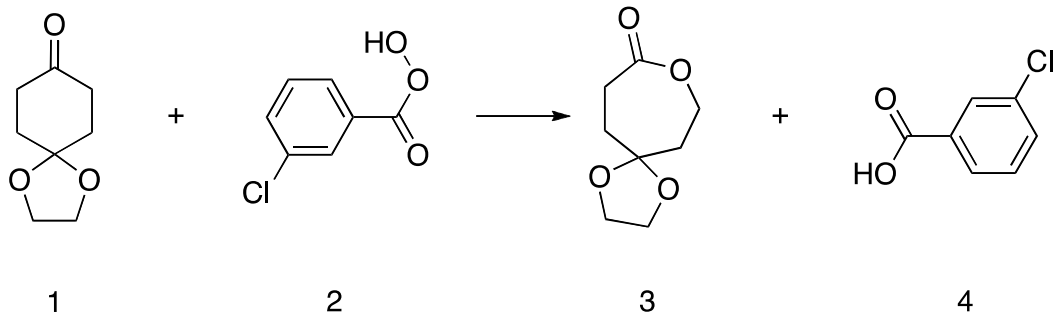

Figure 4-1: Synthesis pathway for the formation of 5-ethylene ketal ε-caprolactone (3) [166]**.**

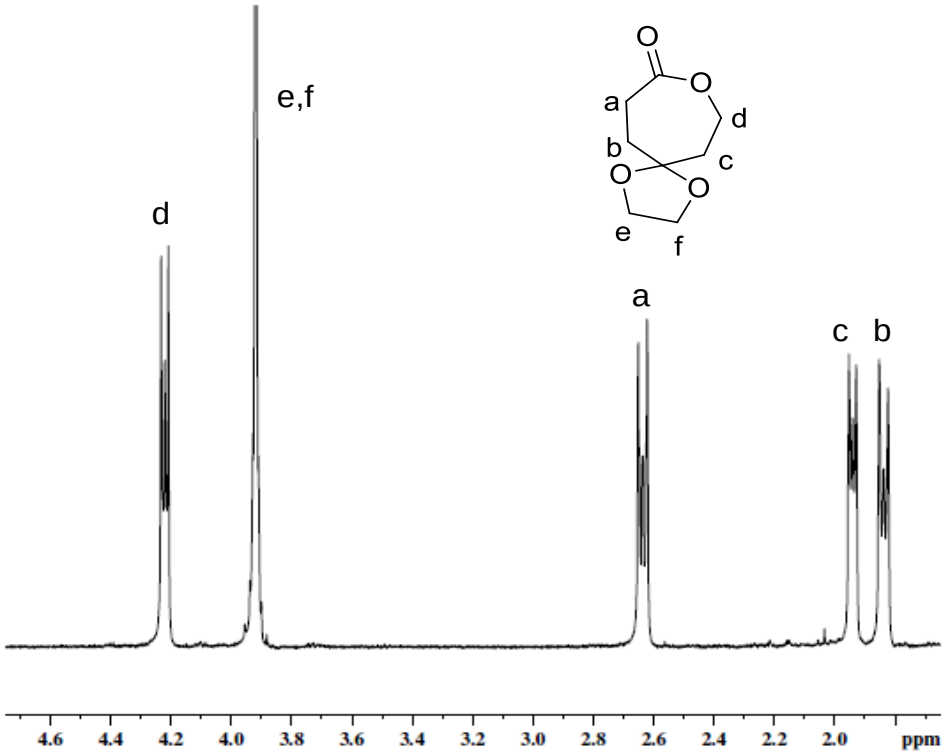

Figure 4-2: ^{1}H-NMR spectrum of 5-ethylene ketal ε-caprolactone obtained in $CDCl_3$.

4.3.2 Polymerization Kinetics

The kinetics of the homopolymerization and copolymerization with DLLA initiated with octan-1-ol was studied over 18 hours. Monomer conversion was determined using ^{1}H-NMR spectroscopy by following the intensity of the peak at 2.7 ppm associated with the EKC monomer and the same peak in the growing polymer at 2.35 ppm. For these experiments, a 0.5 g polymer batch size was used. Figure 4-3A shows the conversion of the EKC monomer with time during homopolymerization while Figure 4-3B shows the conversion of EKC and DLLA with time during copolymerization

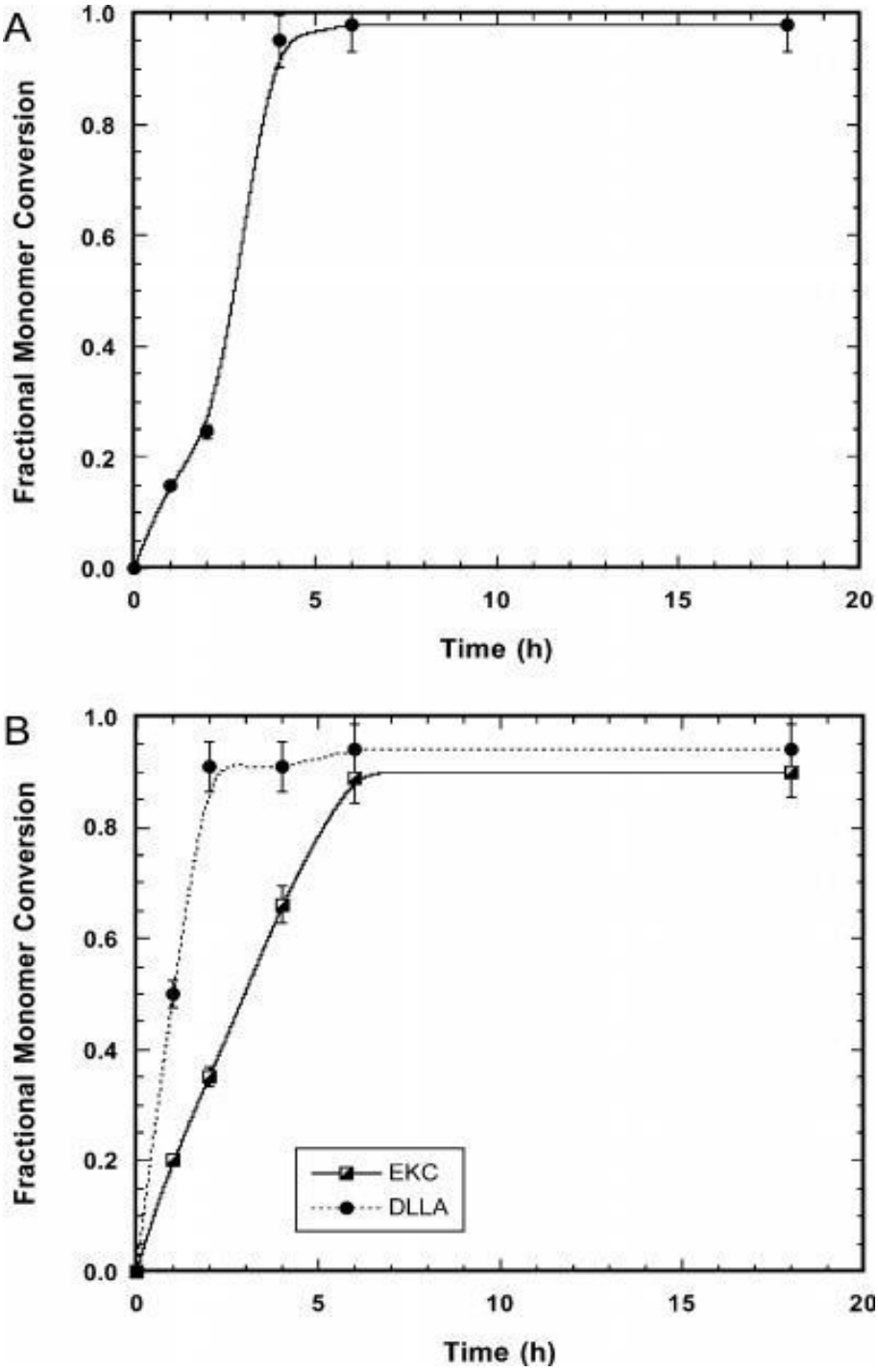

Figure 4-3: Monomer conversion during ring opening polymerization using octan-1-ol as initiator and stannous octanoate as catalyst at a temperature of 110ºC. (A) EKC in OCT-PEKC (B) EKC and DLLA in OCT-PEKCDLLA.

For PEKC initiated with octan-1-ol, monomer conversion is almost complete after about 6 hours under these conditions. For copolymers with DLLA initiated with octan-1-ol, the polymerization of the EKC reached about 90% completion at about 6 h while the DLLA reached about 95% completion. EKC polymerized more slowly in the presence of DLLA compared to its homopolymerization. This slower polymerization is attributed to the differences in monomer reactivity. DLLA has a higher reactivity compared to ε-caprolactone, [168] and ε-caprolactone and EKC have the same reactivity [148]. Thus, DLLA would be incorporated into the polymer at a faster rate compared to EKC. This difference in reactivity may lead to copolymers with blocky structures; however because of the small molar ratio of DLLA to EKC and the low molecular weight, the block lengths would be small.

A polymerization temperature of 110ºC was chosen because above this temperature the 5-ethylene ketal functional group was unstable and deacetylated to form a ketone pendant group. A ^{1}H-NMR spectrum of PEG-PEKCDLLA, obtained at a polymerization temperature of 120ºC for 24 hours, is provided in appendix A. The spectrum shows the appearance of peaks between δ= 2.7 and 2.9 ppm, corresponding to a ketone pendant group[166, 169, 170]. Pyrolysis of the polymer ester groups at 120ºC was also evident, in the form of carboxylic acid (δ = 12 ppm) and unsaturated (δ = 5.7 ppm, 5.9 ppm, 6.3 ppm) terminal groups. A similar pyrolysis mechanism has been reported for the thermal degradation of poly(2-oxepane-1,5-dione-ran-ε-caprolactone) in the presence of trace amounts of tin [169].

4.3.2 Polymer Characterization

Figure 4-4 shows the ^{1}H-NMR spectrum of OCT-PEKCDLLA as obtained in DMSO-d6. The spectrum confirmed the expected major peaks associated with the backbone polymer and the end groups.

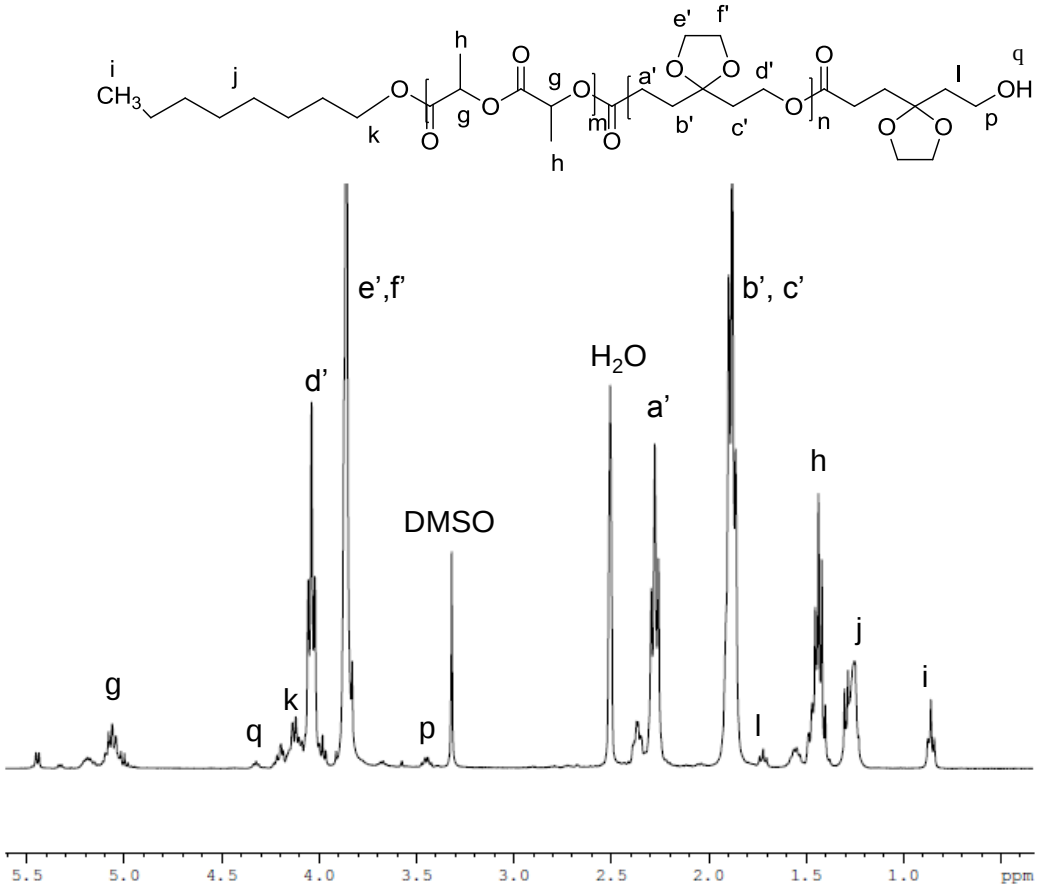

Figure 4-4: ^{1}H-NMR of octan-1-ol initiated poly(5-ethylene ketal ε-caprolactone-ran-D,L-lactide, obtained in DMSO-d6.

The number average molecular weight of the product polymers was calculated by end-group analysis using the ^{1}H-NMR spectra and the signal intensity of the methyl group from octan-1-ol at δ = 0.85 ppm and methyl group of MPEG 350 at δ = 3.2 ppm as the reference end group peaks, and the methylene group at δ = 2.3 ppm for EKC and the methine group of DLLA at δ = 5.1 ppm as the reference monomer peaks. The number average molecular weight was then calculated based on the number of each monomer in the resulting polymer, as calculated by the ratio of the reference monomer peak integration to the reference end group peak integration. This value of the number average molecular weight was then compared to that obtained via GPC measurement. Table 4-1 shows the monomer composition of the

polymers, their number average molecular weights as calculated via end-group analysis as well as by GPC, polydispersity index (PDI) obtained by GPC, and their glass transition temperature (T_g).

Table 4-1: Physical properties of the synthesized polymers.

Monomer feed ratio (EKC:DLLA (mol:mol))	Product monomer ratio (EKC:DLLA (mol:mol))	T_g (^oC)	M_n ^{1}H-NMR (Da)	M_n GPC (Da)	PDI	η_{37^oC} (Pa·s)	E (kJ/mol)
OCT-PEKC (12:0)	13.2:0	-30	2390	2680	1.30	26.3	75.9 ± 2.4
PEG-PEKC (12:0)	12.9:0	-36	2570	2420	1.53	17.5	69.2 ± 2.1
OCT-PEKCDLLA (9.9:3.3)	13.5:3.8	-21	3000	2700	1.32	106.1	92.8 ± 2.7
PEG-PEKCDLLA (9.9:3.3)	10.6:3.5	-24	2610	2330	1.42	40.1	84.9 ± 3.5
OCT-PCLDLLA (12:4)	13.5:4.0	-51	2200	2200	1.23	2.1	51.6 ± 1.1
PEG-PCLDLLA (12:4)	16.6:4.6	-53	2780	2970	1.33	3.0	49.4 ± 1.5

The increments of refractive index (dn/dc) values, used in calculating the molecular weight by GPC, are listed in Table 4-2. The M_n obtained from ^{1}H-NMR end group analysis and from GPC are in good agreement. However, the number average molecular weights of the polymer and the monomer ratios were higher than expected based on total monomer conversion and each initiator initiating a polymer

chain of equal length. This result is attributed to loss of low molecular weight polymer molecules during the purification procedure and incomplete monomer conversion.

Table 4-2: Increment of refractive index of the polymers in THF

Polymer	dn/dc (mL/g) 95% CI*
OCT-PEKC	0.0737 (0.001)
PEG-PEKC	0.0822 (0.001)
OCT-PEKCDLLA	0.0655 (0.003)
PEG-PEKCDLLA	0.0749 (0.003)
OCT-PCLDLLA	0.0682 (0.003)
PEG-PCLDLLA	0.0638 (0.004)

* CI = confidence interval

4.3.3 Polymer Viscosity & Thermal Properties

For the proposed application, an amorphous polymer with viscosity low enough to allow easy injection and high enough to provide control over drug release is required. Previous experience with low molecular weight poly(trimethylene carbonate), indicated that a viscosity of 10-100 Pa·s was desired to provide ready injection through standard gage needles while still producing a non-dispersible implant within the tissue[160]. Based on preliminary studies on the 37ºC viscosity of OCT-PEKC at different number average molecular weight (Figure 4-5), 2200 Da was chosen as a target number average molecular weight (M_n) for comparing the various polymers.

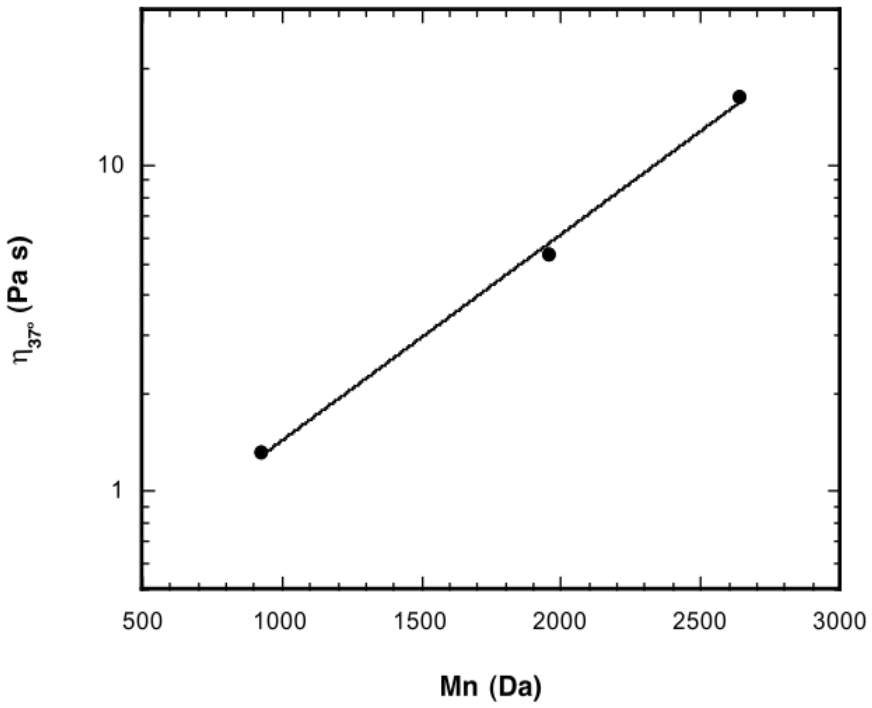

Figure 4-5: Viscosity measured at 37ºC of low molecular weight OCT-PEKC as a function of their number average molecular weight.

For the copolymers, an EKC to DLLA molar ratio of 3:1 was chosen as a compromise between the anticipated increases in polymer degradation rate versus the increase in viscosity by incorporating a monomer that would increase the glass transition temperature. All the EKC based polymers were amorphous at the molecular weights obtained. The T_g of OCT-PCLDLLA and PEG-PCLDLLA were the lowest of the polymers examined. This result can be attributed to the lower T_g of poly(ε-caprolactone) (-60ºC [171]) relative to PEKC (-35ºC to -14ºC[165]). The influence of the initiator used on the T_g of the resulting polymer is demonstrated by comparing OCT-PEKC to PEG-PEKC; the T_g of PEG-PEKC was - 36ºC compared to OCT-PEKC with similar number of EKC units, which was -30ºC. The lower T_g of the PEG-PEKC is due to the ether bonds in the PEG conferring greater polymer chain flexibility and thus a lower glass transition temperature than is provided by the alkane group in the octan-1-ol. The T_g of these homopolymers are consistent with the -35ºC value reported for PEKC initiated with aluminium isopropoxide in toluene at 25ºC with molecular weight of 2600 Da[165]. The homopolymers had a lower T_g

compared to the co-polymers with DLLA, regardless of the initiator used. This result is due to the higher T_g of DLLA, which is about 55ºC, depending on molecular weight [172].

The zero shear viscosities of the polymers were closely related to their glass transition temperature and all samples exhibited Newtonian flow behaviour. The viscosities ranged from 2.1 to 106.1 Pa·s at 37ºC (Table 4-1). The Newtonian flow behaviour indicated that the polymers have molecular weights low enough that the polymer chains in the melt are not extensively entangled. For polymers and liquids at temperatures above their T_g, the zero shear viscosity η, is related to temperature by the following Arrhenius-type equation [173].

$$\ln \eta = \ln \eta_r + \frac{E}{RT} - \frac{E}{RT_r} = k + \frac{E}{RT} \qquad (1)$$

In Eq (1) η_r is the zero shear viscosity at reference temperature T_r, E is the activation energy required for flow, R is the gas constant, and k is a constant. By fitting Eq (1) to the viscosity data plotted *vs*. T^{-1} (Figure 4-6), the slope of each curve (E/R) was obtained from which the activation energy was calculated.

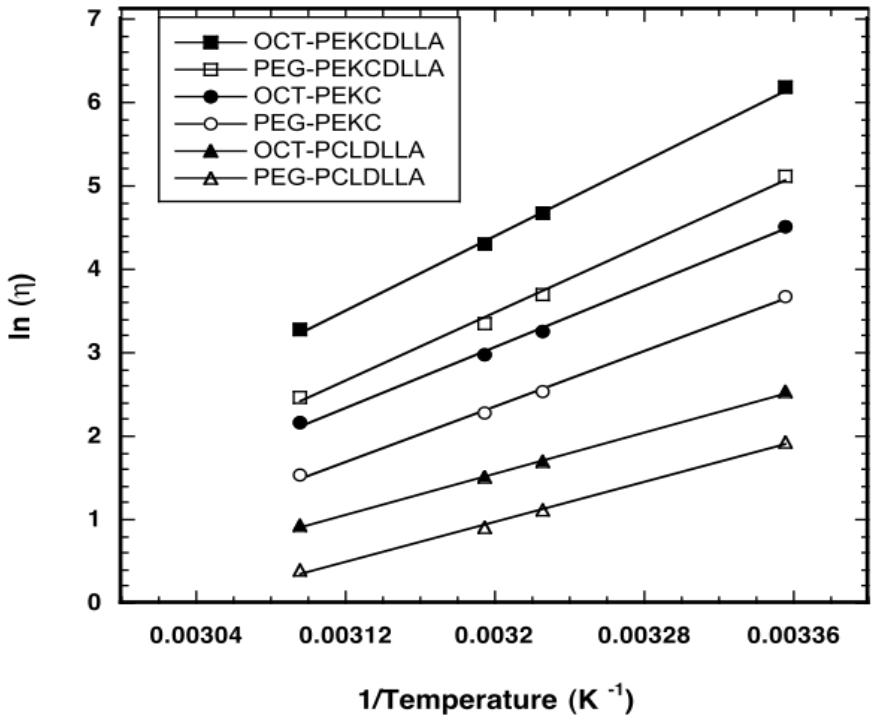

Figure 4-6: Viscosity temperature dependence. The solid lines represent fits of the Arrhenius expression (Eq (1)) to the data.

These activation energy values are listed in Table 4-1. The activation energy required for flow is influenced by the same properties as the glass transition temperature, and increases as polymer chain flexibility decreases.

4.3.4 *In Vitro* Degradation

As aliphatic polyesters, these polymers undergo hydrolysis in aqueous media. *In vitro* degradation of the polymers was done at a pH of 7.4 and temperature of 37ºC to gain an understanding of the influence of the hydrophilicity of the initiator used (MPEG versus octan-1-ol), and the influence of copolymerization with DLLA, on the rate of hydrolysis. The results would also give insight into how long the polymer would remain at the injection site after the drug has been delivered. Changes in sample weight, average molecular weight, composition and T_g with time were studied over 24 weeks.

The change in sample weight was determined by comparing the weight of the dry polymer at each time point to the weight of the dry polymer before degradation. Initially yellow and clear, the layer of the polymer directly in contact with water became opaque in the buffer due to water absorption (Appendix B). The weight loss with time of the EKC based polymers is given in Figure 4-7A while that of CL based polymers is given in Figure 4-7B.

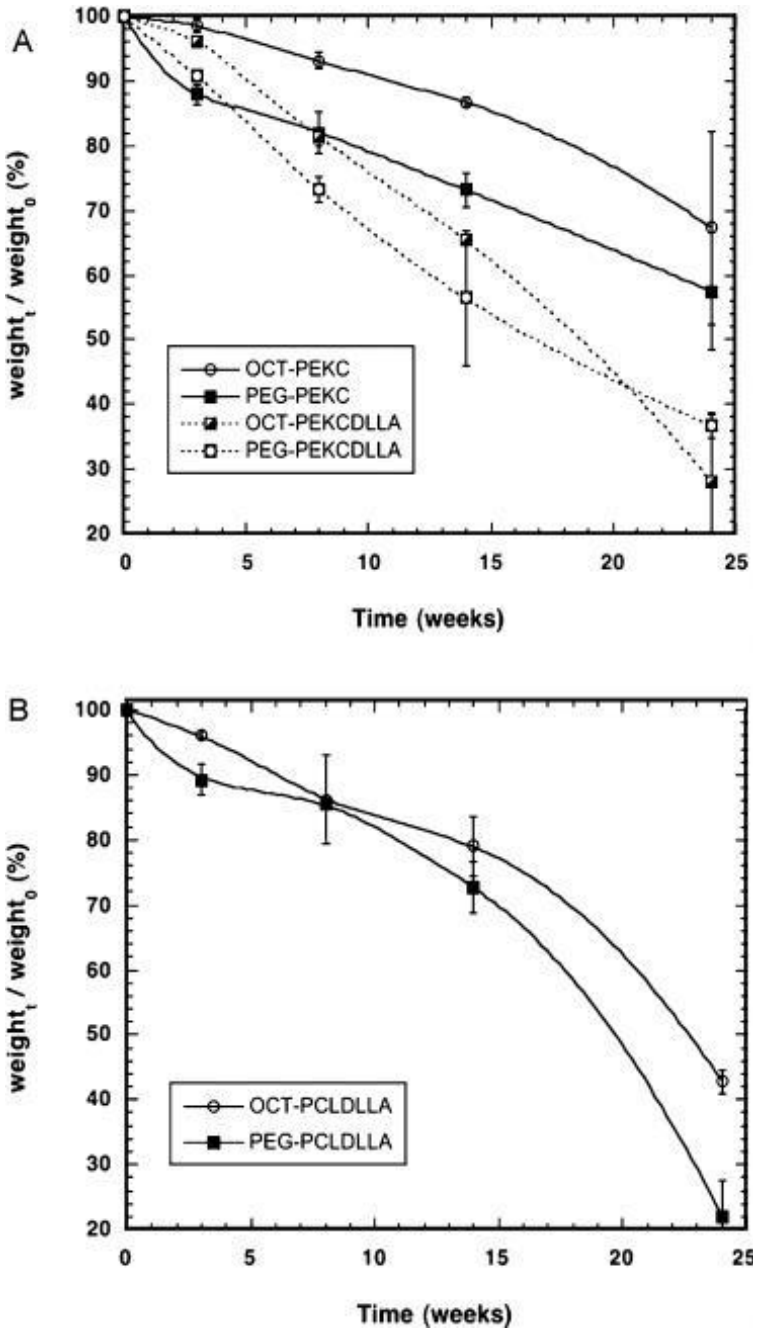

Figure 4-7: Weight loss of the polymers during in vitro degradation in pH 7.4 PBS at 37ºC (A) influence of initiator and incorporation of DLLA for EKC containing polymers, and (B) comparative degradation of copolymers of CL with DLLA initiated with octan-1-ol and PEG.

The EKC homopolymer initiated with MPEG 350 initially lost weight faster than the homopolymer initiated with octan-1-ol; however, after 3 weeks there was no significant difference in the rate of weight loss of the homopolymers, but the weight loss of the PEG-initiated polymers was greater

than those of the octan-1-ol initiated polymers as a result of the greater initial weight loss. Similarly, there was no significant difference in the degradation rate of the EKCDLLA copolymers with respect to the initiator used. Thus, the hydrophilicity of the initiator had no significant effect on the rate of polymer hydrolysis after 3 weeks. The initial weight loss of the MPEG-initiated polymers could not be attributed to the presence of unreacted MPEG in the polymer, as the absence of unreacted MPEG and monomer in the purified polymers was confirmed via ^{1}H-NMR (Appendix C). The ^{1}H-NMR spectrum confirmed the absence of the OH peak associated with unreacted MPEG 350 at $\delta = 4.55$ ppm and the proton peak (H_a) at $\delta = 2.7$ ppm associated with the EKC monomer.

As anticipated, incorporation of DLLA resulted in an increase in degradation rate of the copolymers over that of the EKC homopolymers (Figure 4-7A). For all EKC polymers and copolymers, after the first 3 weeks the degradation rate was nearly constant, while for CL based copolymers weight loss was slower initially, but increased noticeably between 14 and 24 weeks (Figure 4-7B). This latter degradation profile is characteristic of bulk erosion [174]. Moreover, the EKC based copolymers degraded at a faster rate than the CL based copolymers. For example, by 14 weeks, PEG-PEKCDLLA had lost 43.6 ± 10.4 % of its initial mass whereas PEG-PCLDLLA had lost 27.3 ± 3.9 %. Analysis of the ^{1}H-NMR spectra of the degraded PEG-PCLDLLA and PEG-PEKCDLLA showed that there was significant cleavage of the ester bond between PEG and the aliphatic polyester as indicated by a significant reduction of the peak at $\delta = 3.23$ ppm, assigned to the CH_3 end group of the MPEG, with time (Appendix D and E). As a result, the molecular weight change with degradation time could only be reliably determined by GPC and not end group analysis.

As shown in Figure 4-8, the number average molecular weight of the EKC based homopolymer and copolymer initiated with octan-1-ol did not change significantly over the 24-week period. For the PEG initiated EKC homopolymer and EKCDLLA copolymer, the molecular weight increased slightly over the first 3 weeks due to the loss of the low molecular weight polymer fraction, then stayed relatively

constant, except for PEG-PEKCDLLA; by 24 weeks, the molecular weight of PEG-PEKCDLLA had decreased slightly. This loss in molecular weight was primarily a result of the hydrolysis of the ester bond associated with the PEG portion of the polymer. The molecular weight of the OCT-PCLDLLA and PEG-PCLDLLA polymers did not change over the first 8 weeks; however at 14 weeks and afterwards, there was a significant decrease in molecular weight, which was more notable for PEG-PCLDLLA. By 24 weeks the molecular weight of PEG-PCLDLLA was too low to be reliably measured.

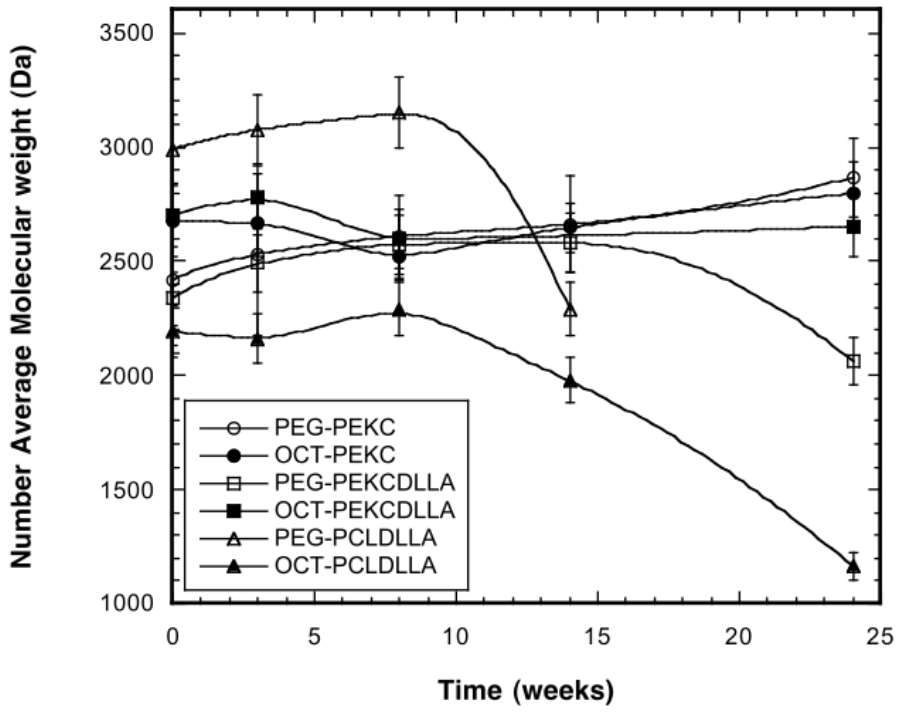

Figure 4-8: Number average molecular weight change of the polymers during *in vitro* degradation as measured using GPC.

To gain insight into the difference in rate of weight loss between the EKC and the CL based copolymers, the ratios of EKC to DLLA and CL to DLLA in the degrading copolymers were measured at each time point. The ratio of the monomers in the degraded polymers was determined using ^{1}H-NMR by comparing the signal intensity at δ= 2.3 ppm for EKC and CL and 5.1 ppm for DLLA. The result is

shown in Figure 4-9. For the EKCDLLA copolymers, the ratio of EKC to DLLA remained the same over the 24-weeks period, whereas for the CLDLLA copolymers, the ratio of CL to DLLA remained the same for 14 weeks, after which the ratio became significantly greater. These results indicate that the EKC-EKC and EKC-DLLA ester bonds are as likely to undergo hydrolysis as the DLLA-DLLA bonds, whereas CL-CL bond cleavage is less likely to occur than DLLA-DLLA cleavage.

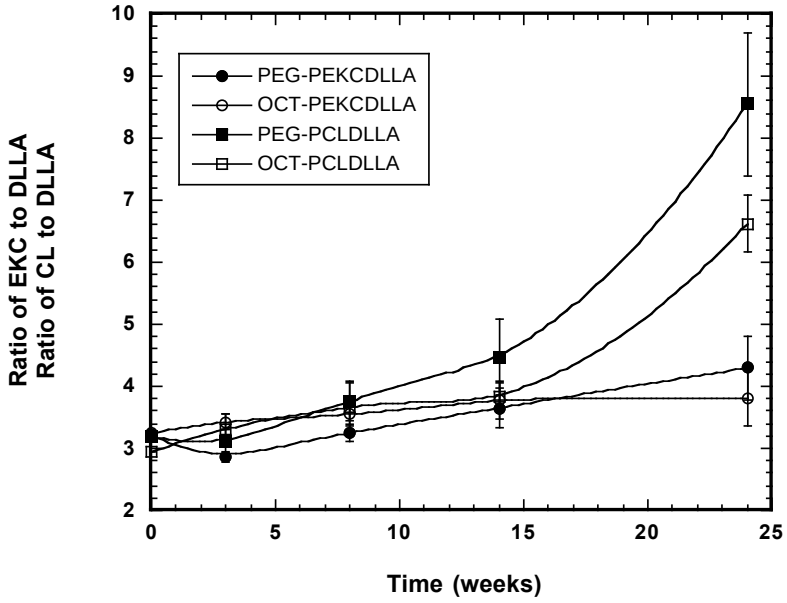

Figure 4-9: Change in monomer ratio of CL or EKC to DLLA during *in vitro* degradation.

Following buffer removal and drying with a flow of air to remove surface water, the white, opaque polymer layers in contact with the buffer solution were separated and their thermal characteristics measured. Representative thermograms are given in Figure 4-10A for the EKC containing polymers at week 3.

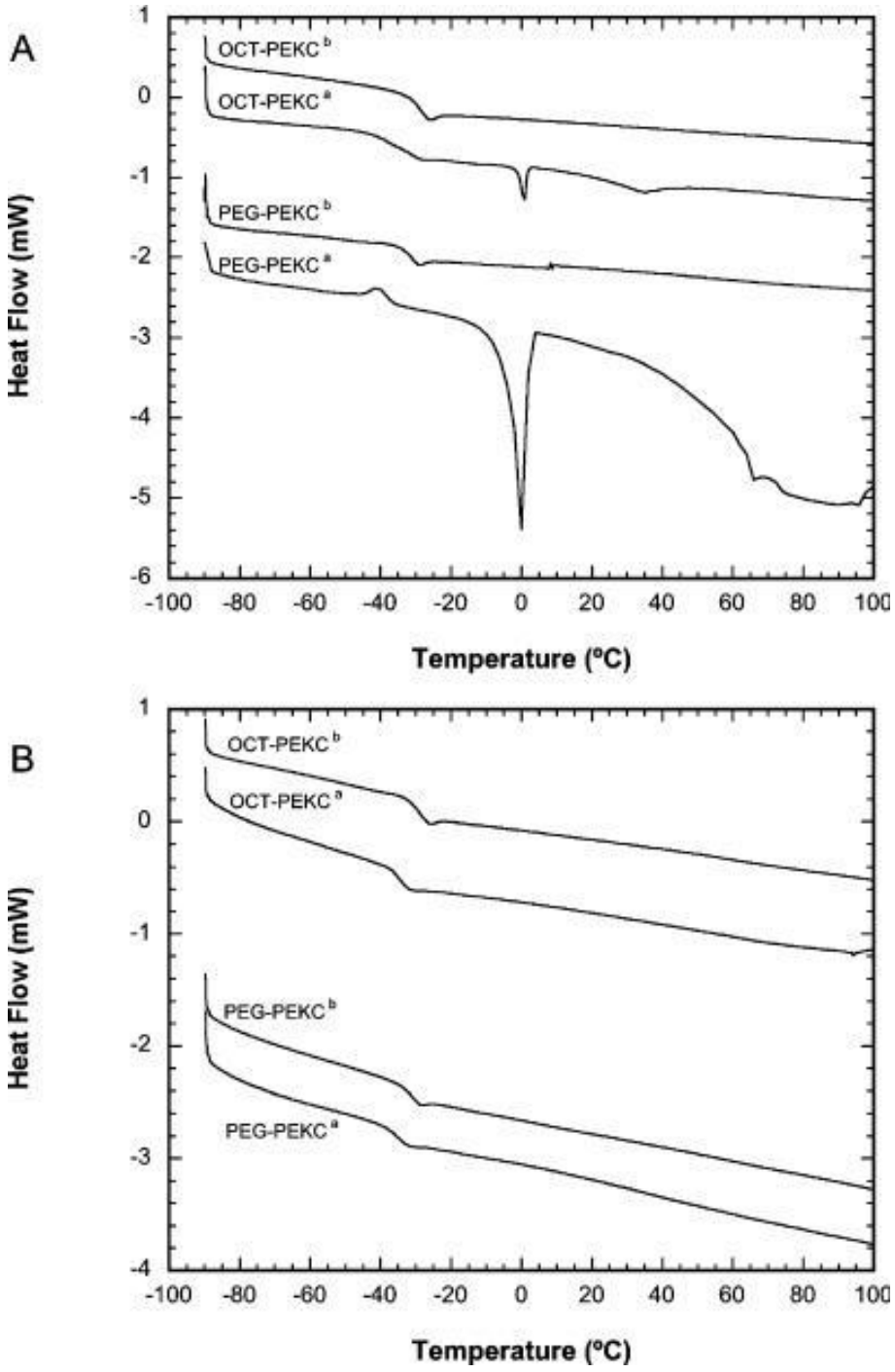

Figure 4-10: DSC thermograms of A) the hydrated polymer layer in contact with the buffer solution, and B) the inner bulk of the polymer after 8 weeks incubation in buffer. [a] indicates the first heating cycle, and [b] indicates the second heating cycle, obtained following holding the polymer at 105°C for 5 minutes, followed by cooling to -90°C.

A distinct endotherm was observed in the first heating cycle, centred on 0ºC for both the PEG-PEKC and OCT-PEKC, indicative of the melting of free water within this polymer layer. The glass transition during the first heating cycle is also broader, and at a lower temperature. Moreover, a broad evaporation endotherm is also observed. Following water evaporation by holding the polymer at 105ºC for 3 minutes then cooling and re-heating, a more distinct glass transition is apparent, occurring at a higher temperature, and the endotherms are no longer present. The thermal characteristics of the clear bottom layer of the degrading polymers were also measured to determine the degree of water penetration into the degrading polymer with time (Figure 4-10B). The melting endotherms are absent in the first heating cycles, showing that there was no free water in the polymer bulk. However, the glass transition observed during the first heating cycle was lower than that observed following holding the polymer at 105ºC for 3 minutes then cooling and running the second heating cycle. As the molecular weight of the polymer does not change during degradation, this result indicates that water must have been present in the bulk phase and that it plasticized the polymers.

The first heating cycle was used to measure the glass transition temperature of the hydrated polymer, and was then compared to glass transition temperature of the polymer following drying. The glass transition temperature (T_g) of the wet polymers was consistently lower than when dry, signifying that there was plasticization of these polymers due to the absorbance of water. Moreover, the T_g of the wet and dry EKC based polymers did not change markedly over the 24-week time period just as the molecular weight did not significantly change over the same time frame (appendix F). For the CLDLLA copolymers, the T_g did not significantly change over the first 14 weeks; however at 24 weeks, the T_g was significantly lower (appendix G). This latter result can be attributed to a combination of loss of the DLLA from the polymer combined with the reduction in polymer molecular weight. Furthermore, the influence of water plasticization on T_g on the CL based polymers was less pronounced at the initial time points, but became more significant as degradation proceeded.

Aliphatic polyesters typically degrade in a bulk erosion fashion. In this process, water penetrates the polymer more rapidly than the ester bonds are cleaved by hydrolysis. The ester bonds are cleaved in a random fashion, forming hydroxyl and carboxylic acid end groups. The acidic degradation products formed auto-catalyse hydrolysis and the degradation rate accelerates with time. Degradation products are eventually formed that are soluble in water and weight loss begins. Furthermore, the ester bonds of the more hydrophilic monomer in a copolymer degrade first[174]. The CLDLLA copolymers exhibit this type of erosion, with an onset of weight loss corresponding to a decrease in molecular weight, a decrease in T_g, and an increase in the CL component of the non-degraded polymer as degradation proceeded. By contrast, the EKC based polymers exhibited nearly linear weight loss, as well as constant T_g, composition, and M_n with degradation time. This result cannot be ascribed to classical surface erosion, because in classical surface erosion, the rate of water penetration into the polymer is slow in comparison to the rate of bond cleavage via hydrolysis and so hydrolysis is limited to a thin region near the surface [175]. Although the EKC-based polymers exhibit surface erosion-like aspects, it is unlikely that classical surface erosion is occurring, as some water does penetrate into the bulk of the EKC-based polymers because the polymers were plasticized by water, and this occurs to a greater extent than within the CL-based copolymers, at least during the beginning stages of degradation. The degradation behavior of the EKC based polymers is a result of the fact that the EKC-EKC bonds are as likely to undergo cleavage as the DLLA-DLLA bonds combined with the facts that the EKC monomer is more polar than CL and so is likely to yield degradation products that are soluble in water at a higher M_n, and that the initial polymer molecular weight is low. As hydrolysis is random, few bond cleavages are required to form a water-soluble degradation product, which would be of an intermediate molecular weight. To support this explanation, 2 mL of pH 7.4 PBS were added to 40 mg of PEG-PEKCDLLA and PEG-PCLDLLA in a glass vial and incubated at 37ºC for 24 hours. The supernatant was collected, frozen and lyophilized for 48 hours. The solid was dissolved in DMSO-d6 and the M_n calculated from ^{1}H-NMR data. The molecular weight and the ratio of CL to DLLA of the PEG-PCLDLLA in the supernatant were 935 Da and 2:1, respectively, while the molecular weight and ratio of EKC to DLLA of the PEG-PEKCDLLA in the supernatant was

1320 Da and 3.3:1, respectively. Furthermore, there is a hydrated layer of polymer in contact with the buffer solution. Thus, weight loss is nearly linear likely because water-soluble degradation products are more rapidly formed in this hydrated layer and transported relatively quickly to the surface and therefore do not accumulate within the bulk. Water penetration into the polymer bulk occurs, but the degradation rate within the bulk is slower due to a lower amount of water present.

4.3.4 Monomer Cytotoxicity

To assess the potential of the EKC-based polymers as implantable biomaterials, the cytotoxicity of the degradation products of the monomer towards 3T3 fibroblasts was measured. As shown in Figure 4-11, following exposure of the degradation products of the EKC monomer to 3T3 fibroblast cells, about 80% of the cells retained metabolic activity comparable to unexposed controls.

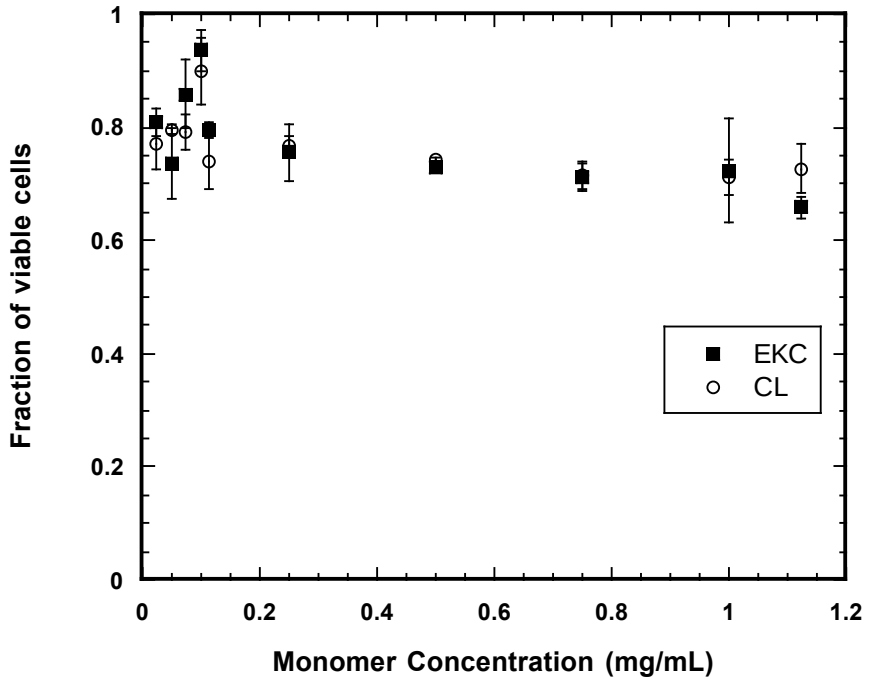

Figure 4-11: Cytotoxicity of degradation products of EKC and CL monomer to 3T3 fibroblast cells.

This result was similar to the activity of 3T3 fibroblast cells exposed to the same concentration of the degradation products of ε-caprolactone monomer. Thus, the degradation products of EKC monomer were no more toxic than ε-caprolactone monomer. Homo and copolymers of ε-caprolactone have a long history of safe clinical use, and so this result implies that the EKC homo and copolymers may be non-toxic *in vivo*.

4.4. Conclusions

Low molecular weight poly (5-ethylene ketal ε-caprolactone) and its copolymer with D,L-lactide were prepared and their properties investigated as potential biodegradable, hydrophobic liquid injectable vehicles for local drug delivery. The polymerization was done at 110ºC to prevent backbone pyrolysis and deacetylation of the 5-ethylene ketal side group. The polymers were amorphous with low viscosity and therefore injectable at 37ºC. The viscosity was tuneable by choice of initiator and/or by copolymerizing with D,L-lactide; lower viscosity was attained by using PEG 350 as an initiator in comparison to octan-1-ol as initiator while incorporation of D, L-lactide increased viscosity. The initiator used had no significant effect on the rate of mass loss *in vitro*, after the first three weeks. Co-polymers with D,L-lactide degraded faster than 5-ethylene ketal ε-caprolactone (EKC) homopolymers, due to the higher hydrophilicity of the D,L-lactide. For the EKC based polymers, a nearly linear degradation rate was observed. This finding was attributed to the hydrolytic susceptibility of the EKC-EKC ester linkage, which was comparable to that of the DLLA-DLLA linkage, coupled with the intermediate molecular weight of the water-soluble degradation product and the low molecular initial weight of the EKC-based polymers. Moreover, cytotoxicity of the hydrolysed EKC monomer to 3T3 fibroblast cells was the same as ε-caprolactone, suggesting that polymers prepared from EKC may be well tolerated upon *in vivo* implantation.

Chapter 5

OSMOTIC PRESSURE DRIVEN PROTEIN RELEASE FROM VISCOUS LIQUID INJECTABLE POLYMERS BASED ON 5-ETHYLENE KETAL Ɛ-CAPROLACTONE

Iyabo Oladunni Babasola and Brian G. Amsden [†]

Department of Chemical Engineering, Queen's University, Kingston, ON, Canada

[†]Human Mobility Research Centre, Kingston General Hospital, Kingston, ON, Canada

This paper is focused on the second and third specific objectives of this research, which is to investigate the potential of polymers based on 5-ethylene ketal ε-caprolactone to deliver a protein using the osmotic release mechanism and to elucidate the mechanism by which proteins are released from the polymer.

Abstract

In this study, the potential of low molecular weight, viscous liquid polymers based on 5-ethylene ketal ε-caprolactone for localized delivery of proteins via an osmotic pressure release mechanism was investigated. Furthermore, the osmotic release mechanism from viscous liquid polymers was elucidated. 5-ethylene ketal ε-caprolactone was homopolymerized or copolymerized with D,L-lactide (DLLA) by ring-opening polymerization. Polymer hydrophobicity was adjusted by choice of initiator; hydrophobic polymers were prepared by initiating with octan-1-ol while more hydrophilic polymers were prepared by initiating with 350 Da methoxy polyethylene glycol (PEG). Particles consisting of bovine serum albumin (BSA) as a model protein drug were co-lyophilized with trehalose at 50:50 and 10:90 (w/w) ratios and were mixed into the polymers at 1 and/or 5% (w/w) particle loading. The release and mechanism of release of BSA from the polymers were assessed *in vitro*. BSA was released in a sustained manner, with a near zero-order release profile, and with no initial burst effect for 5 to 80 days depending on the polymer's hydrophilicity; the release was faster from the PEG initiated polymers than from the octan-1-ol initiated polymers. Increasing the particle loading from 1 to 5% (w/w) resulted in a more noticeable burst effect, but did not significantly increase the mass fraction release rate. Using fluorescently labeled BSA and a laser scanning confocal microscope, this release behaviour was determined to proceed as follows. Release from the polymer was triggered by the water activity gradient between the surrounding aqueous medium and the saturated solution, which forms when water is absorbed from the surrounding medium to dissolve a given particle. The generated pressure initiates swelling around the particle/polymer interface, and creates a highly hydrated polymer region through which the solute is transported by convection, at a rate determined by the osmotic pressure generated and the hydraulic conductivity of the polymer. These studies indicate that low molecular weight 5-ethylene ketal ε-caprolactone based polymers may be suitable as a viscous, injectable medium for localized delivery of therapeutic proteins via the osmotic release mechanism.

5.0 Introduction

Protein and peptide therapeutics have become an important class of drugs, and numerous protein therapeutics have been approved for use or are in advanced clinical testing [176]. Due to the intrinsic physico-chemical and biological properties of these proteins, a safe, effective and patient friendly delivery approach for these proteins remains a challenge [91, 149]. To improve patient compliance and achieve the optimal therapeutic effects without toxicity and unfavorable side effects, it would be ideal to have injectable formulations that could provide local and sustained release of protein therapeutics within the therapeutic range over a period of several days, weeks or even months.

For this purpose, liquid, injectable, hydrophobic and biodegradable polymeric vehicles may be advantageous as they allow facile incorporation of thermally sensitive drugs such as proteins and peptides by simple mixing [131, 133], and they are injectable through standard gauge needles, and so can be administered via minimally invasive means [131, 177]. There is restricted water penetration into these polymers, which may provide enhanced stability for drugs such as proteins incorporated as solid particles [30]. The viscosity and thus the injectability of the polymers can be controlled by appropriate selection of monomers and initiator [30, 130, 131]. For this strategy to be effective there must be a compromise between injectability and effective depot formation. The polymer must be have a viscosity low enough to allow easy injection while still high enough to reduce dispersion within the tissue and thus provide control over drug release. Previous work by Timbart and co-workers[30, 160] indicated that a viscosity of 10-100 Pa·s was necessary to provide ready injection through standard gauge needles while still producing a non-dispersible implant within the tissue.

Poly(5-ethylene ketal ε-caprolactone) (PEKC) could be a promising injectable delivery system for protein therapeutics. PEKC has a similar chemical structure as poly(ε-caprolactone), except that the gamma carbon is substituted with an ethylene ketal pendant group (Figure 5-1). PEKC is amorphous and has a low viscosity of 17.5 to 26.3 Pa·s at a molecular weight of about 2500 Da and at 37ºC, depending on the initiator used (Table 5-1) [130]. EKC can be readily copolymerized with other monomers, such as D,L-lactide, to control viscosity (Table 5-1), and biodegradability (Figure 5-2) [130]. Viscosity can also be controlled by adjusting molecular weight (Table 5-1). The pendant ketal group increases the hydrophilicity of the polymer, which enhances its hydrolytic degradation. Low molecular weight PEKC, and its copolymers, degrade by surface erosion (Figure 5-2),[130] a feature that might be advantageous in preserving the bioactivity of incorporated therapeutic proteins.

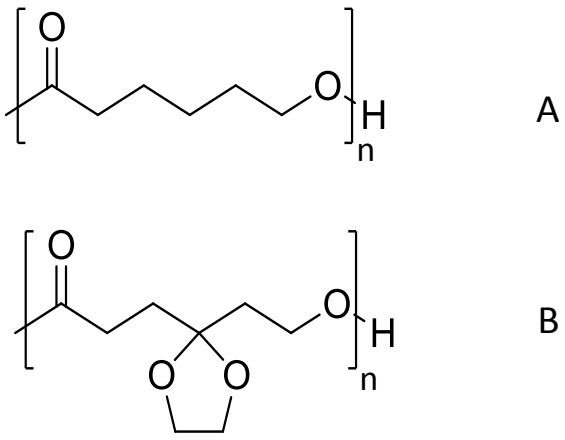

Figure 5-1: Structure of: A) poly(ε-caprolactone) and B) poly(ethylene ketal ε-caprolactone).

Table 5-1: Physical characteristics of the polymers used [130]

Polymer Designation	monomer ratio (EKC:DLLA (mol:mol))	T_g [a] (^oC)	M_n [b] (Da)	PDI [c]	η_{37^oC} [d] (Pa·s)
OCT-PEKC	13.2 : 0	-32.4	2390	1.40	26.3
PEG-PEKC	12.9 : 0	-35.7	2570	1.17	17.8
OCT-PEKCDLLA 1	10.0 : 3.5	-22.1	2340	1.32	79.4
OCT-PEKCDLLA 2	13.0 : 4.0	-19.7	2810	1.26	129.0
PEG-PEKCDLLA	10.6 : 3.5	-25.0	2610	1.26	55.2

[a] glass transition temperature, [b] number average molecular weight, [c] polydispersity index, [d] zero shear rate viscosity at 37ºC.

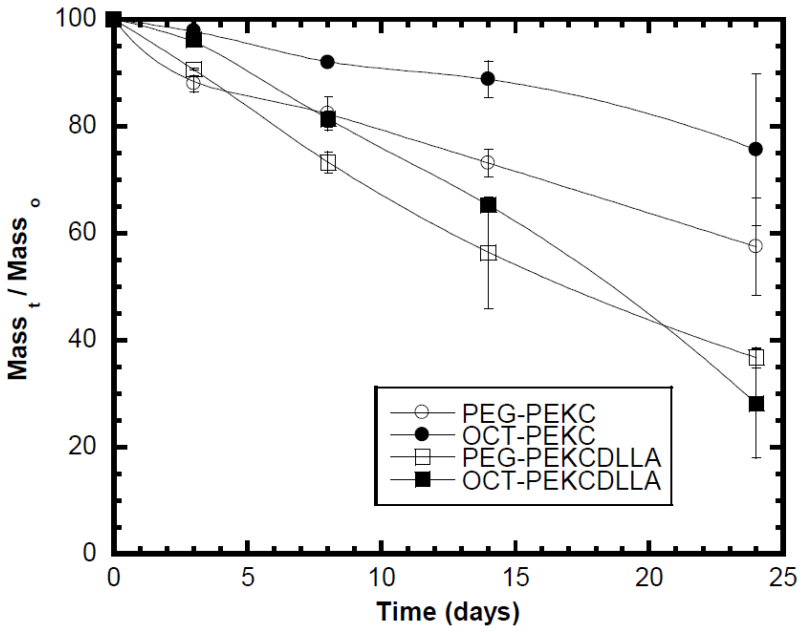

Figure 5-2: Degradation profile of PEKC and EKC copolymerized with DLLA, prepared with either octan-1-ol (OCT-PEKC, OCT-PEKCDLLA) or 350 Da methoxy poly(ethylene glycol) (PEG-PEKC, PEG-PEKCDLLA) in 0.1 M PBS at 37 °C and pH 7.4 (reproduced from [130], used with permission).

An osmotic pressure release mechanism was used as it can provide a linear release profile with very minimal initial burst[30]. The osmotic pressure release mechanism for viscous liquid polymers is incompletely understood, but is believed to occur as follows [133, 147]. Water from the surrounding medium dissolves into and diffuses through the polymer matrix until it encounters a polymer-enclosed drug particle. At the particle/polymer interface, the water phase dissolves a portion of the particle to form a saturated solution. The water activity in the saturated solution formed is much less than that in the surrounding aqueous medium. This difference generates an activity gradient between the solution at the particle surface and the surrounding medium. The activity gradient draws water into the polymer to generate an osmotic pressure equal to the osmotic pressure of the saturated solution. The pressure generated drives the solution through the polymer towards the surface, where the pressure is lower. The means by which the solution is moved through the polymer phase has not yet been clarified.

Most proteins have low solubility in water and generate low osmotic pressures. For example, a saturated solution of bovine serum albumin (BSA) with a molecular weight of 66 kDa would generate an osmotic pressure of approximately 12 atm at 25°C[178]; this is not sufficient osmotic activity to drive its release [30, 178]. However, a saturated solution of the non-reducing sugar trehalose, can provide an osmotic pressure of 92 atm at 37°C [147]which is sufficient to drive the release of proteins from viscous liquid polymers to the release medium[30]. Thus, intimately mixing trehalose with the protein can be used to generate the necessary osmotic pressure to drive the release of the protein, plus trehalose, from the polymer.

The first objective of this study was to explore the potential of an injectable delivery vehicle consisting of low molecular weight poly(5-ethylene ketal ε-caprolactone) (PEKC) or its copolymer with D,L-lactide (DLLA) for the delivery of proteins using the osmotic pressure release mechanism. For this purpose, BSA as a model protein was used because it has previously been shown to release at the same rate with therapeutic protein such as VEGF, using the osmotic release mechanism. The second objective was to more clearly elucidate the mechanism of osmotic release of proteins from viscous liquid polymers, and in particular, the means by which the dissolved solute is transported through the polymer phase to the release medium.

5.1.Materials

1,4-cyclohexanedione monoethylene ketal (97% purity), meta-chloroperoxybenzoic acid (MCPBA) (97% purity), octan-1-ol (anhydrous, 99% purity), stannous 2-ethylhexanoate (95% purity), Dulbecco's phosphate buffered saline (PBS), sulphuric acid, phenol, methoxy poly(ethylene glycol) with an average molecular weight of 350 Da (MPEG 350), bovine serum albumin (≥ 98% purity), D-(+)-trehalose dihydrate (≥ 99% purity), and succinic acid (99% purity) were obtained from Sigma-Aldrich, ON, Canada. D,L-lactide was obtained from Purac, the Netherlands and purified by recrystallization from dried toluene. The bicinchoninic acid (BCA) protein assay kit was purchased from Pierce, Rockford, IL, USA.

5.2 Methods

5.2.1 Synthesis of 5-ethylene ketal ε-caprolactone-based copolymers

The 5-ethylene ketal ε-caprolactone monomer was prepared by the Baeyer-Villiger oxidation of 1,4-cyclohexanedione monoethylene ketal by meta-chloroperoxybenzoic acid

(MCPBA), and used to prepare EKC homopolymers and copolymers with DLLA, initiated with octan-1-ol and methoxy PEG, via ring-opening polymerization utilizing stannous 2-ethylhexanoate as a catalyst, as described previously [130]. The properties of these polymers are listed in Table 5-1.

5.2.2 Preparation of protein particles

The protein particles were prepared by dissolving trehalose and BSA at a weight ratio of 50:50 and 90:10 in 10 mL of 0.5 mM pH 7 succinate buffer. This solution was frozen in liquid nitrogen, then lyophilized on a Modulyo D freeze dryer (Thermosavant, USA) at -50°C and 100 mbar. The resulting powder was sieved through a #325 Tyler sieve to yield < 45 μm particles.

5.2.3 *In vitro* BSA release

A known amount of lyophilized protein particles was suspended with a known amount of polymer by physical mixing. The lyophilized particles were loaded into the polymer at 1 and 5% (w/w). To facilitate mixing, the polymer was initially warmed to 40°C. Following mixing, the protein-loaded polymer was drawn into a plastic 1 mL syringe, and approximately 100 mg dispensed into the base of a 2 mL glass vial to fill the bottom of the vial to a height of approximately 3 mm. The exact weight of the mixture in each vial was recorded. The vials were filled with 0.8 mL of 37°C pH 7.4 PBS containing 0.02% (w/v) Tween 20 and 0.02% (w/v) sodium azide. The Tween 20 was added to prevent non-specific adsorption of the BSA to the glass vials [133] and sodium azide was added as an antimicrobial. The vials were capped and placed on a rotary mixer rotating at 300 rpm and maintained at 37°C. For each condition, triplicate samples were prepared. As controls, polymer-only samples were also prepared. At frequent

sampling intervals, the buffer was replaced with fresh buffer. The removed buffer was stored at -80°C until analyzed.

The BSA concentration in the release medium was measured on a microplate spectrophotometer at a single wavelength of 562 nm using the bicinchoninic acid (BCA) protein assay in accordance with the supplier's protocol. The released trehalose was quantified by using a phenol-sulfuric acid calorimetric assay as follows [30]. 5 µL of 80% phenol in distilled water was added to 0.3 mL of diluted released media, gently mixed, and 1 mL of concentrated sulfuric acid was added, the stream of acid being directed against the liquid surface. After 10 minutes, the liquid was vortexed and left for 20 minutes at 30°C, after which 100 µL was placed in triplicate in a 96 well plate and absorbance measured at 480 nm. The concentration of trehalose in the release medium was determined by using calibration curves of known concentrations of trehalose varying from 0 to 300 µg/mL in PBS.

5.2.4 Elucidation of Release Mechanism

To investigate the release mechanism, fluorescein isothiocyanate conjugated BSA (FITC-BSA) was incorporated into the protein particles. The particles were prepared by dissolving 183.9 mg of trehalose, 23.6 mg of BSA and 4.1 mg of (FITC-BSA) in 20 mL of 0.5 mM, pH 7.4 succinate buffer. The solution was lyophilized, and the resulting particles sieved to < 45 µm and loaded into the OCT-PEKCDLLA 2 at 1% (w/w) loading as described above. About 18 mg of the protein-loaded polymer was injected into a glass tube with an internal diameter of 0.8 mm and a length of 3.5 cm. The polymer filled the tube to a height of ~ 10 mm. The tube was then filled with release buffer to a height of 3 cm and placed upright in an oven maintained at 37ºC. At given

time points, the tube was removed from the oven and mounted flat on the stage of an Olympus FV1000 confocal microscope. The FITC-BSA particle loaded polymer was imaged prior to release at depths of up to 300 μm from the surface, at a step size of 10 μm, and at days 7 and 14 via laser scanning confocal microscopy and brightfield microscopy.

5.3 Statistics

All release experiments were done in triplicate and results are reported as the average ± the standard deviation about the average. Evaluations of significant difference between group means were assessed using a one-way Kruskal-Wallis ANOVA. A p value of less than 0.05 was considered significant.

5.4 Results

5.4.1 *In vitro* BSA release

Due to the low viscosity of the polymers, the trehalose-BSA particles were evenly distributed throughout the polymers by physical mixing (Figure 5-3). The average diameter of the particles was less than 45 μm as anticipated. To form solid particles with an osmotic activity capable of driving BSA release from the polymer, BSA was lyophilized with trehalose, which is a compatible osmolyte that has been used previously to drive the release of VEGF from poly(trimethylene carbonate)[30]. The release experiments were performed in such a manner as to approximate release from a slab configuration, under near perfect sink conditions.

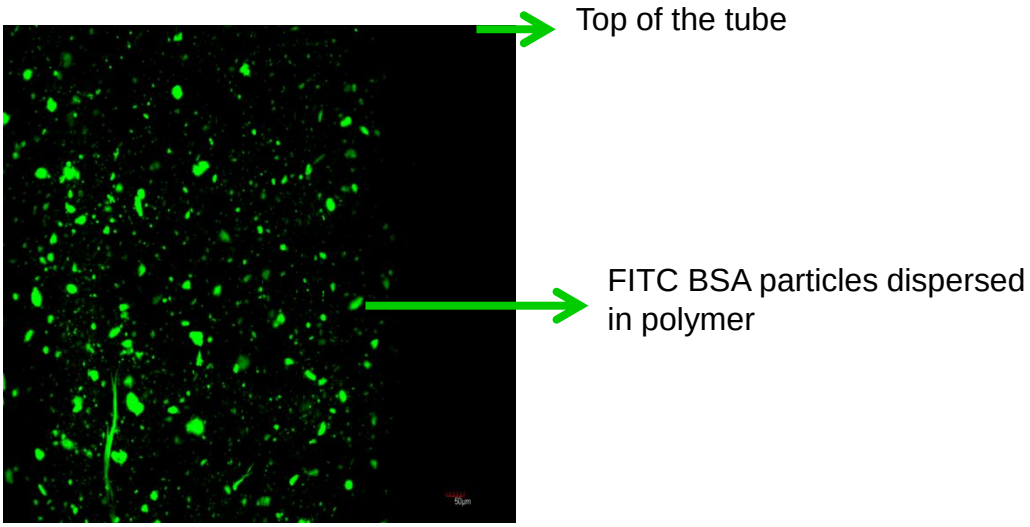

Figure 5-3: Image of lyophilized trehalose and BSA containing FITC-BSA loaded into OCT-PEKCDLLA at 1 % loading obtained using a laser scanning confocal microscope. The image was taken from the top of the tube, prior to adding water and was generated by stacking images taken at different depths. The scale bar represents 50 µm.

5.4.2 Effect of initiator hydrophilicity and copolymerization with DLLA on release

Previous work by Sharifpoor and Amsden showed that almost 100% of incorporated vitamin B12 was released from 1315 Da poly(trimethylene carbonate) in a sustained manner via the osmotic release mechanism [147]. This release was achieved by lyophilizing trehalose and vitamin B12 at a weight ratio of 50:50, sieving the particles to less than 25 µm, and loading the particles in the polymer at 1% (w/w). Vitamin B12 was released faster from a copolymer of ε-caprolactone with trimethylene carbonate (viscosity of 2.7 Pa·s) compared to poly(trimethylene carbonate) (viscosity of 16.8 Pa·s) of similar molecular weight, suggesting that polymer viscosity influenced release. Furthermore, the release mechanism relies on water imbibition into the polymer. It was thus expected that utilizing PEG as the initiator would result in an increase in the release rate over that observed for polymers initiated with octan-1-ol, as PEG is more hydrophilic

and would allow for faster and increased water penetration into the polymer. To test this hypothesis, BSA release from EKC based polymers with varying viscosities and with PEG and octan-1-ol as the initiators was investigated using a BSA : trehalose weight ratio of 50:50 and a 1% particle loading.

For all the polymers examined, release proceeded with a very low burst amount (less than 6%), after which a constant release phase was observed. The duration and rate of the constant release phase varied, depending on the nature of the initiator used to prepare the polymer. When the hydrophobic initiator (octan-1-ol) was used, the release of BSA appeared to be influenced by polymer viscosity (Figure 5-4A). The release rate of BSA increased as polymer viscosity decreased (Figure 5-4B), with release rates of 1.2 ± 0.1, 5.4 ± 0.6, and 9.4 ± 0.4%/day, for OCT-PEKCDLLA 2 (η_{37^oC} = 129 Pa·s), OCT-PEKCDLLA 1 (η_{37^oC} = 79.4 Pa·s), and OCT-PEKC (η_{37^oC} = 26.3 Pa·s), respectively ($p = 0.03$).

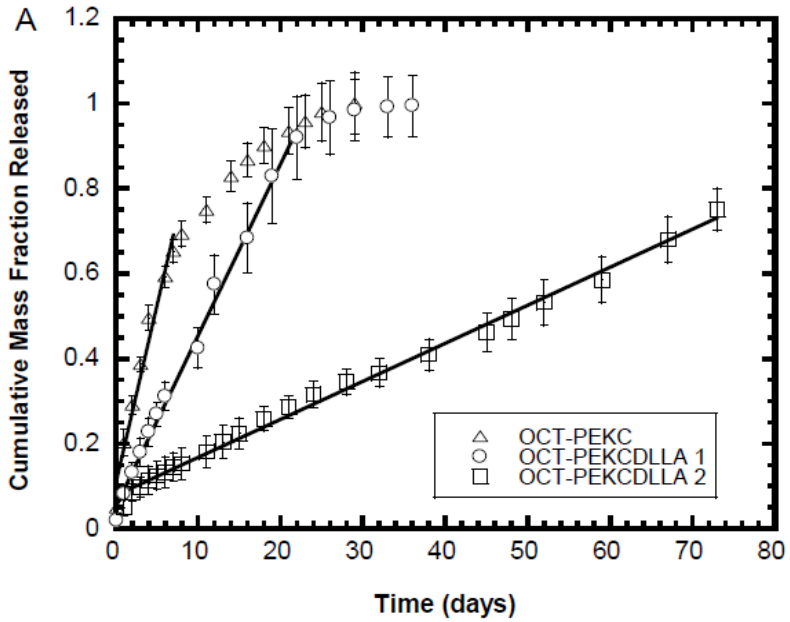

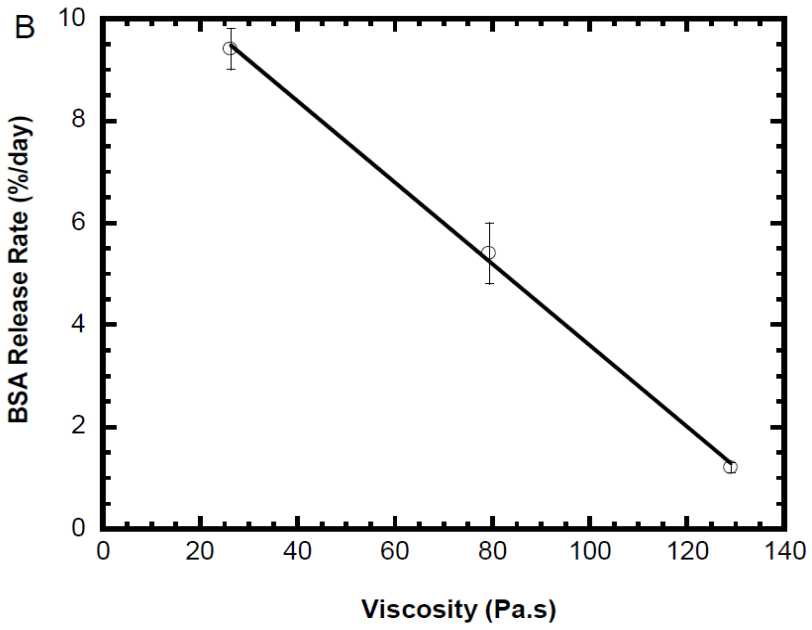

Figure 5-4 A) Cumulative mass fraction release of BSA from octan-1-ol initiated polymers of comparable number average molecular weight. B) BSA release rate versus viscosity of octan-1-ol initiated polymer. The error bars indicate the standard deviation of 3 independent release experiments. The straight lines in A represent linear regressions over the times indicated by the length of the line. For each regression, the coefficient of determination was ≥ 0.92.

As proposed, BSA was released faster from the PEG initiated polymers (Figure 5-5). However, for these polymers, BSA release did not increase as polymer viscosity decreased. The BSA was released faster from PEG-PEKCDLLA (η_{37^oC} = 55.2 Pa·s) than from PEG-PEKC (η_{37^oC} = 17.8 Pa·s) (p = 0.049). Over the first 5 days, the release rate of BSA from PEG-PEKC was 14.7 ± 0.3%/day, while that for PEG-PEKCDLLA was 18.6 ± 0.7%/day.

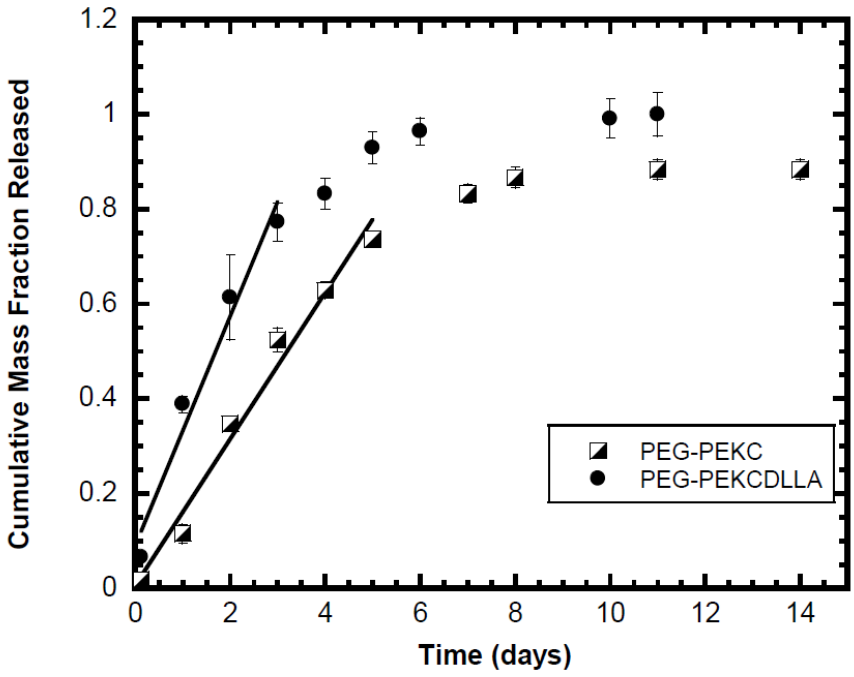

Figure 5-5: Cumulative mass fraction release of BSA from PEG-initiated polymers of comparable number average molecular weight. The error bars indicate the standard deviation of 3 independent release experiments. The straight lines represent linear regressions over the times indicated by the length of the line. For each regression, the coefficient of determination was ≥ 0.92.

The release profile of BSA from PEG-PEKC and PEG-PEKCDLLA might be suitable for proteins that need to be released in less than 10 days, but not for proteins that need to be released over longer time periods. As multi-week, and nearly constant, protein release is advantageous in a number of applications, formulations using OCT-PEKCDLLA 2 as a basis were examined further.

5.4.3 Effect of particle trehalose content and total particle loading on release

Based on previous work for osmotically driven release from liquid injectable polymers[147], low melting point microspheres [179] and elastomers [123, 125], it was expected that BSA release would increase as trehalose content in the particle increased due to an increase in solution osmotic pressure generated upon dissolution of the particles in the polymer. To determine the extent of increase in release rate in the EKC-based polymers, formulations containing trehalose content of 90% (w/w) in the particles, and a particle loading of 1% (w/w) in OCT-PEKCDLLA 2 were examined. Linear release profiles were again obtained (Figure 5-6), with the release rate being higher for the formulation containing 90% (w/w) trehalose in the particles. By increasing the trehalose concentration in the particle from 50% (w/w) to 90% (w/w), the release rate increased by 27%; BSA was released from the formulation containing 50% (w/w) trehalose at 0.96 ± 0.02%/day compared to 1.24 ± 0.02%/day from the formulation containing 90% (w/w) trehalose for the first 70 days.

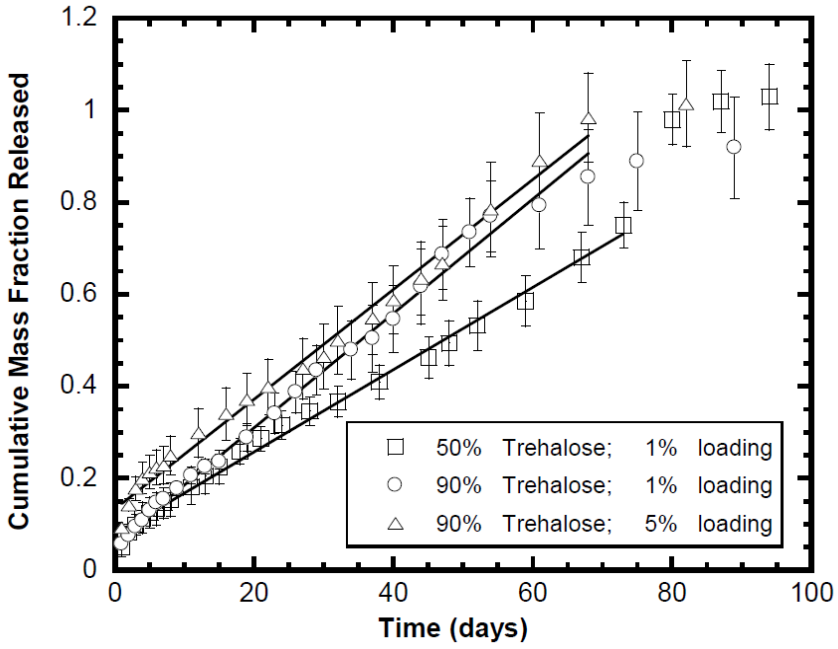

Figure 5-6: BSA release from OCT-PEKCDLLA 2 loading with 1% and 5% particles containing 90% trehalose and 10% BSA. The error bars indicate the standard deviation of 3 independent release experiments. The straight lines represent linear regressions over the times indicated by the length of the line. For each regression, the coefficient of determination was ≥ 0.99.

For release from elastomer systems, increasing the particle loading increased the release rate [31, 123]. The influence of loading on release from liquid injectable polymer systems has not yet been elucidated. To determine whether the BSA release rate from the OCT-PEKCDLLA 2 was influenced by the total loading of particles into the polymer, BSA release from particles containing 90% trehalose was examined with particle loadings of 1% and 5% (w/w). Increasing the particle loading from 1 to 5% (w/w) resulted in a slightly longer time frame before linear release was observed (Figure 5-6). Linear release was noticeable after 1 day for the 1% particle loading formulation, whereas linear release was not observable until after 4 days for the 5% particle loading formulation. The total mass fraction of BSA released during the initial periods of

nonlinear release were ~ 10% for the 1% (w/w) particle loading case and 21% for the 5% (w/w) particle loading case. Following the initial period of nonlinear release, the linear release rates for both formulations were statistically equal ($p = 0.83$). BSA was released from the formulation with 1% (w/w) loading at 1.24 ± 0.02%/day compared to 1.17 ± 0.02%/day for the 5% (w/w) loading case, over the same time frame.

In a previous study[30], vascular endothelial growth factor (VEGF) and trehalose were released at the same rate from liquid poly(trimethylene carbonate) as would be expected if a similar osmotic pressure release mechanism as proposed for release from elastomers was driving the release for viscous liquid polymers. In this study, with the formulation containing particles with 50% (w/w) trehalose, trehalose and BSA were also released at the same rate (Figure 5-7A). However, for formulations containing particles with 90% trehalose, trehalose was released at a slightly greater rate than was BSA (Figure 5-7B). With particle compositions of 90% (w/w) trehalose, the particles loaded at 1% (w/w) released trehalose faster than the particles loaded at 5% (w/w) in the early stages of release.

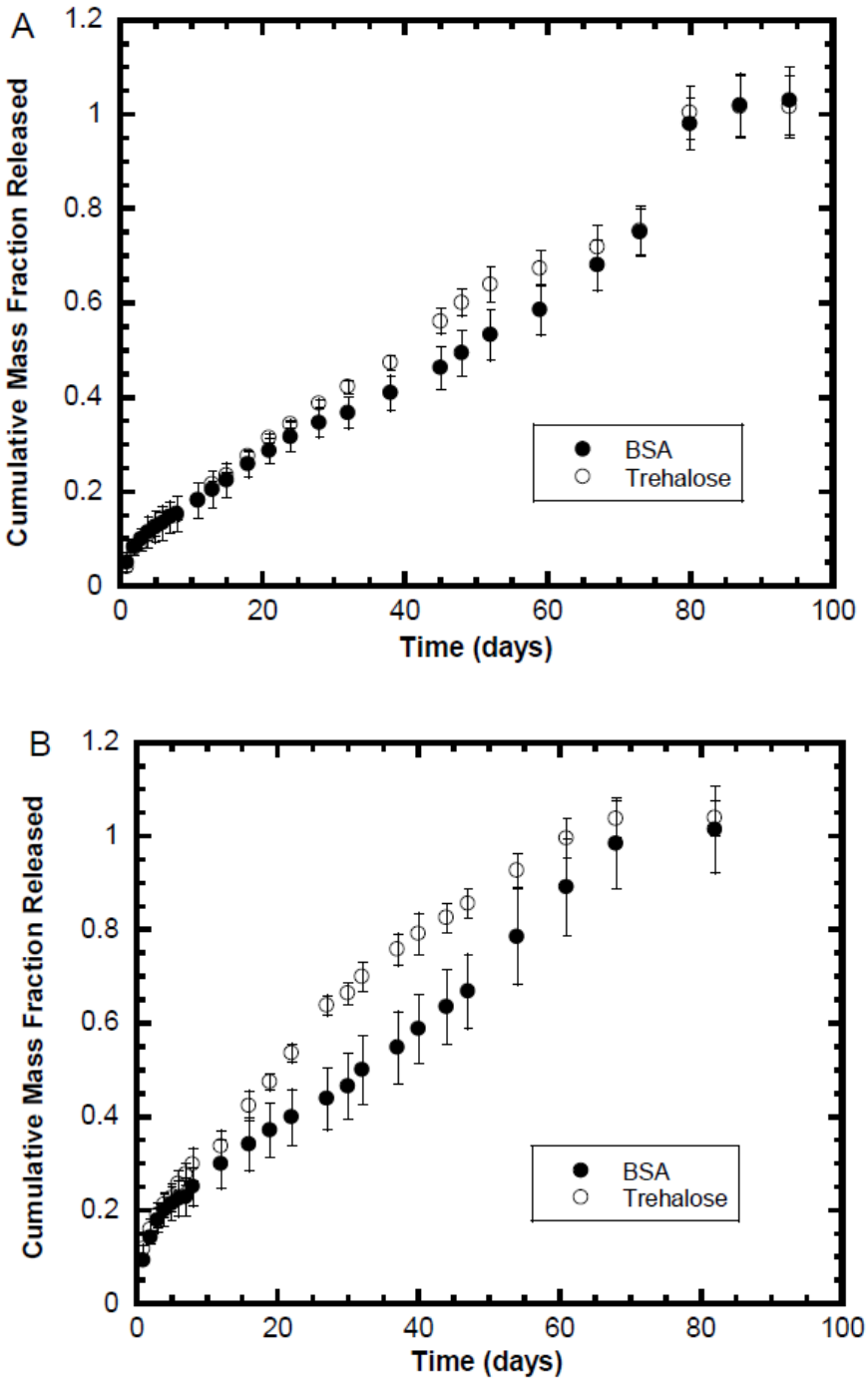

Figure 5-7:Mass Fraction of trehalose and BSA released from OCT-PEKCDLLA 2 using particles with a trehalose to BSA weight ratio of (A) 50 : 50 at 1 % (w/w) loading and (B) 90 : 10 at 5 % (w/w) loading.

5.4.4 Release mechanism

In order to elucidate the release mechanism, the release of FITC-BSA with time from OCT-PEKCDLLA 2 was studied visually using images taken with a laser scanning confocal microscope. In Figure 5-8, the fluorescent image obtained from the laser scanning confocal microscope has been overlaid with the corresponding brightfield image.

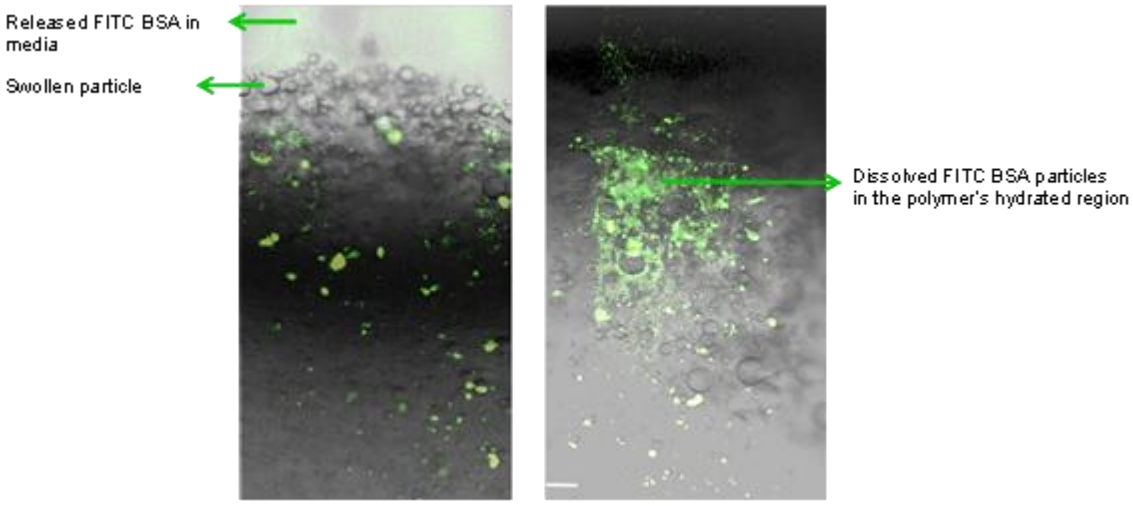

Figure 5-8:Confocal laser scanning microscope images showing water penetration into OCT-PEKCDLLA 2 containing dispersed FITC BSA particles taken at day 7 (left) and at day 14 (right). The scale bar represents 50 µm.

The image on the left and the image on the right were taken at day 7 and 14 respectively. As was shown in Figure 5-3, prior to adding water to the tube, the particles were evenly dispersed in the polymer. By day 7, water had diffused into the upper region of the polymer, and had begun dissolving dispersed particles. The solution formed created swollen capsules that are clearly visible in the brightfield image. Capsules very near the interface can be seen that also contain undissolved solid particles fluorescing green in the overlay image. By day 14, a fluorescent halo

surrounded the capsules visible in the overlaid brightfield/fluorescent images. The polymer region surrounding the capsules also fluoresced green, with this region of fluorescence extending towards and reaching the polymer/aqueous medium interface. Also apparent is dissolved and released FITC-BSA in the aqueous medium above the polymer.

5.5 Discussion

The release results show that BSA and trehalose are being released at almost the same rate, therefore release must be dominated by convective flow and not diffusion. Moreover, the imaging experiments show FITC-BSA in the polymer region surrounding the swelling particles, and that this fluorescence is nearly homogeneous, indicating that distinct pores are not being formed. Based on these observations, the following release mechanism is proposed. Upon contact with the release medium, particles resident at the surface, and those particles in contact with them, dissolve and diffuse into the release media. This phase of release corresponds to the observed burst. Water from the surrounding medium also dissolves into, and diffuses through, the polymer matrix until it encounters a polymer-enclosed drug particle. At the particle/polymer interface, the water dissolves a portion of the particle to form a saturated solution. An activity gradient is generated between the saturated solution and the surrounding aqueous medium. The activity gradient draws water into the polymer to generate an osmotic pressure equal to the osmotic pressure of the saturated solution at the particle/polymer interface. The pressure causes the capsule to swell, with the swelling extent determined by the polymer's hydraulic conductivity and hydrophilicity. As a result of the pressure generated and the low molecular weight of the polymer, water is forced into the polymer region surrounding the capsules. The water forced into the surrounding polymer forms what have been termed "zones of excess hydration"[180]. At some

point in time, these zones overlap to form a continuous pathway extending to the surface. The dissolved solutes are transported by convection through this hydrated region, driven by the osmotic pressure difference between the dissolved solute at the particle/polymer interface and the external medium. A pictorial representation of the proposed release mechanism is shown in Figure 5-9.

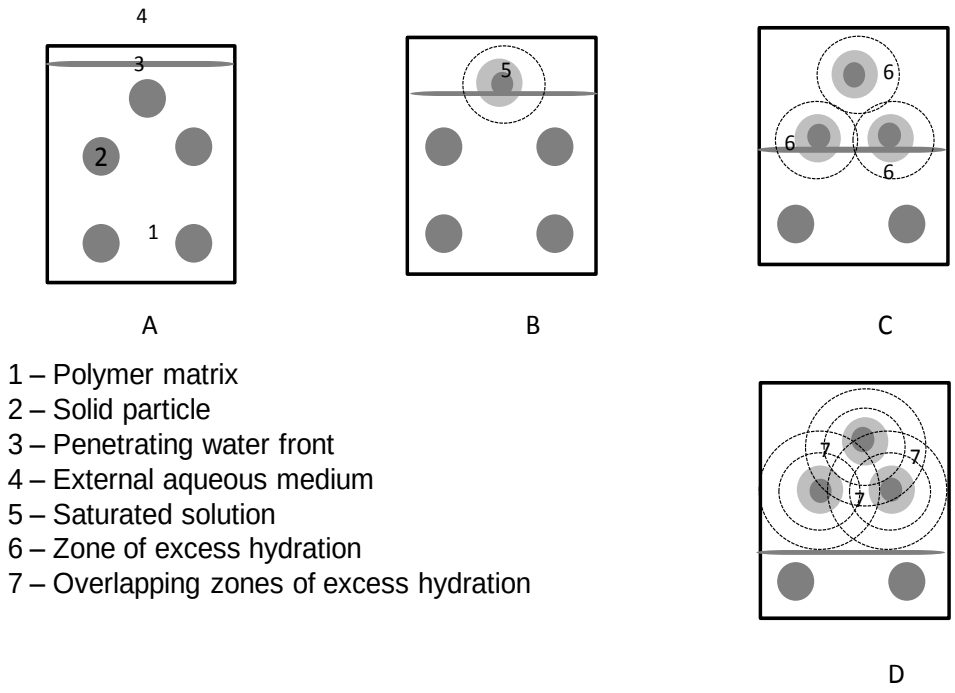

Figure 5-9: Pictorial representation of proposed osmotic swelling mechanism that involves zones of excess hydration where solute transport is facilitated. (A) Water from the surrounding medium dissolves into and diffuses through the polymer matrix until it encounters a polymer-enclosed drug particle (B) At the particle/polymer interface, the water phase dissolves a portion of the particle to form a saturated solution. (C) This activity gradient between the solution at the particle surface and the surrounding medium draws water into the polymer to generate an osmotic pressure equal to the osmotic pressure of the saturated solution. The pressure generated drives the solution to the surrounding polymer known as the "zone of excess hydration" (D) More solute is diffused through the swollen polymer or clusters of water dispersed in the polymer causing an overlap of these zones of excess hydration as it extends towards and reaches the polymer/aqueous medium interface.

This release process is analogous to the Starling model for convective flow through a semi-permeable membrane, expressed as [181]

$$J = k(\Delta P) C_s \quad (1)$$

In Equation (1) J is solute flux, k is the hydraulic conductivity of the polymer, ΔΠ is the osmotic pressure difference between the water at the particle/polymer interface and the external medium, and C_s is the solute concentration in the hydrated region.

From the proposed release mechanism, the observed release results can be explained as follows. The release rate of the encapsulated solid agent is determined by the amount of water within the zones of excess hydration. This is in turn determined by the hydraulic conductivity of the polymer. The PEG initiated polymers are more hydrophilic compared to the hydrophobic octan-1-ol initiated polymers [182, 183]. As a result, the hydraulic conductivity of the PEG initiated polymers is greater. They absorb more water and water absorption is faster, creating a larger "zone of excess hydration", and therefore releasing more solute at a given time to the polymer/aqueous phase interface compared to the more hydrophobic octan-1-ol initiated polymers. With the PEG initiated polymers, BSA release was independent of viscosity; however, with the hydrophobic polymers, viscosity appeared to be influential. The influential factor in the release kinetics is the hydraulic permeability of the polymer; when hydraulic permeability of the polymer is high, viscosity is less influential.

BSA release from the more hydrophobic polymer (OCT-PEKCDLLA 2) increased as trehalose content in the loaded particles increased due to the increase in osmotic pressure generated upon dissolution of a particle in the polymer, as anticipated. This finding has been noted in osmotically driven release from liquid injectable polymers[147], low melting point microspheres [179] and elastomers [123, 125]. Our result indicate that more water was absorbed into the polymer as a result of the osmotic pressure generated, increasing the extent of the zone of excess hydration, which increased solute release. The almost complete, sustained and near zero order release profile observed as a result of osmotic pressure generated upon dissolution of the particle was expected, based on previous results [30, 147]. The particle loading used was 1% w/w or 5% w/w; this value is below the percolation threshold, which is about 33% for most geometries [122, 147]. The percolation threshold is defined as the volume fraction of dispersed particles at which enough particles are touching so as to form a path spanning the thickness of the device[122]. The osmotic pressure release dominates when the total volumetric loading of the particle in the polymer is below the percolation threshold[123, 184].

Based on previous osmotically induced studies from elastomers, where solute release is determined by the mechanical properties of the device, [123, 125], increasing the particle loading increased release rates due to the resulting thinner polymer wall that surrounded a given entrapped particle. In elastomeric devices, due to the pressure gradient generated when water is drawn into the capsule, cracks are formed, which connect the content of the capsule to the pore network, allowing transport of the dissolved contents towards the surface [123, 125]. However, in our studies where solute is released through the "zone of excess hydration", by increasing the particle loading from 1% (w/w) to 5% (w/w), a short, non-linear initial burst release was observed at

higher particle loading due to the expected increase in fraction of the particles that would reside at the surface. Increasing the total particle loading, provided it remains below the percolation threshold, would result in the overlap in the zones of hydration to occur sooner. Nevertheless, the hydraulic permeability and osmotic driving force would remain the same, and so the near zero order mass fraction release rate is unaffected.

It must also be noted that the polymer is undergoing hydrolytic degradation during the release phase. Nonetheless, with this polymeric delivery system, the acidic degradation products formed are water soluble and do not accumulate within the polymer but are released to the release media shortly after they are formed, confining polymer degradation and thus solute release to the surface. However, given that extended periods of constant release were observed when non-hydrolyzable poly(trimethylene carbonate) was used [30] which were similar in time scale to the release duration in this study when OCT-PEKCDLLA 2 was used, it would appear that the influence of polymer degradation on the release rate is not large. The low impact of polymer degradation on release may be due to the fact that degradation is proceeding more slowly than solute is being released.

5.6 Conclusions

These studies indicate that low molecular weight poly(5-ethylene ketal ε-caprolactone) based polymers have many suitable qualities to act as a viscous, injectable polymer for localized delivery of therapeutic proteins in a sustained manner, with a near zero-order release profile and with minimal burst effect via the osmotic release mechanism. BSA encapsulated with trehalose as the osmotigen was transported by convection driven by the osmotic pressure generated, through

interconnected hydrated regions formed by the transport of excess water into the swelling particle region. The osmotic pressure generated by the dissolved particle and the hydraulic permeability of the hydrated zone surrounding the swelling particle region determines to a large extent the rate of solute release from these delivery systems. The hydraulic permeability of the polymer can be varied by the choice of initiator used in the ring opening polymerization and/or by copolymerizing with D,L-lactide.

Chapter 6

IN VIVO DEGRADATION AND TISSUE RESPONSE TO OCTAN-1-OL INITIATED POLY(5-ETHYLENE KETAL Ɛ-CAPROLACTONE-CO-D,L LACTIDE)

Iyabo Oladunni Babasola, Juares Bianco[†] and Brian G. Amsden[†]

Department of Chemical Engineering, Queen's University, Kingston, ON, Canada

[†]Human Mobility Research Centre, Kingston General Hospital, Kingston, ON, Canada

This paper focuses on the fourth specific objective of this thesis, which was to investigate the *in vivo* biodegradation and tissue response to octan-1-ol initiated poly(5-ethylene ketal ε-caprolactone-co-D,L lactide) when subcutaneously implanted in rats. The sectioning of the tissue after retrieval from the animal, the histology and immunohistological stainings and macrophage count were done by Juares Bianco, the second author of this paper.

Abstract

The purpose of this study was to measure the *in vivo* biodegradation rate and assess the tissue response to octan-1-ol initiated poly(5-ethylene ketal ε-caprolactone-co-D,L-lactide) (OCT-PEKCDLLA) after subcutaneous injection in rats. The mass loss, change in molecular weight, change in composition and thermal properties of the polymer were monitored and evaluated as a function of implantation time over an 18 week period. The tissue response was assessed histologically using Masson's trichrome staining and immunohistochemically by staining for CD68 positive cells. The polymer lost weight with time in a nearly linear fashion and this was not accompanied by a significant change in number average molecular weight, polydispersity index, glass transition temperature and monomer ratio for 18 weeks, indicating a surface erosion process. A moderate foreign body reaction with the infiltration of numerous cells into the implantation site with no fibrous capsule formation was observed in the first week. The infiltrated cells at the implantation site consisted of granulocytes, fibroblasts and macrophages adjacent to the polymer-tissue interface, which persisted with the formation of fibrous capsule around the implant. The inflammatory response decreased with implantation time, but was still ongoing at 18 weeks, due to incomplete resorption of the polymer. The tissue response to the polymer was moderate and comparable to that reported in the literature for poly(trimethylene carbonate), poly(lactic acid) and poly(lactic-co-glycolic acid). This study demonstrates that OCT-PEKCDLLA biodegrades *in vivo* in a surface erosion fashion, with a moderate tissue response to the degradation products of the polymer, indicating that the polymer is biocompatible. These findings make this polymer a potential candidate for injectable drug delivery, and other biomedical applications.

6.0 Introduction

There is an increased demand for drug-delivery systems that can provide local, controlled and sustained release of drugs via a minimally invasive procedure. To meet these demands, a number of different polymer formulation approaches have been investigated that can be injected directly into the required site without the need for surgical implantation and retrieval, and once injected, form a depot. Such approaches include in situ crosslinked systems[35, 36], in situ thermo-gelling systems[139], and liquid injectable hydrophobic polymers [30, 130, 131, 160]. Polymers investigated as liquid injectable hydrophobic polymers include poly(ortho esters) (POEs),[131, 132, 152-155], low molecular weight poly(α-hydroxy acids) [157, 164, 185, 186], hexyl-substituted poly(lactide) [187-190], and poly(trimethylene carbonate)[30, 160]. The advantages of the use of liquid injectable hydrophobic polymers are the relatively straightforward drug incorporation procedure and the lack of mechanical irritation of the surrounding tissue. Mechanical irritation of the surrounding tissue can result in a thicker fibrous encapsulation layer, [191, 192] which may retard drug absorption into the tissue. Furthermore, the polymer viscosity and thus the injectability can be controlled by appropriate selection of monomer and initiator [30, 130, 160].

Recently, we have investigated the use of 5-ethylene ketal ε-caprolactone (EKC) based, low molecular weight polymers as injectable drug delivery vehicles [130]. These polymers degrade *in vitro* by surface erosion [130], a feature that might be advantageous in preserving the bioactivity of incorporated therapeutic proteins. EKC has been homopolymerized and copolymerized with D,L-lactide using either 350 Da methoxy poly(ethylene glycol) (PEG) or octan-1-ol as initiators. The resulting polymers were amorphous, liquid, and possessed a low viscosity making them injectable. The viscosity and the *in vitro* degradation rate were controlled by the hydrophilicity of

the initiator used and/or by copolymerizing with D,L-lactide. The copolymer of EKC with DLLA initiated with octan-1-ol was chosen for further investigation because of its ability to deliver a model protein drug, BSA, in a sustained manner, with near zero order release profile, and with no burst release for an extended period of time (Chapter 5). The higher viscosity imparted on the polymer by copolymerizing with D,L-lactide would ensure that the polymer formed an effective depot at the injection site.

Important criteria for the practical *in vivo* application of this polymer are an understanding of both the host tissue response after implantation, and the *in vivo* degradation rate and process. The objectives of this study were therefore to measure the *in vivo* biodegradation rate and assess the tissue response to octan-1-ol initiated poly(5-ethylene ketal ε-caprolactone-co-D,L-lactide) following subcutaneous injection in rats. The mass loss, change in molecular weight, change in composition and thermal properties of the polymer were monitored and evaluated as a function of implantation time. The tissue responses were assessed histologically using Masson's trichrome staining and immunohistochemically by staining for CD68 positive cells.

6.1 Materials

1,4-cyclohexanedione monoethylene ketal (97% purity), meta-chloroperoxybenzoic acid (MCPBA) (97% purity), octan-1-ol (anhydrous, 99% purity), stannous 2-ethylhexanoate (95% purity), and Dulbecco's phosphate buffered saline (PBS) were obtained from Sigma-Aldrich, ON, Canada. D,L-lactide was obtained from Purac, the Netherlands and purified by recrystallization from dried toluene. 1% (w/v) bovine serum albumin (BSA type V) was obtained from Sigma, St Louis, USA, primary antibody mouse anti-rat CD68 was obtained from AbD Serotec, UK, (cat#

MCA341R), secondary antibody anti-mouse IgG was obtained from VectaStain ABC KIT, US (cat# PK-6102), streptavidin-peroxidase and 3.3-diaminobenzidine were obtained from Sigma, St. Louis, USA, Harris' hematoxylin permont was obtained from (Fisher Scientific, US, (cat# SP15-100), and Masson's trichrome was obtained from Sigma Aldrich, Oakville, ON.

6.2 Methods

6.2.1 Synthesis of poly(5-ethylene ketal ε-caprolactone- co-D,L-lactide)

The 5-ethylene ketal ε-caprolactone monomer was prepared by the Baeyer-Villiger oxidation of 1,4-cyclohexanedione monoethylene ketal by meta-chloroperoxybenzoic acid (MCPBA), and used to prepare the copolymer by polymerizing with D,L-lactide via ring-opening polymerization utilizing stannous 2-ethylhexanoate as a catalyst and octan-1-ol as initiator. The copolymerization was done in the bulk at 110ºC for 24 hrs. The initial physical properties of the polymer thus prepared are shown in Table 6-1 [130].

Table 6-1: Physical properties of OCT-PEKCDLLA. [130]

monomer ratio (EKC:DLLA (mol:mol))	T_g[a] (°C)	M_n[b] (Da)	PDI[c]	$\eta_{37°C}$[d] (Pa·s)	$\eta_{40°C}$[e] (Pa·s)
3.2 : 1	-17.3	2740	1.1	180.0	122.0

[a] glass transition temperature, [b] number average molecular weight, [c] polydispersity index, [d] zero shear rate viscosity at 37ºC, and [e] zero shear viscosity at 40ºC.

6.2.2 *In vivo* Biocompatibility and Biodegradation Studies

The animal experiments were done in accordance with the guidelines of the Canadian Council on Animal Care code of ethics governing animal experimentation (protocol # Amsden 2007-043-R1). The polymers were loaded into 1 mL plastic syringes, which were then sterilized by germicidal UV source (Phillips; G30T8) (253.7nM) for 30 minutes. Prior to injection, the polymers were preheated to 40 ºC in a water bath. A total of 16 male Wistar rats, weighing approximately 340 g, were used. The rats were anesthetized with 2% isoflurane (Baxter Corp.) in oxygen by an Engler ADS 1000 (Benson Medical Industries) at a flow rate of 0.2 $mL \cdot min^{-1}$ of O_2. At a level of surgical anesthesia (i.e., lack of tail and corneal reflexes), the rats were shaved at the site of implantation, the shaved area was disinfected with Hibitane, and 100 µL (120 mg) of the polymer was injected through an 18 1/2 G 1.5" needle. Three animals were used for each time point, with three injection sites per animal. The implanted polymers were excised on weeks 1, 4, 8, 12 and 18. At each explantation time point, the rats were anesthetized with 2% isoflurane (Baxter Corp.) in oxygen followed by an intraperitoneal injection of Somnotol (65 $mg \cdot kg^{1}$). The site of implantation was shaved and the skin was dissected back. One tissue sample containing the implanted polymer was harvested from one implantation site from each animal and fixed in 4% paraformaldehyde in phosphate-buffered saline for histological analyses. The tissue surrounding the other two implantation sites from each animal were carefully removed, and put into glass vials. This tissue was frozen at -80°C then cut into small pieces with a scalpel. The diced tissue was immersed in dichloromethane (DCM) and vortexed until the polymer is dissolved and centrifuged to extract the polymer from the tissue. The DCM phase was gently decanted into a previously weighed eppendorf tube. This process was repeated twice. The DCM was evaporated

at 50°C for 2 days, and then residual DCM was removed via lyophilization. The mass of the extracted polymer was measured and used to calculate the percent weight loss.

The polymers' number average molecular weight (M_n), weight average molecular weight (M_w), and polydispersity index (PDI), were obtained by gel permeation chromatography (GPC). The GPC apparatus consisted of a Waters 1525 Binary HPLC pump and a Precision Detectors Enterprise PD2100 Series combined refractive index and light scattering detector. Samples were prepared in anhydrous tetrahydrofuran (THF) at concentrations of 30 $mgmL^{-1}$. They were filtered through a 0.45 µm filter and 100 µL was injected into an Ultrastyragel column (500 Å, 7.8 × 300 mm^2) at 1.0 $mLmin^{-1}$ and a temperature of 30 ºC. Data acquirement and processing were conducted using the Precision Detectors' Aquire32 and Discovery32 software programs. The increment of refractive index (0.065 mL/g)) used in the molecular weight calculations was measured using a Wyatt Optilab rEX as described previously [130].

^{1}H-NMR spectra of the polymers were recorded in DMSO-d6 on a 400 MHz Bruker Avance spectrometer. The polymer number average molecular weights were calculated by end group analysis from the signal intensity of the methyl group of octan-1-ol at δ = 0.85 ppm and PEG at δ = 3.23 ppm, and the methylene group at δ = 2.3 ppm for EKC and methine group at δ = 5.1 ppm for DLLA. The ratio of EKC to DLLA in the polymer was obtained by comparing the integration of the EKC peak at δ = 2.3 ppm to the integration of the DLLA peak at δ = 5.1 ppm.

The glass transition temperature was obtained using a DSC 1 STARe system (Mettler Toledo). The samples were run at a heating and cooling rate of 10 °C/min using the following

temperature program. The sample was first cooled from 25°C to -90°C and held at -90°C for 3 minutes, followed by heating from -90°C to 105°C with a hold time of 3 minutes at 105°C. It was further cooled from 105°C to -90°C and held at -90°C for 3 minutes. The sample was finally heated from -90°C to 105°C. The glass transition temperature (T_g) was obtained from the inflection point of the second heating cycle.

6.2.3 Histological and Immunohistochemistical Analyses

The explants were fixed in 4% paraformaldehyde in phosphate-buffered saline immediately after extraction. The tissues were then transferred to 70% v/v ethanol in distilled water and stored at 4ºC until processing. The tissues were re-hydrated in graded ethanol, cleared in toluene, and then embedded in paraffin. Tissue sections were cut at 5 μm intervals and stained with Masson's trichrome. The sections were observed and photographed with a Zeiss Imager M1 microscope. For immunohistochemistry, endogenous peroxidase activity was blocked using 3% (v/v) H_2O_2 in distilled water, followed by incubation in 1% (w/v) bovine serum albumin in 0.01M phosphate buffer (pH 7.4) (BSA type V, Sigma, St Louis, USA). The tissues were then incubated with the pan-macrophage primary antibody mouse anti-rat CD68 diluted in 0.2% (w/v) BSA in 0.01M phosphate buffer pH 7.4. After incubation in the primary antibody at 4°C overnight, a secondary antibody anti-mouse IgG was used for 2 hours at room temperature. The sections were incubated with streptavidin-peroxidase followed by 0.5 mg/mL 3,3-diaminobenzidine and 0.3% (v/v) hydrogen peroxide treatment in distilled water. The sections were counter-stained with Harris' hematoxylin and mounted under a cover slip. Each immunohistochemical experiment included one negative control. For the negative controls, the primary antibody was replaced by normal rabbit/mouse serum. The sections were also observed and photographed with a Zeiss

Imager M1 microscope. For each sample, multiple sections were cut and a total of ten images from each sample were captured using Zeiss Axio Vision (version 4.6). On these images, the fibrous capsule area was measured and the macrophages in this area were counted using Axio Vision, Zeiss, Germany, version 4.7.0.0. A final total score for each animal per time point was averaged (n=3) and the number of macrophages per 10^4 μm^2 was calculated.

6.3 Statistics

All polymer property measurements were done on triplicate samples and are reported as the average ± the standard deviation about the average.

6.4 Results

Prior to injection, the polymer was a viscous, transparent, and yellow liquid. Due to its low viscosity when pre-warmed to 40 ºC, the polymer was injectable through an 18 ½ G needle. All the animals gained weight and showed no sign of discomfort or adverse responses such as sores on the skin throughout the study period. Figure 6-1 shows representative images of polymer samples within the subcutaneous tissue at weeks 1, 4, 12 and 18. The injected polymer samples presented a cohesive mass at the implantation site. Due to absorption of water from the surrounding tissue, the polymers appeared opaque after implantation.

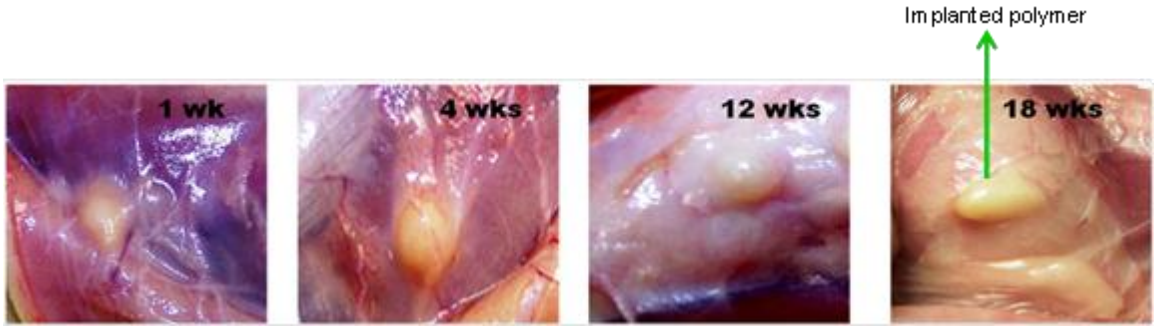

Figure 6-1: Representative photographs of OCT-PEKCDLLA samples in the subcutaneous tissue before explanting at weeks 1, 4, 12 and 18.

6.4.1 *In vivo* biodegradation

Figure 6-2 shows the *in vivo* weight loss of the polymer from week 1 to week 18. Mass loss was nearly linear with time. By week 4, OCT-PEKCDLLA had lost 14.8. ± 8.4 % of its initial weight *in vivo*, which increased to 52.2 ± 19.1 % by week 18 (Figure 6-2). The large variability could be attributed to the assumption that exactly 100 µL of the polymer was injected through the syringe, which was measured to weigh 120 mg. Although significant care was expended in retrieving the polymer from the tissue, it is also possible that the polymer was not completely retrieved from each sample. Figure 6-3 shows the ^{1}H NMR spectra of the polymer before implantation and at 8 and 18 weeks after implantation. Only the polymer was extracted from the tissue, as no peaks apart from the expected polymer peaks were observed, indicating that the mass loss measured was not influenced by the extraction of lipids from the surrounding tissue. Furthermore, the physical properties of the polymer did not change significantly over the 18 weeks of the *in vivo* implantation time frame (Table 6-2).

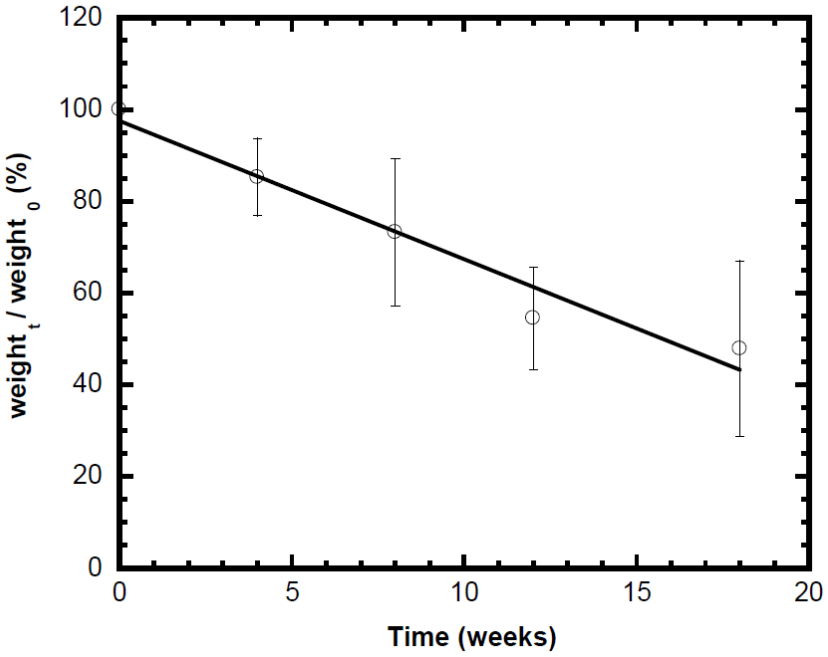

Figure 6-2: Weight loss of the polymers during *in vivo* and *in vitro* degradation. The error bars indicate the standard deviation of 6 samples (2 from each rat). The solid line is a linear curve fit to the data over the time period indicated by the length of the line (coefficient of determination for the linear regression was = 0.97).

Table 6-2: Physical properties of *in vivo* degraded polymer with time

Time (weeks)	**T_g[a] (^oC)**	**M_n[b] (Da)**	**PDI[c]**	**EKC:DLLA**
0	-17.3	2740 ± 90	1.09 ± 0.01	3.3 ± 0.2
1	-17.6	2810 ± 100	1.09 ± 0.01	3.4 ± 0.2
4	-17.2	2760 ± 90	1.10 ± 0.01	3.4 ± 0.1
8	-17.5	2720 ± 70	1.09 ± 0.01	3.7 ± 0.1
12	-17.5	2720 ± 100	1.09 ± 0.02	3.6 ± 0.3
18	-15.8	2490 ± 70	1.08 ± 0.00	3.0 ± 0.4

[a] glass transition temperature [b] number average molecular weight (GPC), [c] polydispersity index.

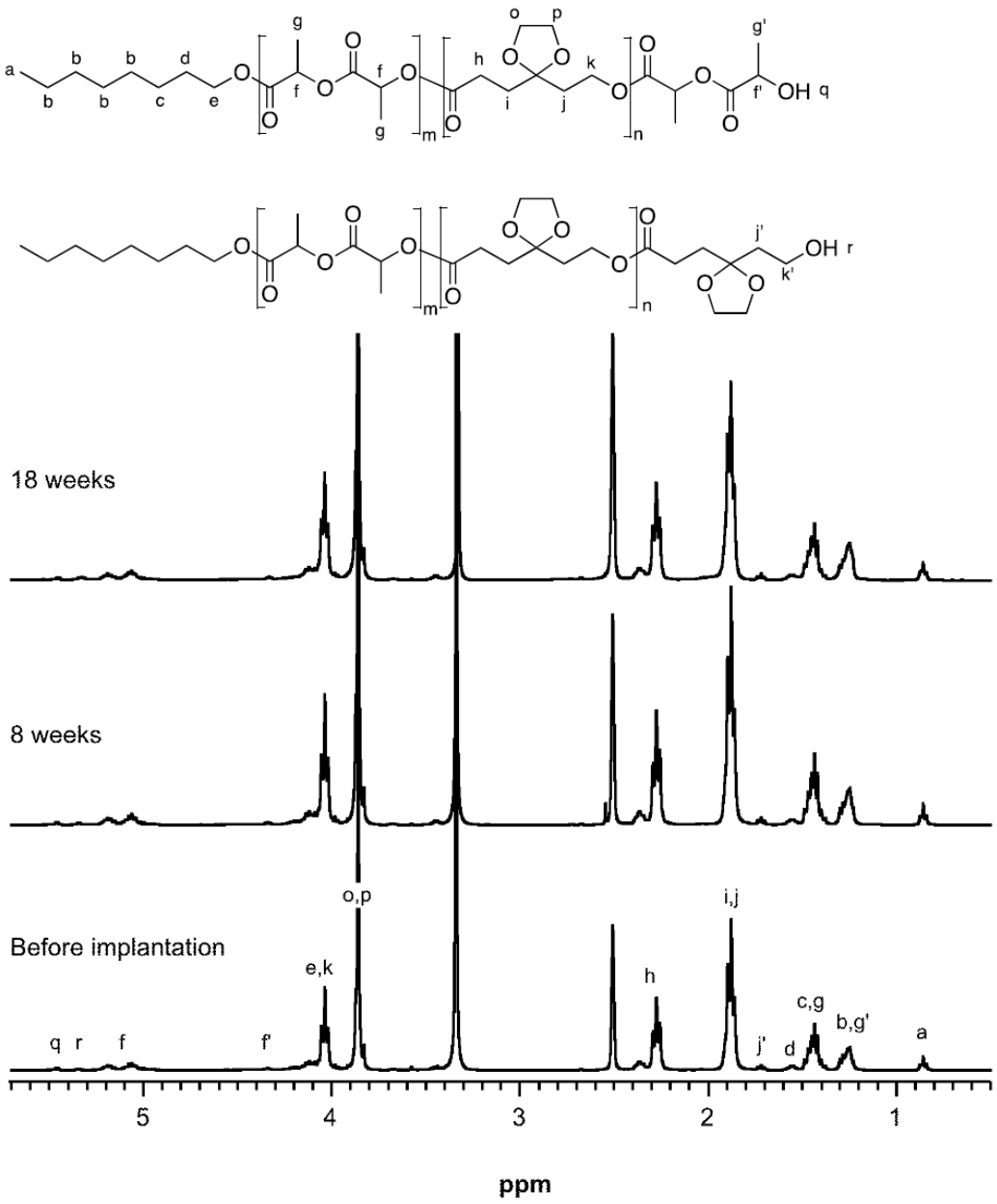

Figure 6-3: ^{1}H-NMR spectra of OCT-PEKCDLLA before implantation and at 8 and 18 weeks after implantation.

6.4.2 Histology and Immunohistochemistry

Tissue sections were stained with Masson's trichrome to determine the host tissue reaction to the implant. Masson's trichrome stains collagen blue, cytoplasm and muscle fiber red and nuclei black. The areas evaluated were the implant-tissue interface and the surrounding fibrous capsule. The cellular compositions around the implants were determined in conjunction with the immunostaining and the thickness of the fibrous capsule formed around the implant was measured using Image J (version 1.45). Representative photomicrographs of tissue sections stained with Masson's trichrome are shown in Figure 6-4, while the thickness of the fibrous capsule surrounding the implant with time is shown in Figure 6-5.

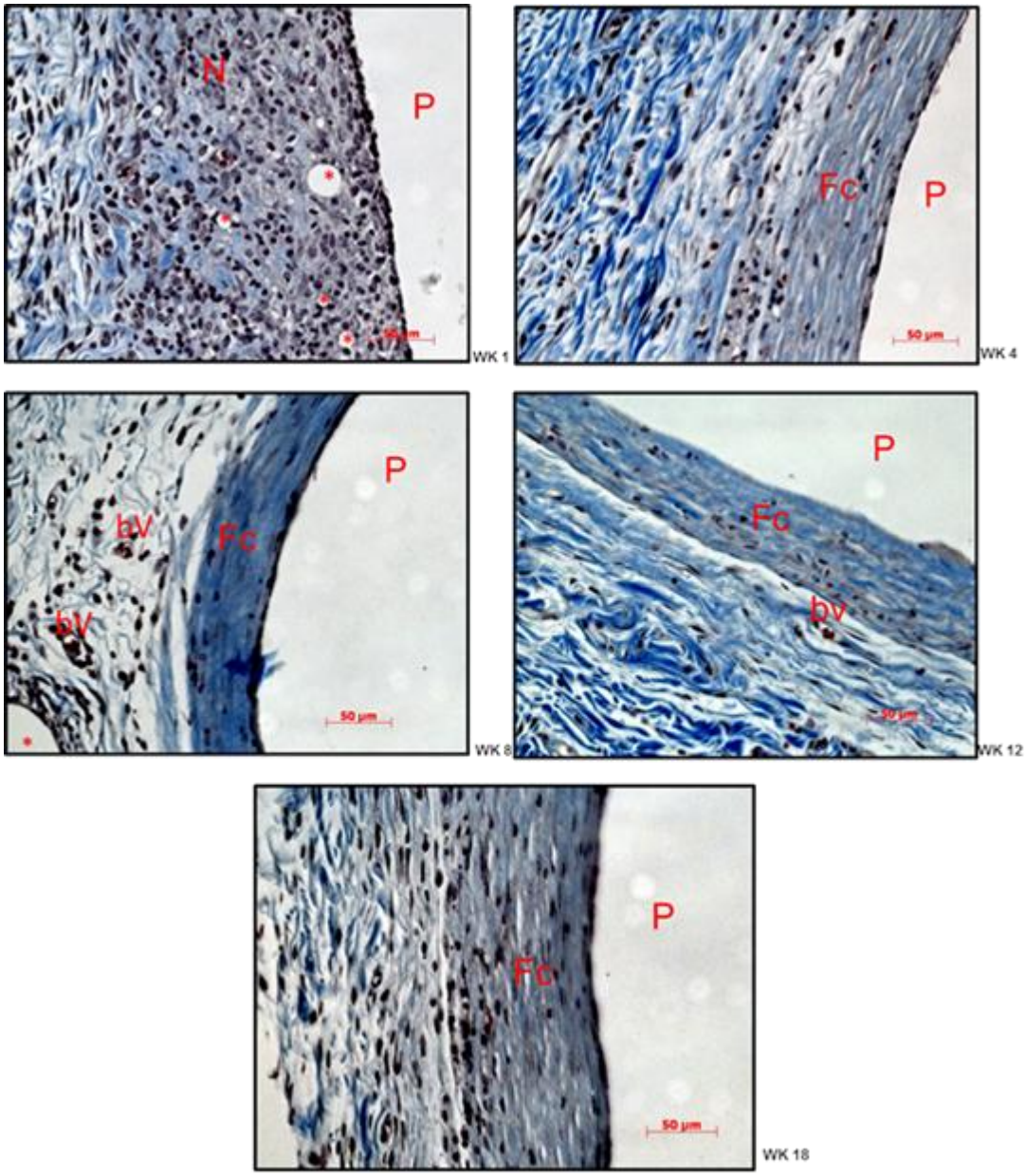

Figure 6-4:Photomicrographs of tissue sections of implanted OCT-PEKCDLLA stained with Masson's trichrome after 1, 4, 8, 12 and 18 weeks of implantation in rats. (P) polymer, (Fc) Fibrous capsule, (*) probably polymer droplet, (bv) blood vessels, (N) probably neutrophils.

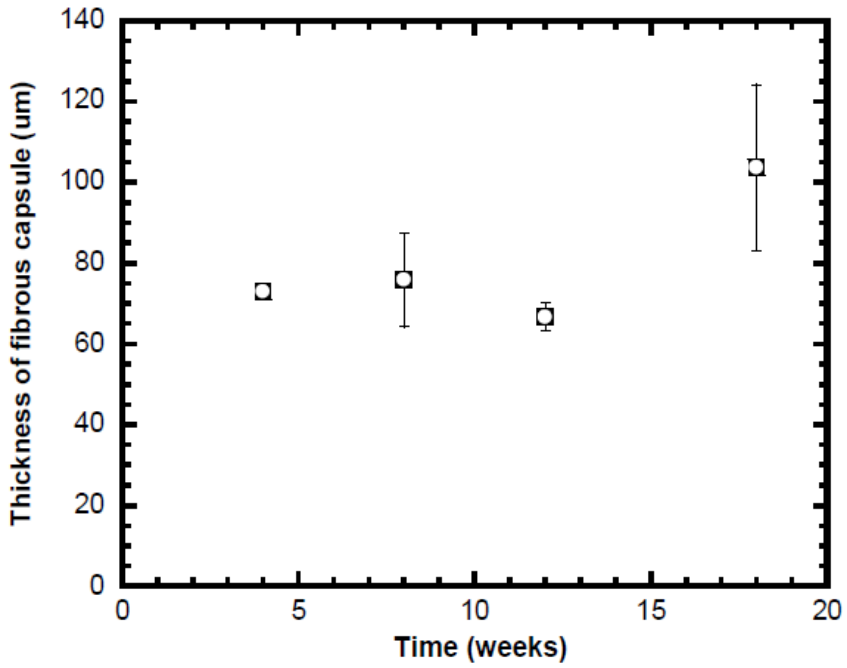

Figure 6-5: Thickness of fibrous capsule formed around the implant after 4, 8, 12 and 18 weeks of subcutaneous implantation in rats.

By week one, there were several layers of cell infiltrate at the implantation site, which included fibroblasts, granulocytes and macrophages with no evidence of fibrous capsule formation. There were small polymer droplets in the tissue surrounding the implant site. These small droplets were also surrounded by a layer of granulocytes, macrophages and fibroblast cells. By week 4, a fibrous capsule with a thickness of 73 ± 5 µm had formed around the implant and the number of cells in the inflammatory zone had decreased significantly compared to that observed in the first week. These cells were concentrated within the implant-tissue interface and the surrounding fibrous capsule, and consisted of macrophages and fibroblasts. There were fewer polymer droplets in the tissue surrounding the implant compared to what was observed in week 1, and these polymer droplets were also surrounded by cells. By week 8 and 12, the thickness of the

fibrous capsule formed around the implant was similar to that observed in week 4, but the macrophage infiltrate to the implantation site had been further reduced. Foreign body giant cells (FBGCs) were seen at week 8. By week 18, the fibrous capsule thickness had increased to 103 ± 20 μm and the macrophage invasion was greater than that in week 12, but was comparable to that observed in week 8.

Macrophages are cells produced by the differentiation of monocytes within tissues. Their role is to phagocytose cellular debris, pathogens and foreign materials. They also secrete chemotactic signals to other cells types that will participate in the wound healing process [134]. It is important to estimate the number of macrophages at the site of implantation because the extended presence of macrophages and FBGCs at the site of implantation is an important marker of chronic inflammation [136]. In order to quantitatively determine the number of macrophages and FBGCs, tissue sections were stained for the macrophage marker CD68 by immunostaining. CD68 is a glycoprotein that binds to low density lipoprotein, and is highly expressed on monocytes and macrophages[193]. CD68 positive cells are stained brown in Figure 6-6.

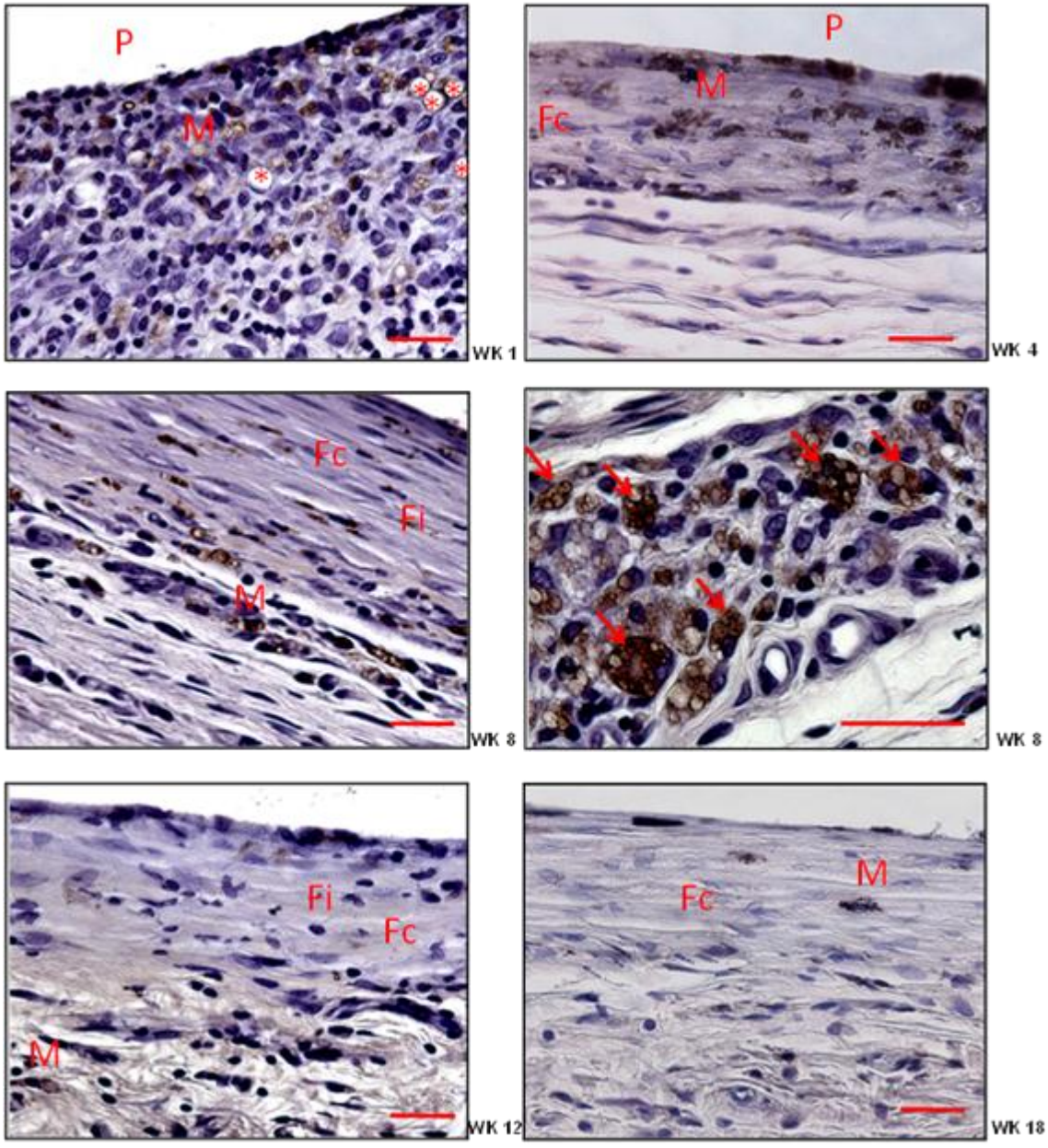

Figure 6-6: Photomicrographs of tissue sections of implanted OCT-PEKCDLLA stained for CD68 after 1, 4, 8, 12 and 18 weeks of implantation in rats. (P) site of polymer implantation, (Fc) Fibrous capsule, (*) probably polymer droplet, (arrow) multi nucleated giant cells, (Fi) fibroblast and (M) macrophages. Bar is 40 µm. The photomicrograph on the right labelled wk 8 is a higher magnification.

The sites of interest were the interface between the implant and the tissue, and the fibrous capsule formed. The number of macrophages (CD68+) within a selected area was counted and expressed as the number of macrophages/10^4 μm^2 (Figure 6-7). By week 1, 11 ± 3 macrophages and foreign body giant cells /10^4 μm^2 were found at the implant site, and they were evenly distributed in the surrounding tissues. A layer of macrophages was also found around the small polymer droplets and cellular debris in the surrounding tissue. By week 4, the area of the inflammatory zone had decreased and a fibrous capsule had been formed around the implant. About 12 ± 3 macrophages /10^4 μm^2 were found in the inflammatory region. The macrophages were concentrated within the fibrous capsule formed, mainly at the polymer-tissue interface and at the edge of the fibrous capsule, where the fibrous capsule interfaced with the surrounding tissue. At this time, the number of cells per 10^4 μm^2 that were positively stained for macrophages were not different from that observed in week 1. By week 8 and week 12, the intensity of the inflammatory cell infiltrate had further reduced. About 6 ± 4. and 4 ± 1 macrophages / 10^4 μm^2 respectively were found adjacent to the implant, and the surrounding fibrous capsule respectively. By week 8, some macrophages had fused together to form FBGCs, but the number of FBGCs seen by week 12 had decreased. By week 18, the macrophages still persisted with 7 ± 0 macrophages / 10^4 μm^2 and were mostly at the interface between the tissue and the polymer, but the number of macrophages per 10^4 μm^2 was still comparable to that observed at week 8.

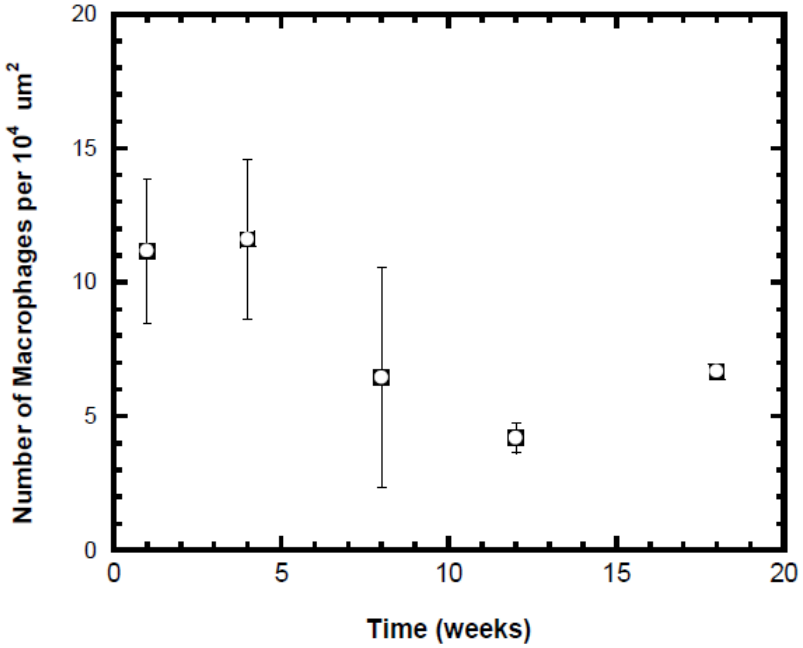

Figure 6-7: Number of macrophages and foreign body giant cells at the interface between the implant and the surrounding capsule per 10^4 μm^2. The error bars indicate the standard deviation of 3 samples (1 from each rat, multiple sections were used with a total of 10 images from each sample).

6.5 Discussion

The purpose of using a controlled delivery device is to locally deliver drugs with controlled dose within therapeutically relevant concentrations, to minimize undesirable side effects and to protect the bioactivity of the drug. However, the implantation of a controlled delivery device evokes an inflammatory response that may influence its performance. The onset of the foreign body reaction shares several aspects of wound healing, which starts after the tissue is damaged by some sort of injury leading to clot formation, coagulation, and the deposition of a provisional matrix around the implant for phagocyte invasion[136 134]. These series of events is then followed by the acute inflammatory phase, chronic inflammatory phase, granulation tissue

formation, foreign body reaction and fibrous capsule formation. As part of the inflammatory response to implanted foreign body, neutrophils in the early stage, followed by monocytes and macrophages in the latter stage are attracted to the implant under the influence of secreted chemokines[140,136]. The secreted chemokines activate macrophages to synthesize nitric oxide which kills pathogens and prevents further infection. The macrophages also secrete enzymes and reactive oxygen species on the enclosed polymer surface in an effort to degrade it [135]. In addition, macrophages phagocytose foreign and debris material, however, due to the large size of the implanted material, macrophages may undergo "frustrated phagocytosis" and fuse together to form foreign body giant cells (FBGCs) under the influence of secreted cytokines such as interleukin-4 (IL-4) in an attempt to increase their effectiveness against larger and more resistant foreign bodies. The formation of FBGCs usually occurs after the third week [134, 135,136].

Fibroblast like cells (myofibroblasts) subsequently induces the formation of fibrotic scar tissue around the implant [134, 136]. The situation becomes especially complex if the implant becomes a source of irritation to the surrounding tissue due to mechanical irritation and/or the release of degradation products from the polymer [142, 143]. In this case, the presence of inflammatory cells at the implantation site would persist in an attempt to phagocytose the polymer and its degradation products. Moreover, the macrophages would secrete chemokines that would attract more macrophages to the site. As a result, the inflammatory response may not subside until the polymer fully degrades and the degradation products are eliminated from the implant site [191, 192]. The resolution of the foreign body reaction occurs when the polymer fully degrades. The inflammatory stimulus is removed, and the macrophages migrate away from the site towards the draining lymph nodes[134]. The fibroblasts produce collagenase that degrades the

fibrous capsule, thus initiating repair [134]. The nature and timing of the transition from inflammation to repair and the extent of clinical manifestation of the inflammation will depend on the reaction of the tissue to the polymer and its degradation products.

The tissue response to the OCT-PEKCDLLA was characterized by the presence of fibroblasts, granulocytes and macrophages at the implant-tissue interface with no formation of fibrous capsule in the first week, signifying the acute inflammatory phase. The macrophage invasion at the site of implantation persisted in the fourth week with subsequent encapsulation to wall off the polymer in a fibrous capsule with thickness of 73 ± 5μm. From week 8 to week 12, the thickness of the fibrous capsule was not different from that observed at week four, while the macrophage invasion per 10^4 μm ^{2} had reduced compared to that observed in week 4. By week 8, some macrophages had fused together to form FBGCs. By week 18, thickness of the fibrous capsule formed and the macrophage invasion per 10^4 μm^2 increased slightly. This could be in response to the acidic degradation products formed upon polymer backbone hydrolysis, which accumulated at the polymer/tissue interface due to the thicker fibrous capsule that surrounded the implant. Thus, the progression of the inflammatory response was decreasing with time, but was still ongoing because the polymer was not completely degraded.

The thickness of the fibrous capsule formed was 73 ± 5 μm at week 4, which increased to 103 ± 20 μm by week 18. The thickness of the fibrous capsule formed after 18 weeks of subcutaneous implantation in rats was less than the 140 μm reported for poly(lactic-glycolic acid) (PLGA) disk [192] after 2 weeks of implantation, 200 μm reported for PLA rod after 18 months of subcutaneous implantation in rabbits[191], and 132 ± 10 μm reported for 2400 Da liquid injectable

poly(trimethylene carbonate) developed within the first week of subcutaneous implantation in rats [160]. However, the fibrous capsule thickness is higher than the 15 ± 9 μm reported for 620 Da liquid injectable poly(trimethylene carbonate) developed within the first week of subcutaneous implantation in rats [160] and 45 μm reported for poly(glycerol sebacate) slab which developed within 5 weeks after subcutaneous implantation in rats [192].

The progression of macrophage invasion at the site of implantation, though not quantitatively determined in other studies, is similar to that observed for subcutaneously implanted PLA rod and disk in rats[191, 194] and poly (trimethylene carbonate) (PTMC) films in rats[195] which is at the maximum when the polymer is actively degrading. Considering the observed tissue response to the implanted OCT-PEKCDLLA, it can be concluded that the EKC-based copolymer elicits a moderate tissue response comparable to that observed for biodegradable polymers in clinically used devices.

Depending on polymer properties, degradation of polymers *in vivo* is as a result of either hydrolysis and/or cell mediated processes such as enzymatic action or reaction with reactive oxygen species [135]. The *in vitro* degradation of the homopolymers of EKC and copolymers of EKC with DLLA has been previously reported [130]. During 24 weeks of *in vitro* degradation in phosphate buffer saline solution at pH 7.4 and a temperature of 37°C, the homopolymers and copolymers lost weight with time in a nearly linear fashion with no significant change in T_g and M_n. With the copolymer, the ratio of EKC and DLLA remained essentially the same throughout the study period. Minimal water penetration into the bulk polymer occurred, and mass loss was confined to the interface of the polymer with the aqueous media. The above *in vivo* degradation

of the polymer was characterized by similar results. The mass decreased with time in a nearly linear fashion, and there was no change in M_n, T_g and the EKC to DLLA ratio, suggesting surface erosion as observed *in vitro*.

6.6 Conclusions

In vivo, following subcutaneous implantation in rats, low molecular weight, viscous liquid octan-1-ol initiated poly(5-ethylene ketal ε-caprolactone-co-D,L lactide) exhibited surface erosion characterized by a nearly linear weight loss with time, with no significant change in M_n, T_g and ratio of EKC to DLLA for 18 weeks. The polymer induced a moderate inflammatory response, which was comparable to that of other clinically used biodegradable polymers. These findings suggest that this polymer has potential as an injectable drug delivery device. Nevertheless, a longer term *in vivo* study, taken up to the point that the polymer is completely resorbed, is necessary to have a complete insight of the host response to this polymer.

Chapter 7

CO-RELEASE OF VEGF AND HGF FROM OCTAN-1-OL INITIATED POLY(5-ETHYLENE KETAL Ɛ-CAPROLACTONE)

Iyabo Oladunni Babasola and Brian G. Amsden[†]

Department of Chemical Engineering, Queen's University, Kingston, ON, Canada

[†]Human Mobility Research Centre, Kingston General Hospital, Kingston, ON, Canada

This paper focuses on the fifth objective of this research, which was to investigate the potential of liquid injectable octan-1-ol initiated poly(5-ethylene ketal ε-caprolactone-co-D,L lactide) to co-release VEGF and HGF at therapeutically relevant concentrations, using the osmotic release mechanism.

Abstract

The potential of a liquid injectable delivery system made from octan-1-ol initiated poly(5-ethylene ketal ε-caprolactone-co-D,L-lactide) (OCT-PEKCDLLA) to release bioactive vascular endothelial growth factor (VEGF) and/or hepatocyte growth factor (HGF), using an osmotic pressure release mechanism for the purpose of treating critical limb ischemia was investigated. Co-release of VEGF with HGF was chosen because of reports of their potential to initiate the proliferation and migration of endothelial cells in a synergistic manner to form stable blood vessels. VEGF and HGF were lyophilized separately with trehalose and bovine serum albumin (BSA), and incorporated into the polymer separately or together by simple mixing. VEGF and HGF were released by convective flow created by the osmotic pressure generated upon dissolution of the particles. When the HGF and VEGF particles were mixed together into the polymer at 5% (w/w) loading each, a nearly zero order, sustained release of bioactive VEGF and HGF for over 41 days with no burst release was achieved under conditions of multidirectional release. VEGF was released at 36 ± 7 ng/day for 41 days, while HGF was released at 16 ± 2 ng/day for 70 days. Factors affecting the release of the growth factors from this delivery device were the solubility of growth factor in the concentrated trehalose solution and hydraulic permeability of the polymer. The released VEGF maintained approximately 90% bioactivity for more than 100 days, while the released HGF maintained approximately 80% bioactivity over 90 days. This formulation approach, of using a low viscosity polymer delivery vehicle, is potentially useful for localized delivery of acid and temperature sensitive proteins, such as VEGF and HGF.

This system may also serve as a platform for controlled and predictable delivery patterns for other therapeutic proteins in other clinical settings.

7.0 Introduction

Peripheral vascular occlusive disease is a gradual illness that results in occlusion of arteries to the limb, due to atherosclerosis of large and medium sized arteries [1]. The flow of blood to the distal tissues is severely impeded as the condition advances, depriving these tissues of oxygen and nutrients, which leads to critical limb ischemia (CLI) in tissues fed by the diseased artery [2]. Symptons experienced by these patients include chronic ischemic rest pain, ulcers, or gangrene in the lower limb, and a poor prognosis [3]. This illness affects roughly 27 million people in the western world [2, 4] and it is estimated that there are 500 new cases of critical limb ischemia per million individuals in the USA and Europe each year [3].

Current therapies for short occlusions of the iliac arteries can only be improved by angioplasty, and long segments of occlusions, especially those distal to the common femoral artery, are best treated by bypass surgery[2, 4] . These treatment options are highly invasive and lead to eventual amputation in more than 50,000 patients each year in the United States [2]. For 10-30% of these patients, revascularization is not a suitable option; greater than 40% of this patient population will require major amputation, and 20% will die within 6 months [3, 4, 8]. The body has the capacity to develop new collateral blood vessels to mediate ischemia by producing endogenous growth factors, but this natural biologic response, termed angiogenesis, is a slow process, and is often unable to replace the lost blood flow completely [9]. As a result, the exogenous administration of these growth factors has been investigated, a treatment termed therapeutic angiogenesis.

Therapeutic angiogenesis can be achieved through the local administration of various growth factors, such as vascular endothelial growth factor (VEGF) [30, 31, 33], hepatocyte growth factor (HGF)[31, 34, 36] and basic fibroblast growth factor (bFGF)[34, 37]. However, the therapeutic use of these growth factors is limited by their short half-lives *in vivo* [37, 133, 196]. The growth factors are quickly cleared or metabolized in the tissue, because of the hostile ischemic environment created by the extensive protein degradation that takes place as part of inflammation and extracellular matrix (ECM) remodeling-induced enzymatic responses [48]. These growth factors must be delivered over a 4 - 6 weeks' time frame, however, to attain therapeutically relevant local concentrations via systemic injection, multiple large doses must be injected, which may result in unwanted blood vessel growth and other undesired side effects [64].

Although delivery of a single growth factor may initiate angiogenesis [30, 64], multiple triggers are needed to work together in a coordinated sequence to complete the angiogenic process and generate stable vessels [40, 60-63]. It is thus generally accepted that the co-administration of multiple growth factors is required to generate effective therapeutic angiogenesis. To overcome formulation complexities associated with sequential delivery of such growth factors, another approach would be the simultaneous delivery of growth factors that act synergistically. One such growth factor combination could be VEGF and HGF. VEGF is the most extensively studied angiogenic growth factor for this purpose, because it promotes the initial stages of angiogenesis by stimulating the proliferation and migration of endothelial cells, which is an essential rate limiting step in physiological angiogenesis [30, 60, 61, 64]. HGF stimulates endothelial cells to proliferate and migrate *in vitro* [42, 52], up-regulates the production of VEGF by human keratinocytes [49, 50]and endothelial cells [50] and acts as a chemoattractant for pericytes [40, 51] to induce

stable blood vessel formation[65]. Studies have shown that the direct effects of HGF on endothelial cell proliferation and migration are similar to that induced by VEGF, and the combination of VEGF and HGF produced a synergistic effect on endothelial cell proliferation and migration[42, 52, 66].

Liquid injectable hydrophobic polymeric vehicles possess certain attributes that make them a potentially attractive delivery vehicle for these growth factors. They allow facile incorporation of thermally sensitive drugs such as proteins and peptides by simple mixing [131, 132], they are injectable through standard gauge needles, and so can be administered via minimally invasive means [131], there is no need for device retrieval, as the polymers are biodegradable [131], and there is restricted water penetration, which may provide enhanced stability for drugs such as proteins incorporated as solid particles[30].

Poly(5-ethylene ketal ε-caprolactone) (PEKC) has several features that qualifies it as a potential injectable delivery system for protein therapeutics. PEKC is amorphous and at low molecular weight, has a viscosity that allows it to be injected through standard gage needles[130]. The EKC monomer also can be readily copolymerized with D,L-lactide, to control viscosity and biodegradability [130]. The pendant ketal group increases the hydrophilicity of the polymer, which enhances its hydrolytic degradation. Additionally, low molecular weight PEKC, and its copolymers, degrades by surface erosion [130], a feature that might be advantageous in preserving the bioactivity of incorporated therapeutic proteins. Furthermore, an octan-1-ol initiated poly(5-ethylene ketal ε-caprolactone-co-D,L-lactide) was well tolerated *in vivo* with a moderate chronic inflammatory response that decreased with implantation time (Chapter 6).

Previous work using bovine serum albumin (BSA) as a model protein drug, demonstrated that 2810 Da octan-1-ol initiated poly(5-ethylene ketal ε-caprolactone-co-D,L-lactide) was capable of releasing almost all entrapped BSA in a sustained manner over a period of months utilizing an osmotic release mechanism (Chapter 5). The osmotic mechanism is considered to proceed as follows. Protein release is governed by the water activity gradient between the surrounding aqueous medium and the saturated solution, which forms when water is absorbed into the polymer from the surrounding medium and dissolves a polymer-encapsulated particle, forming a saturated solution. The activity gradient increases the rate of water transport to the particle surface. The imbibed water generates an internal pressure equal to the osmotic pressure of the saturated solution. This pressure causes some swelling around the dissolving particle, and forms a region of excess hydration within the polymer surrounding the swelling capsule. The dissolved solute is driven through this region of excess hydration by convection induced by the pressure difference between the osmotic pressure in the solution and the surrounding medium. The dissolved solute is driven to the surface of the device through overlapping regions of excess hydration.

The objective of this study was to investigate the ability of low molecular weight, octan-1-ol initiated poly(5-ethylene ketal ε-caprolactone-co-D,L-lactide) (OCT-PEKCDLLA) to serve as a single, or dual, delivery system for the release of VEGF and/or HGF in a sustained manner and in their active form for a period of at least 4 -.6 weeks utilizing the osmotic pressure release mechanism. To accomplish this goal, VEGF or HGF was co-lyophilized with trehalose and BSA, and sieved to produce particles of less than 45 μm diameter. These particles were either incorporated separately at 10% (w/w) loading into the polymer or together at 5% (w/w) loading

each into the polymer, and the *in vitro* release of VEGF and/or HGF from the polymer was assessed. The bioactivities of the released VEGF and HGF were measured using cell-based assays.

7.1 Materials

For the release studies, recombinant human VEGF, HGF, epidermal growth factor (EGF), and a VEGF ELISA kit were purchased from Peprotech Inc., Canada. An HGF ELISA kit was purchased from R&D Systems (USA). For the bioactivity studies, a WST-1 cell proliferation kit was obtained from Roche, Canada and a QuantiFluor™ dsDNA system was obtained from Promega Corporation, USA. 1,4-cyclohexanedione monoethylene ketal (97% purity), meta-chloroperoxybenzoic acid (MCPBA) (97% purity), octan-1-ol (anhydrous, 99% purity), dichloromethane (CH_2Cl_2), hexane, methanol, tetrahydrofuran (THF), ethyl acetate (EtOAc), stannous 2-ethylhexanoate (95% purity), Dulbecco's phosphate buffered saline (PBS), magnesium sulphate ($MgSO_4$), sodium bicarbonate, sulphuric acid, phenol, bovine serum albumin (≥ 98% purity), D-(+)-trehalose dihydrate (≥ 99% purity), and succinic acid (99% purity) were obtained from Sigma-Aldrich, ON, Canada. D,L-lactide was obtained from Purac, the Netherlands and purified by recrystallization from dried toluene.

7.2 Methods

7.2.1 Synthesis of 5-ethylene ketal ε-caprolactone-based copolymers

The 5-ethylene ketal ε-caprolactone monomer (EKC) was prepared by the Baeyer-Villiger oxidation of 1,4-cyclohexanedione monoethylene ketal by meta-chloroperoxybenzoic acid (MCPBA). EKC was copolymerized with D,L-lactide (DLLA) via ring-opening

polymerization, initiated with octan-1-ol utilizing stannous 2-ethylhexanoate as a catalyst (OCT-PEKCDLLA), as described previously [130]. Table 7-1 provides the physical properties of the copolymer.

Table 7-1: Characteristics of OCT-PEKCDLLA used.

monomer ratio (EKC:DLLA (mol:mol))	T_g [a] (°C)	M_n [b] (Da)	PDI [c]	$\eta_{37°C}$ [d] (Pa·s)
13 : 4.0	-19.7	2810	1.3	129.0

[a] glass transition temperature, [b] number average molecular weight, [c] polydispersity index, [d] zero shear rate viscosity at 37ºC.

7.2.2 Preparation of solid particles

VEGF particles were prepared by dissolving trehalose, bovine serum albumin (BSA) and VEGF at a weight ratio of 50:49.8:0.2, 90:9.8:0.2 or 90:9.97:0.03 in 10 mL of 0.5 mM pH 7 succinate buffer. HGF particles were prepared by dissolving trehalose, BSA and HGF at a weight ratio of 90:9.97:0.03, 90:9.985:0.015 and 90:9.9925: 0.0075 in 10 mL of 0.5 mM pH 7 succinate buffer. The solution was sterile filtered and frozen in liquid nitrogen, then lyophilized under sterile conditions on a Modulyo D freeze dryer (Thermosavant, USA) at -50°C and 100 mbar. The resulting powder was sieved through a #325 Tyler sieve to yield < 45 μm particles [30].

7.2.3 *In vitro* release of VEGF

Prior to the release experiment, the polymer was sterilized by germicidal UV source (Phillips; G30T8) (253.7nM) in the laminar flow hood for 30 minutes and the release media used was sterile filtered. To maintain the sterility of the polymer, loading of the particle into the

polymer, dispensing the protein-loaded polymer into vials, and removing and adding release buffers into the vials were all done under sterile conditions in a laminar flow hood. A known amount of lyophilized protein particles was suspended with a known amount of OCT-PEKCDLLA by physical mixing. The designation and composition of the particles and their loading into the polymer are shown in Table 7-2.

Table 7-2: Designation and composition of particles and loading into the polymers

Particle Designation	Particle loading (%)	Trehalose content (% w/w)	BSA content (% w/w)	VEGF content (% w/w)	HGF content (% w/w)
1TB50V (0.2)	1	50	49.8	0.2	0
5TB90V (0.2)	5	90	9.8	0.2	0
10TB90V (0.03)	10	90	9.97	0.03	0
10TB90H (0.03)	10	90	9.97	0	0.03
10TB90H (0.015)	10	90	9.985	0	0.015
10TB90H (0.0075)	10	90	9.9925	0	0.0075

The protein-loaded polymer was initially warmed to 40°C, and about 100 mg was injected into the base of a 2 mL glass vial to fill the bottom of the vial to a height of approximately 3 mm. The exact weight of the mixture in each vial was recorded. The vials were filled with 1 mL of 37°C pH 7.4 phosphate buffered saline (PBS) containing 0.02% (v/v) Tween 20 and 0.02% (w/v) sodium azide. The Tween 20 was added to prevent nonspecific adsorption of proteins to the glass vials [132] and sodium azide was added as an antimicrobial. The release media

used for the bioactivity measurements was PBS at 37°C pH 7.4 containing 1% BSA and 1% antibiotics. The vials were capped, placed on a rotary mixer rotating at 300 rpm, and maintained at 37°C. All release experiments were done in triplicate. Polymer-only samples were also prepared as controls. At frequent sampling intervals, the buffer was replaced with fresh buffer to maintain near perfect sink conditions. The removed buffer was stored at -80°C until used for analysis. Growth factor concentration in the release medium was measured as a function of time using ELISA kits specific for each growth factor, in accordance with the supplier's protocol. The results are presented in terms of fractional cumulative release and/or cumulative mass released as a function of time.

To simulate a more representative *in vivo* release profile, 100 mg of the growth factor loaded OCT-PEKCDLLA was injected into a hollow space created in a hydrogel composed of methacrylated glycol chitosan (MGC). Due to the bigger size of the gel, the sample was placed in a 20 mL glass vial, 3 mL of buffer was added to cover the top of the gel, and the vials were maintained at 37°C in an oven without any agitation. MGC with a degree of *N*-methacrylation (number of *N*-methacrylated residues per 100 residues) of 5%, was prepared as described elsewhere [197]. MGC was chosen because it has a pKa of approximately 6.5 [197], while VEGF and HGF have a pI of 8.5 – 8.9 [45], and 9.5 [53] respectively. Therefore, at the pH of the release medium, MGC and the growth factors would be positively charged and there would be no interaction between them that would affect the observed release kinetics. The water content of the gel was high (~ 94% (w/v)); therefore, there was negligible contribution of the gel phase to the release kinetics and the release from the liquid polymer was rate limiting. To make the mold, a 6.25% (w/v) solution of MGC in deionized water containing 0.8% (w/v) of the photoinitiator I2959 was

poured into a cylindrical Teflon mold (1.6 cm diameter × 1.4 cm). A cylindrical glass rod with diameter of 0.5 cm was placed in the center of the mold, extending 0.7 cm from the surface, before pouring in the MGC solution. The MGC solution was photopolymerized using 30 mW/cm^2 of long-wave (365 nm) UV light for 5 minutes (LIGHTNING CURE ™ from Hamamatsu). The glass rod was gently removed and the other side was exposed to the same intensity of UV light for 5 minutes.

7.2.4 Cell culture

Human Aortic Endothelial cells (HAECs) (Lonza Walkersville Inc., Walkersville, MD) were cultured in endothelial cell growth media (EGM-2) supplemented with 0.04% (v/v) hydrocortisone, 0.1% (v/v) gentamicin amphotericin B (GA-1000), 2% (v/v) fetal bovine serum (FBS), 0.1% (v/v) ascorbic acid, 0.1% (v/v) heparin, 0.1% (v/v) recombinant human epidermal growth factor, 0.1% (v/v) VEGF, 0.4% (v/v) human fibroblast growth factor-B with heparin, and 0.1% (v/v) insulin growth factor-1. Monkey epithelial lung cells (CCL 208) were cultured in Ham's F12-K medium with 2 mM L-glutamine adjusted to contain 1.5 g/L sodium bicarbonate and supplemented with 60 ng/mL epidermal growth factor, 10% (v/v) fetal bovine serum and 1% (v/v) antibiotics. The cells were incubated under standard conditions until they reached greater than 80% confluence.

7.2.5 Bioactivity Assays

The bioactivity of the released VEGF was assessed by determination of its ability to stimulate the proliferation of HAECs as compared to the proliferation obtained with the same concentration of as-received VEGF. After passage 3, 4, or 5, HAECs were rinsed twice, then

suspended in growth factor free basal media containing 0.08% (v/v) hydrocortisone, 0.2% (v/v) GA-1000, 0.5% (v/v) FBS, 0.2% (v/v) ascorbic acid, 0.2% (v/v) heparin at a concentration of 75,000 cells/mL. 100 μL of this cell suspension was added to each well and the plate incubated at 37°C for 1 h. 100 μL of the release medium from each sampled vial at the selected time point was added to a given well. For each bioactivity assay run, VEGF standard solutions with concentrations of 0 to 50 ng/mL were prepared in the same basal media and 100 μL added to release medium-free wells, in triplicate. Cell number was measured using two assays: WST-1 which measures metabolic activity, and QuantiFluor™ dsDNA system which quantifies DNA.

After 72 hours, 20 μL of WST-1 reagent was added and incubated at 37ºC, and an absorbance measurement at 450/690 nm taken after 4 hours (UQuant UV-VIS spectrophotometer). The bioactivity was calculated as a fraction of the activity expressed by the cells incubated with the release medium divided by the activity that would be expressed by cells exposed to an equivalent concentration of as received VEGF, as determined from the standards. The bioactivity of the released HGF was determined using CCL 208 cells, the same culture procedure used to determine the bioactivity of VEGF was used. For DNA quantification, after the medium was aspirated, cells were rinsed with PBS (0.01 M, pH 7.4) solution and were lysed for two hours in 100 μL of 10X trypsin at 37ºC. The cell lysate was mixed with QuantiFlour™ dsDNA dye in equal volume and was incubated for 5 minutes at room temperature protected from light. The fluorescence was measured using a microplate reader (BIOTEK Synergy HI) with 485 nm as excitation and 530 nm as emission. The bioactivity was calculated as a fraction of the activity expressed by the cells incubated with the release medium divided by the activity that

would be expressed by cells exposed to an equivalent concentration of as received VEGF and HGF, as determined from the standards.

7.3 Statistics

All release experiments were done in triplicate and are reported as the average ± the standard deviation about the average.

7.4 Results

7.4.1 In vitro release of VEGF

In an *in vitro* human endothelial cell proliferation and migration assay by van Belle and co-workers, 50 to 100 ng/mL of VEGF and HGF induced maximum cell proliferation and migration over a 48-hour period. This dosing translates to approximately 25-50 ng/day for both growth factors[52]. Therefore, our target was to co-release VEGF and HGF at 25-50 ng/day for at least 4 weeks. Preliminary studies, in which BSA as a model drug was released from an OCT-PEKCDLLA using the 1TB50V (0.2) formulation (Chapter 5), indicated that a release rate of VEGF at ~20 ± 0.4 ng/day could be obtainable with this formulation, assuming that VEGF was released at the same normalized rate as BSA. This assumption was based on the previous finding that BSA and trehalose was released at similar normalized rates (Chapter 5). Using this formulation, VEGF was released from the OCT-PEKCDLLA in a sustained manner with a minimal burst effect (4 ± 0.2%) (Figure 7-1A). However, the VEGF was released at the rate of only 8 ± 0.3 ng/day (0.42 ± 0.02 %/day). In addition, after 122 days, only 33 ± 3% of the incorporated VEGF had been released (Figure 7-1B).

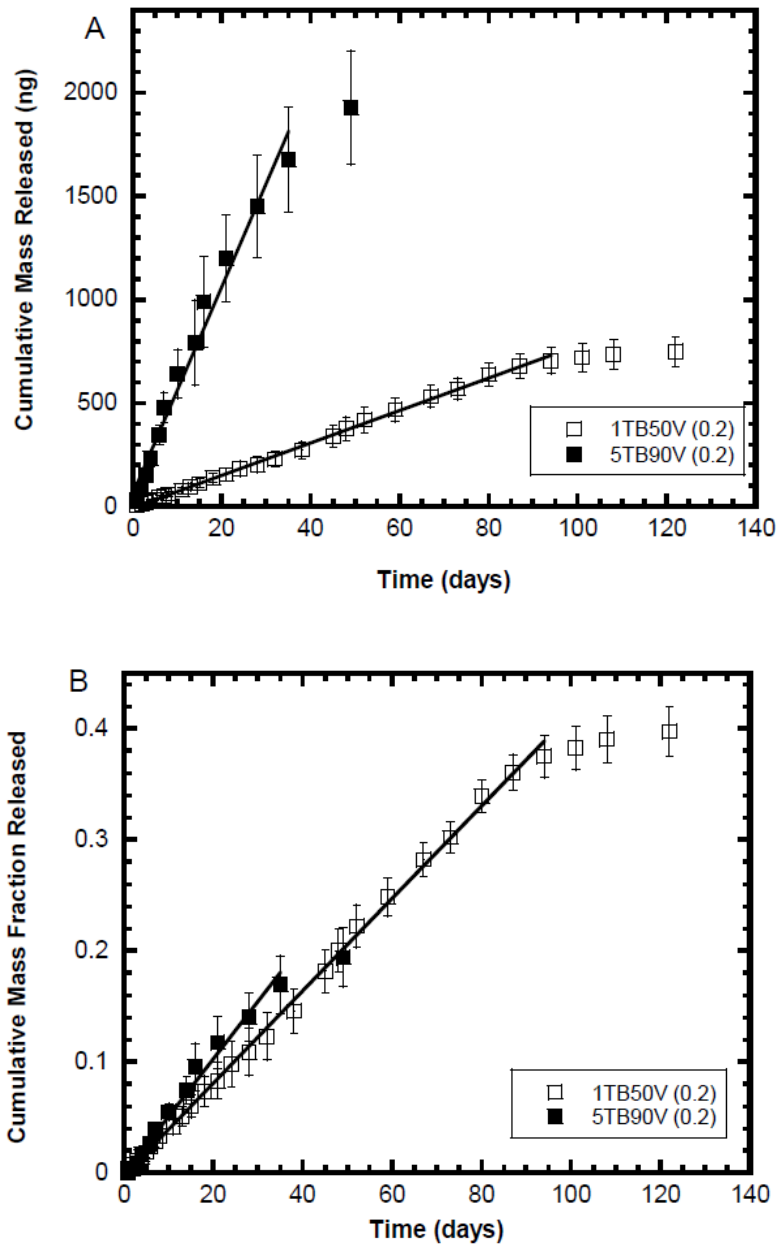

Figure 7-1: Cumulative release of VEGF from 1TB50V (0.2) and 5TB90V (0.2) formulations, demonstrating the influence of trehalose content in the particle and the total loading of particles into the polymer on the release rate. (A) Cumulative mass released and (B) cumulative mass fraction released. The error bars indicate the standard deviation of 3 independent release experiments. The solid lines are linear curve fits to the data over the time period indicated by the length of the line. (Coefficient of determination for the linear regressions were ≥ 0.98)

Based on previous work for osmotically driven release from liquid injectable polymers[147], low melting point microspheres [179] and elastomers [31, 123, 125], it was expected that VEGF release would increase as trehalose content in the particle increased due to an increase in solution osmotic pressure generated upon dissolution of the particles in the polymer. Furthermore, the mass release rate of an agent released via the osmotic mechanism from polymers is proportional to the volumetric loading of the particle, provided the loading is below the percolation threshold [123]. Therefore it was expected that by increasing the trehalose content in the particle from 50% (w/w) to 90% (w/w) and the particle loading from 1% w/w to 5% (w/w) (5TB90V), the release rate and the total amount released would increase. With this formulation, VEGF was released in a sustained manner with no burst effect at a rate of 48 ± 4 ng/day (0.44 ± 0.03 %/day) (Figure 7-1A). The mass release rate is almost 5 times the mass release rate observed using the 1TB50V (0.2) formulation, in accordance with a 5 times increase in the particle loading. Thus, increasing particle loading in the polymer increased the mass release rate. However, increasing trehalose content had no significant effect on the mass fraction released. Moreover, after 49 days, only 19 ± 3 % of the incorporated VEGF had been released (Figure 7-1B).

7.4.2 Effect of VEGF concentration in the particle on its release.

Figure 7-2 shows the mass fraction of trehalose, BSA and VEGF released from the 5TB90V (0.2) formulation. Over the first 7 days, trehalose and BSA were released at almost similar rates, after which trehalose was released faster than BSA. On the other hand, VEGF was consistently released more slowly than both trehalose and BSA (Figure 7-2).

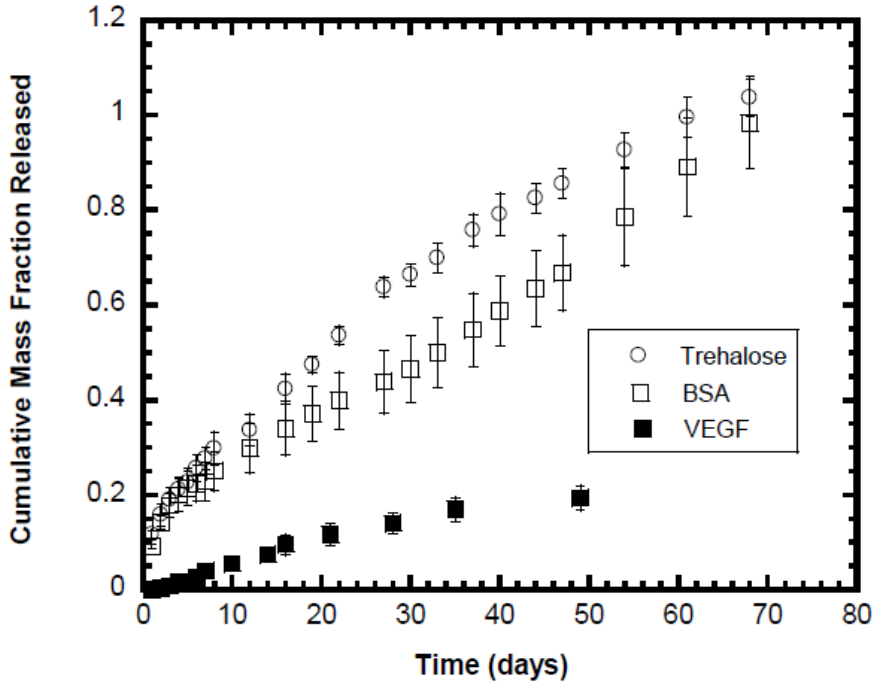

Figure 7-2: Cumulative mass fraction of trehalose, BSA and VEGF released from the 5TB90V formulation.

Since almost all the trehalose in the formulation was released, the low total mass fraction of VEGF released was considered to be a result of the limited solubility of VEGF in the concentrated trehalose solution. In a previous study of VEGF release from liquid poly(trimethylene carbonate) using the osmotic release mechanism driven by trehalose, VEGF was released at the same mass release rate when the concentration of VEGF in the formulation was increased from 0.1 to 0.5% (w/w). The authors speculated that the VEGF had a reduced solubility in the concentrated trehalose solution, when VEGF was loaded at 0.5% (w/w) compared to at 0.1% (w/w) [30]. Thus, it was reasoned that by reducing the concentration of VEGF in the particle to below the solubility limit in a concentrated trehalose solution and increasing the particle loading to 10%, the desired release rate would be obtained and the total amount of VEGF

released would be increased. The solubility of VEGF in the concentrated trehalose solution was estimated based on the release rate of VEGF (48 ± 4 ng/day) and the corresponding initial release rate of trehalose (122 ± 9 μg/day) from the 5TB90V (0.2) formulation. From this calculation, the ratio of VEGF to trehalose in the concentrated trehalose solution was estimated to be approximately 390 ng VEGF/mg of trehalose. Therefore, the concentration of VEGF in the particle was reduced from 0.2% (w/w) to 0.03% (w/w), the particle loading was increased from 5% (w/w) to 10% (w/w), while the trehalose particle content was maintained at 90% (w/w) (10TB90V (0.03)). The cumulative mass fraction of VEGF and trehalose released from the 10TB90V (0.03) formulation is shown in Figure 7-3A, while the cumulative mass of VEGF released is shown in Figure 7-3B.

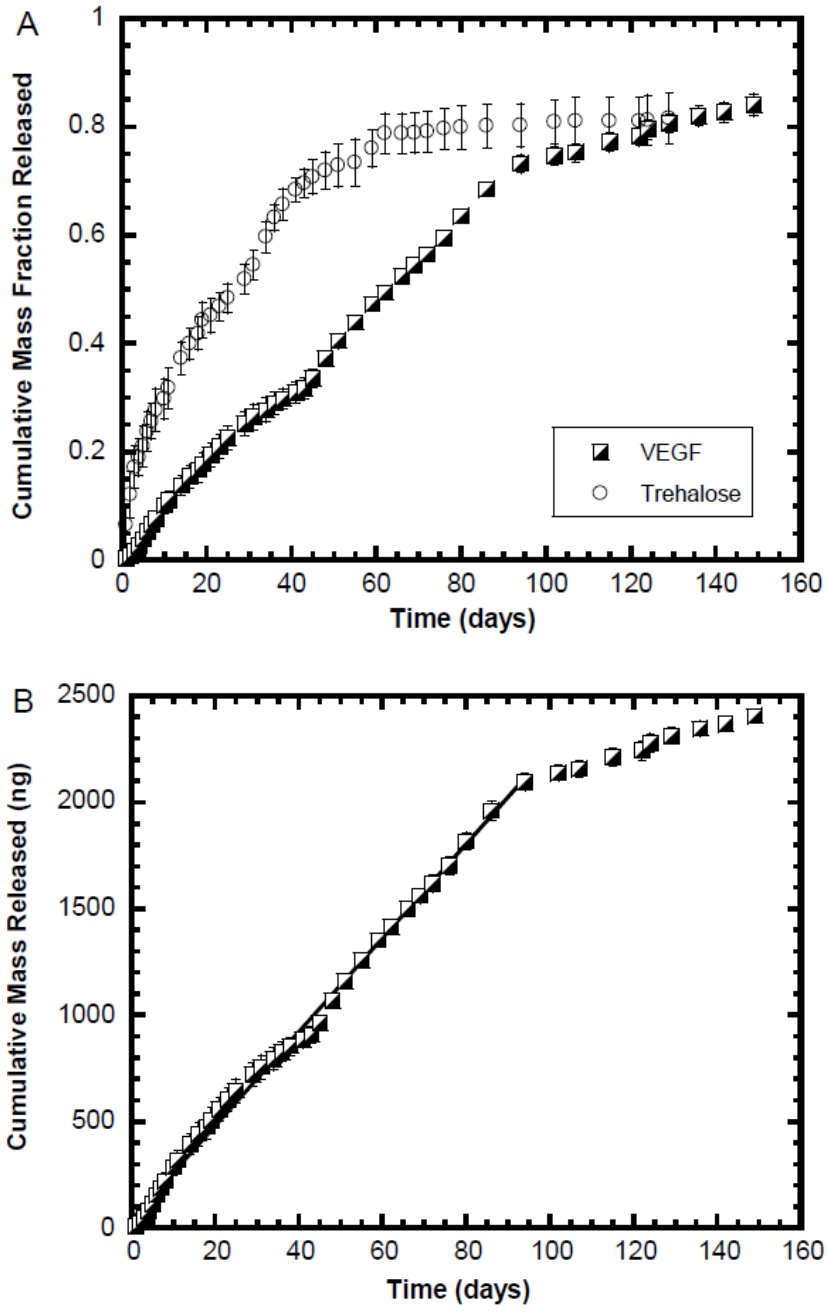

Figure 7-3: (A) cumulative mass fraction of trehalose and VEGF released from the 10TB90V formulation and (B) cumulative mass of VEGF released from the 10TB90V formulation. The error bars indicate the standard deviation of 3 independent release experiments. The solid line in (B) is a linear curve fit to the data over the time period indicated by the length of the line. (Coefficient of determination for the linear regressions was ≥ 0.99)

The VEGF was again released with a minimal burst effect (0.3 % after day 1), and exhibited a nearly linear release profile for 94 days. During the linear release phase, the mass release rate of VEGF was 22 ± 1 ng/day (0.73 ± 0.01%/day), and by the end of the release period, 84 ± 2 % of the incorporated VEGF had been released. Thus, by increasing the particle loading to 10% and reducing the concentration of VEGF in the lyophilized particle from 0.2 %(w/w) to 0.03 % (w/w), the release rate increased by almost two-fold.

7.4.3. *In vitro* release of HGF

Based on the ability to obtain nearly complete release of VEGF at the desired release rate from the 10TB90V formulation, the same formulation was further investigated for HGF. HGF was incorporated in the trehalose + BSA particle in a similar fashion as VEGF, i.e. at a concentration of 0.03% (w/w). These particles were then incorporated into the OCT-PEKCDLLA at 10% (w/w) loading (10TB90H 0.03). HGF was released from the polymer in a sustained manner with no initial burst release for a prolonged period of time. HGF was released at the rate of 13 ± 2 ng/day (0.49 ± 0.07 %/day) and by the end of the release period, 56 ± 8 % of the incorporated HGF was released (Figure 7-4A). Following the trend observed previously, trehalose was released faster than both growth factors, while VEGF was released faster than HGF (Figure 7-4B).

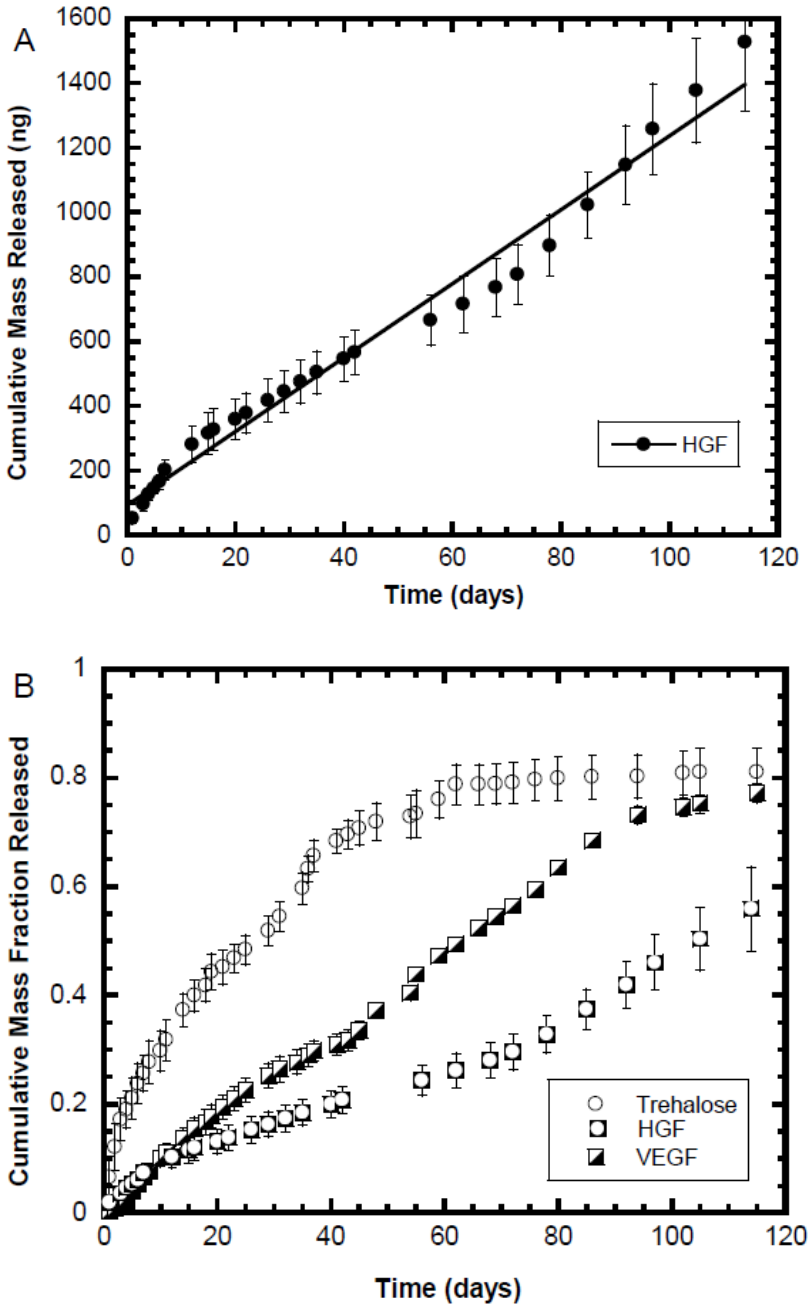

Figure 7-4: (A) Cumulative mass of HGF (10TB90V) released alone from OCT-PEKCDLLA (B) Cumulative mass fraction of trehalose (10TB90V), HGF (10TB90H) and VEGF (10TB90V) released alone from OCT-PEKCDLLA. The error bars indicate the standard deviation of 3 independent release experiments. The solid line in (A) is a linear curve fit to the data over the time period indicated by the length of the line (coefficient of determination for the linear regression was ≥ 0.99).

After the release of VEGF and HGF from the vial, the polymer was dried in the oven for 2 days and then dissolved in dichloromethane (DCM) and centrifuged to remove residual particles. The DCM phase was gently decanted into a previously weighed eppendorf tube and the DCM evaporated at 50°C for 2 days. Any residual DCM was removed via lyophilization. The mass of the extracted polymer was measured and used to calculate the percent weight loss. The T_g, M_n and ratio of EKC to DLLA in the polymer were also measured at 18 and 21 weeks after release of HGF and VEGF, respectively. The polymer used for VEGF and HGF release had lost approximately 35% of the initial weight during the entire release period; however, the molecular weight of the polymer only reduced slightly from 2810 Da to ~ 2500 Da with no significant change in ratio of EKC to DLLA and T_g (Table 7-3). As observed during an in *vitro* degradation study in the absence of trehalose [130], while the physical properties of the polymer remained the same throughout the degradation time, the polymer lost approximately 34.7 ± 0.3% of its initial weight by week 14, which increased to approximately 71.8 ± 10.2 % by week 24. The weight loss of the polymer used for HGF and VEGF release indicates that the polymer used for the release studies degraded slightly slower compared to that in the absence of trehalose (Figure 7-5). This result could be attributed to the slightly lower molecular weight (2700 Da) of the polymer used for the degradation studies done in the absence of lyophilized particles (chapter 5) compared to the molecular weight of the polymer batch used for this studies (Table 7-3). However considering the observed polymer weight loss in the presence versus that in the absence of the trehalose/protein particles, it can be inferred that the degradation mechanism of the polymer during release is the same in each case.

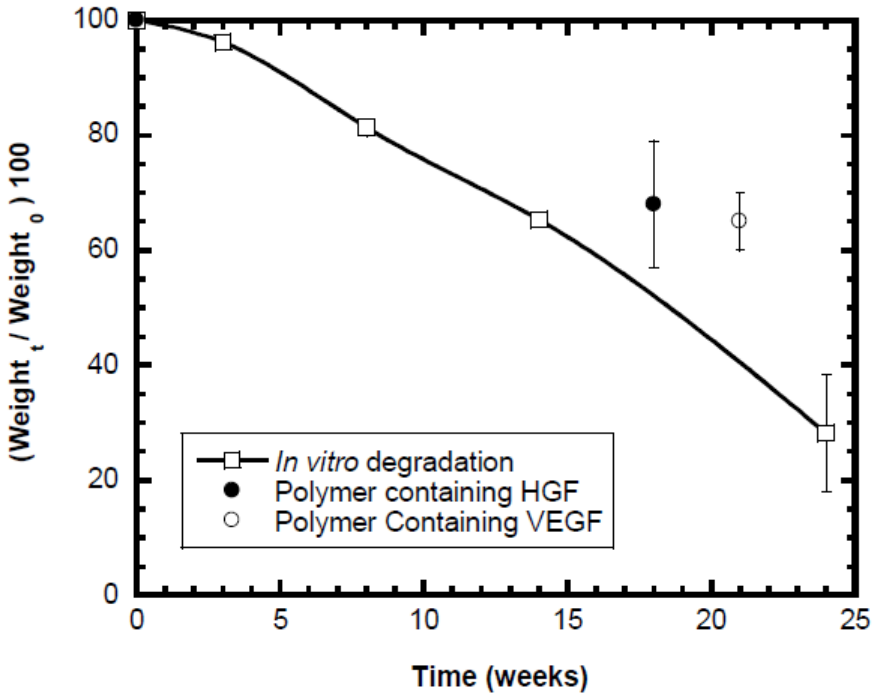

Figure 7-5: Comparison of weight loss of the OCT-PEKCDLLA degraded *in vitro* in the absence and presence of particles containing VEGF or HGF.

Table 7-3: Characteristics of OCT-PEKCDLLA after release of VEGF and HGF.

	% Weight remaining	**T_g (°C)**	**M_n (Da)**	**Molar Ratio of EKC to DLLA**
Polymer before release	100	-19.7	2810	3.6 : 1
Polymer after release of VEGF	65 ± 5 After 21 weeks	-18.5	2490	3.8 : 1
Polymer after release of HGF	68 ± 11 After 18 weeks	-18.4	2500	3.4 : 1

7.4.4 Bioactivity of the released VEGF and HGF

The bioactivities of VEGF and HGF in the release media were assessed using an *in vitro* assay based on the proliferation of HAECs and CCL 208 cells, respectively [31]. The bioactivity of the released VEGF and HGF was calculated relative to the proliferation of HAECs and CCL 208 cells grown in the presence of the same concentration of as-received VEGF and HGF respectively. Two cell proliferation assays were used for this purpose, WST-1 and QuantiFluor™ dsDNA system. WST-1 measures cell number by measuring the number of cells that are metabolically active, while Quantiflour™ dsDNA system measures cell number by quantifying the amount of DNA present. The results from the two assays were consistent; the released VEGF retained approximately 90% of the bioactivity of the as-received VEGF throughout the release study (Figure 7-6A), while the HGF retained approximately 80% bioactivity throughout the release studies (Figure 7-6B).

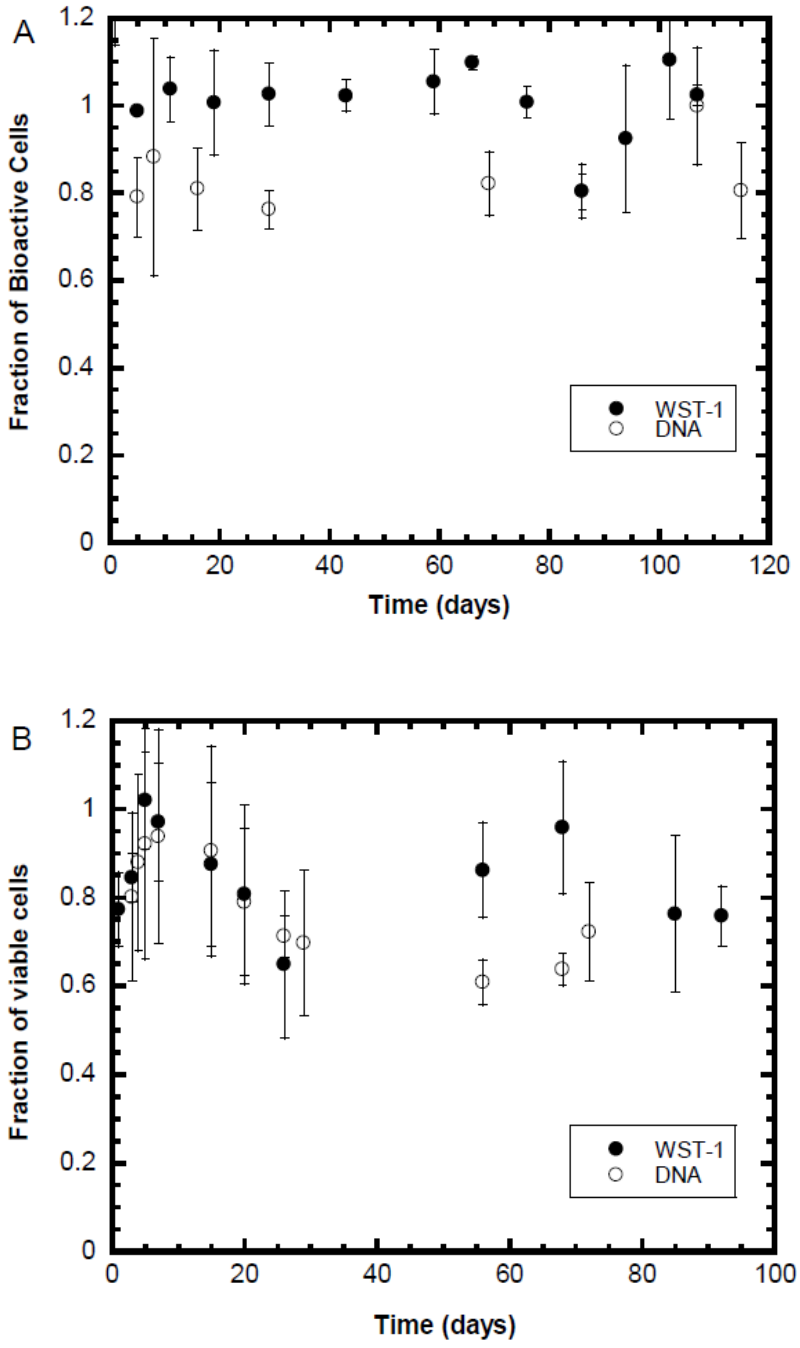

Figure 7-6: Fraction of bioactive cells in the release media relative to the same concentration of as-received growth factors using WST-1 and QuantiFlour™ (A) VEGF and (B) HGF. Each point represents the average of the released protein from three samples with 2 replicates per sample for each experiment.

7.4.5 *In vitro* release from the hydrogel mold

It was easier and faster to assess formulation parameters by placing the polymer/particle suspension in the bottom of a vial. However, the release rate obtained in this manner would be slower than that expected *in vivo* because release from the vial was unidirectional, while the release *in vivo* would be multidirectional. In order to simulate the release rate of the growth factors *in vivo*, 100 mg of protein-loaded polymer was injected into a hollow space created in a hydrogel prepared from *N*-methacrylate glycol chitosan (MGC). As expected, both VEGF (10TB90V 0.03) and HGF (10TB90H 0.03) were released faster when the formulation was injected in the gel mold than when injected into the bottom of the vial. VEGF release was sustained for the first 31 days at 69 ± 6 ng/day (1.9 ± 0.1 %/day), while HGF was sustained for 9 days at 64±7 ng/day (2.0 ± 0.3 %/day) and at 18.6 ± 3.5 ng/day (0.6 ± 0.1 %/day) thereafter. (Figure 7-7A and 7-7B).

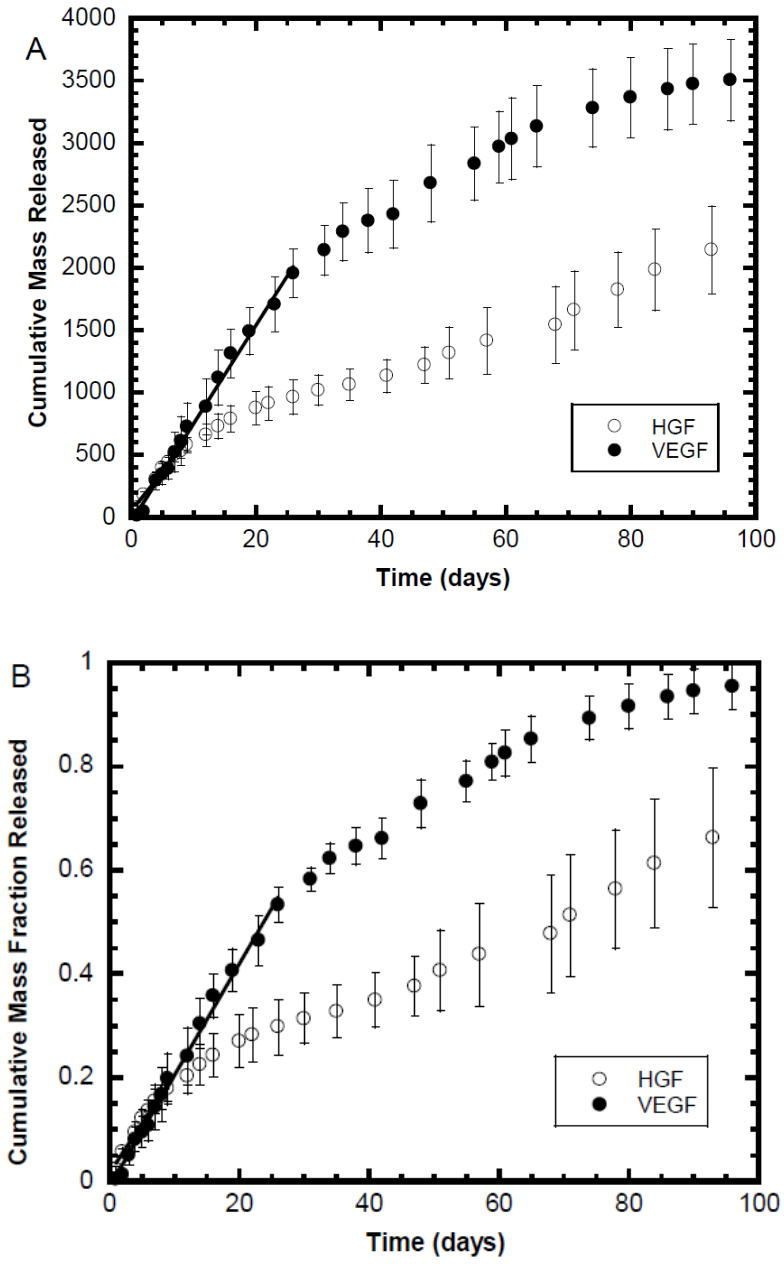

Figure 7-7: Cumulative release of VEGF and HGF from OCT-PEKCDLLA when the formulation was injected into the MGC gel mold, demonstrating the difference in release kinetics of VEGF and HGF when formulated under the same conditions. (A) Cumulative mass released and (B) cumulative mass fraction released. The error bars indicate the standard deviation of 3 independent release experiments. The solid lines are linear curve fits to the data over the time period indicated by the length of the line. (Coefficient of determination for the linear regressions was ≥ 0.97)

These release rates were calculated via a linear regression, and in all cases the coefficient of determination was > 0.97. By the end of the release study, 95 ± 4 % of the incorporated VEGF had been released while 66 ± 13 % of the incorporated HGF had been released (Figure 7-7B). When the growth factors were released from the OCT-PEKCDLLA within the gel mold, the initial release rate of VEGF was approximately 3 times faster than the release rate from the vial, while the release rate of HGF was approximately 5 times faster than the release rate from the vial. Moreover, a nearly linear release is no longer observed for a long time frame when the release was multidirectional compared to when the release of the growth factors was unidirectional.

7.4.6 Co-release of VEGF and HGF

The VEGF (10TB90V 0.03) and HGF (10TB90H 0.03) particles were also loaded into the polymer at 5% particle loading each and injected into the MGC gel mold, to assess the feasibility of concurrent release of the two growth factors from the OCT-PEKCDLLA vehicle. It was also important to ascertain why VEGF was consistently released faster than HGF; therefore, the amount of trehalose released with time was compared to the VEGF and HGF release. The release profiles from the single and dual factor-loaded systems coincided, at least for the first 41 days (Figure 7-8). Trehalose, VEGF and HGF were released in a sustained manner, but at different rates. VEGF was released at 36 ± 7 ng/day (2.2 ± 0.3 %/day) for 41 days while HGF was released at 16.1 ± 1.5 ng/day (0.95 ± 0.05 %/day) for 70 days. On the other hand, trehalose was almost completely released by the seventh day at the rate of 11.0 ± 0.8%/day, which is approximately 5 times faster than the release rate of VEGF and about 10 times faster than the release rate of HGF in the same time frame.

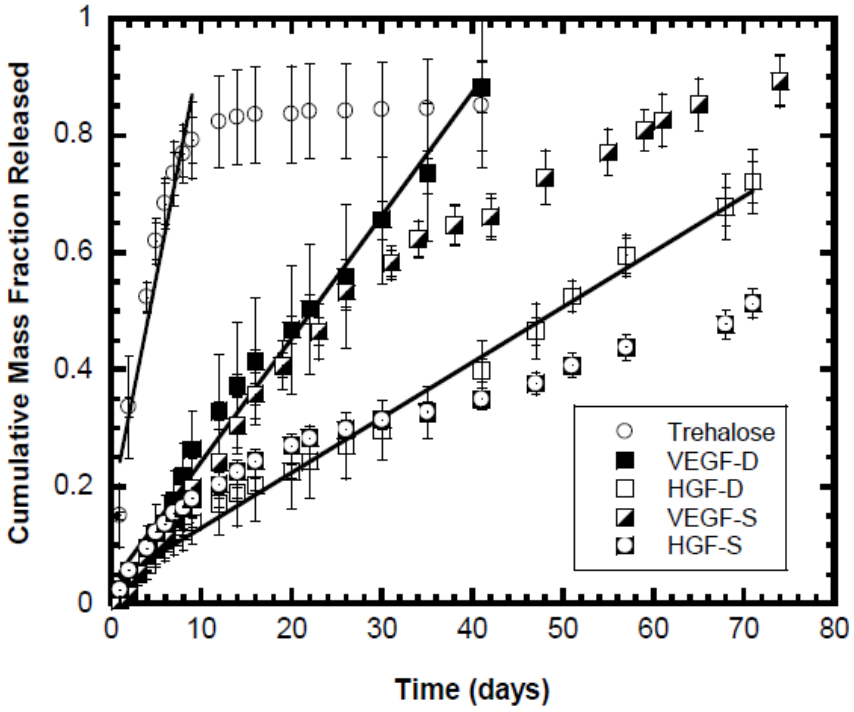

Figure 7-8: Cumulative release of trehalose, VEGF and HGF from OCT-PEKCDLLA when injected into the MGC gel mold. In the legend, VEGF-D and HGF-D refer to the release of each growth factor when incorporated into the polymer together and VEGF-S and HGF-S when delivered from the polymer separately. The error bars indicate the standard deviation of 3 independent release experiments. The solid lines are linear curve fits to the data over the time period indicated by the length of the line. (Coefficient of determination for the linear regressions was ≥ 0.97)

7.4.6: Effect of HGF concentration in the particle

HGF in all cases was released consistently slower than VEGF. This finding led to a similar hypothesis as that proposed for VEGF release: that the solubility of HGF in the trehalose solution formed by dissolving the particle was less than the HGF content in the particle. To test this hypothesis, the vial approach was used, the concentration of HGF in the particle was reduced to 0.0075% (w/w) and 0.015% (w/w), incorporated into the OCT-PEKCDLLA at 10% loading,

and the release results compared (Figure 7-9A). The release kinetics showed that there was an increase in cumulative mass fraction release rate when the concentration of HGF was reduced to 0.015% (w/w). However, a further decrease in HGF concentration in the particle did not have any significant effect on release rate (Figure 7-9A). The release profile of VEGF from the 10TB90V (0.03) formulation was compared to the release profile of HGF from 10TB90H (0.015) formulation, with these formulations, the fractional release of HGF was slightly faster than that observed for VEGF Figure 7-9B. This further indicates that the release of VEGF and HGF is limited by their concentration in the concentrated trehalose solution.

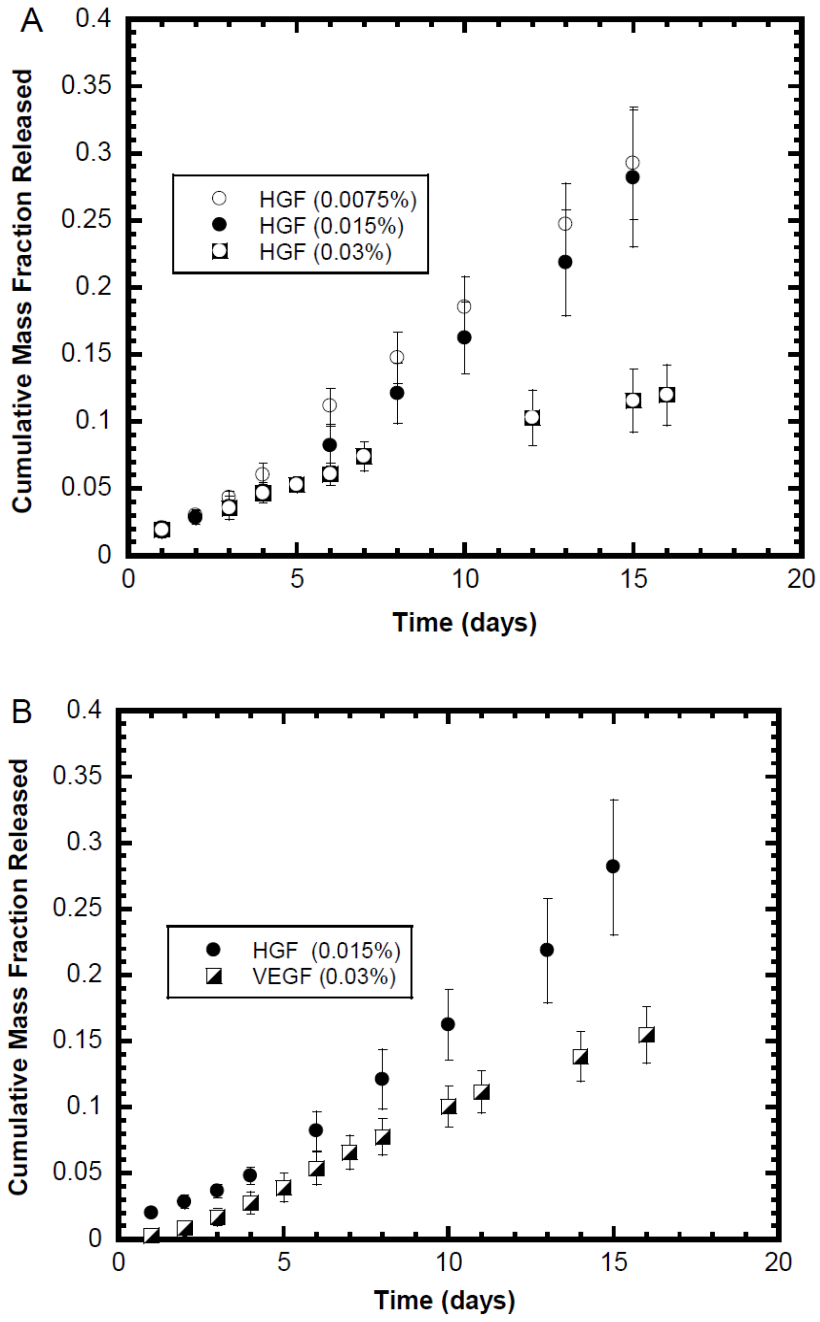

Figure 7-9: (A) Cumulative mass fraction release of HGF showing effect of concentration of HGF in the particle on release rate. (B) Cumulative mass fraction release of HGF (0.015%) and VEGF (0.03%). The error bars indicate the standard deviation of 3 independent release experiments.

7.5 Discussion

The ultimate goal was to develop an injectable polymeric delivery system made from a copolymer of 5-ethylene ketal ε-caprolactone and D,L-lactide, that could provide sustained and complete release of VEGF and HGF at a minimum of 25 ng/day for at least 4 weeks with a minimal burst, while maintaining their bioactivity. To accomplish these goals, an osmotic release mechanism was employed. Trehalose was chosen as the osmotigen for this study because it is a compatible osmolyte that has been used previously to drive the release of VEGF from liquid injectable 1600 Da poly(trimethylene carbonate) [30].

VEGF and HGF were co-lyophilized with trehalose and BSA and the particles thus formed incorporated into the polymer by simple mixing. According to the release mechanism proposed by Babasola and Amsden (Chapter 5), solute release from the polymer was initiated by the water activity gradient between the surrounding aqueous medium and the saturated solution formed when water from the surrounding medium dissolves a polymer-enclosed drug particle. The activity gradient draws water into the polymer to generate an osmotic pressure equal to the osmotic pressure of the saturated solution at the particle/polymer interface. The generated pressure initiates swelling around the particle/polymer interface, and creates a highly hydrated polymer region surrounding the particle that ultimately overlaps with the hydrated regions of neighboring particles, forming a pathway to the surface through which the dissolved solutes are transported by convection. The rate of transport is determined by the osmotic pressure generated and the hydraulic conductivity of the hydrated zone (Chapter 5).

As anticipated, release was slower when release was from one direction compared to when release was from multiple directions. As observed with BSA release, increasing the particle loading of VEGF from 1% (w/w) to 5% (w/w) increased the mass release rate but had no significant effect on the mass fraction release rate. Increasing the total particle loading, provided it remains below the percolation threshold, would result in the overlap in the zones of hydration to occur at a faster rate. Nevertheless, because the hydraulic permeability and osmotic driving force remained the same, the fractional release rate did not change appreciably. By increasing the particle loading to 10% (w/w) from 5% (w/w) while decreasing the concentration of VEGF in the particle from 0.2% (w/w) to 0.03% (w/w), the fractional release rate and total fraction released was significantly increased by almost two fold. This finding suggests that when the concentration of VEGF is at or near 0.2% (w/w) in the particle, a smaller fraction of the VEGF in the particle is soluble in the saturated trehalose solution formed upon dissolution of the particle. At 0.03% (w/w), the concentration of VEGF is low and as a result, a greater fraction of the VEGF is soluble in the saturated trehalose solution formed. In a previous study by Amsden and co-worker, [151] it was observed that there was no significant effect on the fractional release rate from liquid poly(trimethylene carbonate) when the concentration of VEGF in equivalent particles was increased from 0.1 % (w/w) to 0.5% (w/w). This previous finding and the findings of this study further confirms that VEGF release from this formulation was limited by its solubility in the concentrated trehalose solution formed by dissolving the particles.

Using the VEGF formulation conditions to formulate HGF did not lead to the same HGF release rate as observed for VEGF, suggesting that HGF had a lower solubility limit in the concentrated trehalose solution formed than did VEGF. This explanation was supported by the

faster release observed upon reducing the concentration of HGF in the particle to 0.015% (w/w) and 0.0075% (w/w) from 0.03% (w/w). Moreover, the release rate of HGF from formulation 10TB90H (0.015) was slightly higher than the release of VEGF from formulation 10TB90V (0.03). This further confirms that the release of HGF and VEGF was determined by their solubility in the concentrated trehalose solution. When VEGF and HGF were released simultaneously from the OCT-PEKCDLLA injected into the MGC gel mold, the fractional release rates were comparable to those achieved when the growth factors were incorporated into the polymer separately. Moreover, VEGF and HGF were released close to the targeted therapeutically relevant concentrations, in a sustained manner, with a near zero order release profile, and with no burst release. VEGF was released at a rate of 36 ± 7 ng/day for 41 days, while HGF was released at a rate of 16 ± 2 ng/day for 70 days, which is close to the minimum targeted delivery rate of 25 ng/day for both growth factors.

In all formulations tested, the more hydrophilic trehalose was released faster than the release of the co-excipient BSA, and the incorporated growth factors, irrespective of the geometry of the system. In this formulation, trehalose was almost completely released by 12 days, however, the release of VEGF and HGF were still continuous in a sustained manner, with a near zero order release profile. The continuous and almost linear release profile observed after almost all trehalose has been released could be as a result of the pathway already created by the released trehalose, the increased solubility of the growth factors as a result of reduction in trehalose concentration and the fact that the polymer degrades by surface erosion. For trehalose to be completely released by day 12, water must have penetrated into the bulk of the polymer and the absorbed water must have increased the hydraulic permeability of the polymer. However, because

the properties of the polymer did not change significantly after release studies even after losing about 35% of the initial weight, it can be inferred that hydrolysis of the ester bonds is more significant at the interface between the polymer and the aqueous medium, therefore confining the release of the dissolved growth factor in that layer. Low molecular weight polymer degradation products are formed at the surface that are dissolved into the release medium while the higher molecular weight degradation products that are not water soluble remain entrapped in the polymer, but at the interface of the polymer with the aqueous medium. All these factors will result in continuous release of the growth factors even after all the trehalose has been released.

In an *in vivo* angiogenesis assay in rats, Richardson and co-workers showed that VEGF released from PLGA (85/15) retained biological activity for up to 2 weeks. By using an *in vitro* VEGF receptor ELISA, which binds specifically to the receptor domain of VEGF, Cleland and co-workers showed that VEGF released from PLGA (50/50) was stable for up to 8 days [46]. Oseki and co-workers showed that HGF released from gelatin was bioactive for up to 2 weeks [59] using cell based assays. In the above studies, significant neovascularization was induced *in vivo* by the released growth factors compared to controls without growth factor, but a quantitative analysis of the actual percentage of bioactive growth factors released was not provided. In a recent study, using a similar cell based assay for measuring bioactivity (WST-1), greater than 95% of VEGF released from poly(trimethylene carbonate) [30] and greater than 80% of VEGF and HGF released from poly(trimethylene carbonate) based elastomers were bioactive [31] after 40 and 8 days of release respectively. HGF is known to lose activity partially when treated with 1M acetic acid [58] while the N-terminal residues of VEGF that participate in receptor binding are prone to deamidation, oxidation and diketopiperazine reactions that occur faster at pH of 5 compared to

pH 8 [43]. However, in this study, using 2 cell based assays, VEGF retained approximately 90% bioactivity for over 100 days when almost 80% of the incorporated protein was released, while HGF maintained approximately 80% bioactivity for over 90 days when over 60% of the incorporated growth factor was released. The high bioactivity of these acid sensitive growth factors can be attributed to the near neutral pH that was maintained within the polymer as a result of the surface degradation mechanism. This bioactivity result is based on the growth factors released from the vial, where the growth factors remained in contact with the polymer for a longer period of time, which represents a worst-case scenario. The bioactivity of the growth factor released from the gel mold would be expected to be greater, considering that the proteins would spend less time within the degrading polymer.

Multiple factor delivery has been described by other groups, applying different delivery systems or different combination of polymers [31, 36, 62, 76]. For example, Richardson and co-workers made porous scaffolds by compressing particulate PLG that was mixed with VEGF that had been co-lyophilized with alginate and NaCl, with microspheres pre-encapsulated with platelet derived growth factor (PDGF-BB) to provide multiple growth factor delivery with a distinct release rate for each factor. PDGF-BB promotes maturation of blood vessels by the recruitment of vascular smooth muscle cells (VSMCs) to the endothelial lining of the developing vasculature [62]. Hao and co-workers used a combination of partially oxidized alginates with low and high molecular weights to produce a hydrogel system that sequentially delivered VEGF and PDGF-BB into the infarcted myocardium [76]. The sequential factor delivery was achieved due to the higher degradation rates of the partially oxidized alginates constituting the hydrogel. Another group of researchers used affinity binding alginate to produce a hydrogel system than sequentially

delivered insulin-like growth factor-1 (IGF-1) and HGF [36] and VEGF, PDGF-BB and transforming growth factor β (TGF-β) [198]. Sequential factor release was achieved by the difference in affinity binding of the growth factor to the affinity binding alginate. The application of these delivery systems induced the formation of stable blood vessels. However, *in vitro* release studies were only done for less than 2 weeks and the growth factors were not completely released at this time point[36, 198.] Though the bioactivity of the released growth factors were not determined, there is possibility of loss of bioactivity of growth factors using this approach due to electrostatic interaction of the affinity binding hydrogel with the growth factors and the large amount of water present in the hydrogel.

Chapanian and Amsden utilized the osmotic pressure release mechanism to achieve both co- and sequential release of VEGF and HGF from cylindrical geometries, made from a biodegradable elastomer composed of photocrosslinked, terminally acrylated star-poly(trimethylene carbonate-co-DL-lactide-co-ε-caprolactone) [31]. Co-release was achieved by distributing lyophilized particles throughout the polymer and photocrosslinking with UV light. Sequential release was achieved when the inner core of the cylinder consisted of HGF particles covered with an outer polymer layer which contained VEGF particles. The HGF particles in the inner layer contained a greater amount of NaCl to drive its release. However, the efficacy of these delivery systems has not been tested *in vivo*.

The OCT-PEKCDLLA delivery system presents a simpler dual-delivery system whereby the growth factors are co-lyophilized with trehalose and BSA and dispersed into the viscous polymer as solid particles by simple mixing. This provides suitable properties as a polymeric

delivery device for protein therapeutics. The device fabrication procedure is simple and avoids the presence of moisture and the use of high temperature that may denature the protein. Since the polymer is viscous at room temperature, the protein-loaded polymer can be easily injected to the affected site through standard gauge needles, providing an effective and patient friendly approach. The polymer degrades by surface erosion *in vitro* (Chapter 4) and *in vivo* (chapter 6) without incorporating trehalose, and the physical properties of the polymer used for release did not change significantly after *in vitro* release of trehalose, VEGF and HGF from the polymer. Moreover, the growth factors were co-released from the polymer with a near zero order release kinetic, with no burst effect and the release could be sustained for over 41 days, within therapeutically relevant concentration. With these distinct properties, the formulation can be manipulated to release growth factors at desired rates. VEGF and HGF were released from the polymer at the rate determined by the hydraulic conductivity of the hydrated polymer region surrounding the particle, the solubility of the growth factors in the concentrated trehalose solution and the hydraulic permeability of the polymer. Though co-release of VEGF and HGF was achieved with this delivery system, a limitation of this approach is that the growth factors were not released at the same rate. However, this could be possible by incorporating the growth factors at concentrations below their solubility limit in the amount of trehalose used as excipient.

7.6 Conclusions

A viscous, liquid injectable polymer made from poly (5-ethylene ketal ε-caprolactone -co -D,L Lactide) provides a simple means of co-delivering bioactive VEGF and HGF in a sustained manner, with a near zero order release kinetics, with minimal burst effect and at therapeutically relevant concentrations. Particles obtained from growth factors lyophilized with trehalose and

BSA can be incorporated in the polymer by simple mixing and released by convection driven by the osmotic pressure generated upon dissolution of the particle. The rate of solute release is determined by the solubility of the growth factor in the concentrated trehalose solution and the hydraulic conductivity of the hydrated region formed upon dissolution of the particle. There is potential for using this delivery system to deliver acid and temperature sensitive drugs without loss of bioactivity as a result of acidic degradation products and high processing temperature, and at similar rates provided the drug is loaded below the solubility limit in the amount of trehalose used as excipient.

Chapter 8

CONCLUSIONS AND RECOMMENDATIONS

8.1 Conclusions

Injectable, and biodegradable polymeric delivery systems based on 5-ethylene ketal ε-caprolactone (EKC) and/or its copolymer with D,L-lactide (DLLA) was successfully synthesized. The flowability, biodegradation rate and protein release was varied by initiating with either a hydrophilic or hydrophobic initiator and copolymerizing with DLLA. The *in vivo* tissue response to the subcutaneously injected polymer was moderate and decreased with time. The *in vitro* and *in vivo* degradation was confined to the surface, characterized by a linear mass loss with time with no change in T_g, M_n and EKC to DLLA ratio. BSA, VEGF and HGF release was by convection via the osmotic pressure generated upon dissolution of the particle at a rate determined by the hydraulic permeability of the polymer and their solubility in the concentrated trehalose solution. Bioactive VEGF and HGF from OCT-PEKCDLLA were released at therapeutically relevant concentrations, with no burst release, with a near zero order release profile, and for a prolonged period of time. These delivery systems may serve as a platform for controlled and predictable delivery of VEGF and HGF for treating critical limb ischemia or other therapeutic proteins in other clinical settings.

8.2 Recommendations

For efficient mass transport between the implant and the surrounding tissue, the thickness of the fibrous capsule formed may be minimized or prevented by co-releasing immunosuppressive anti-inflammatory drugs such as dexamethasone [199].

A longer-term *in vivo* degradation study of the polymer until the polymer is completely resorbed still needs to be done.

It is necessary to study the *in vitro* degradation of the polymer (using the same polymer batch) with or without trehalose incorporated in the polymer to determine the effect of trehalose on the degradation of the polymer.

It is also necessary to correlate *the in vitro* degradation of the polymer and protein release to the *in vivo* degradation of the polymer and protein release using the same polymer batch.

The *in vivo* efficacy of this delivery approach in an hind limb ischemic model needs to be demonstrated.

Chapter 9

CONTRIBUTIONS

The following are my contributions to the literature:

1. Low molecular weight, poly(5-ethylene ketal ε-caprolactone) and its copolymer with DLLA degraded *in vitro* and *in vivo* in a surface erosion fashion.

2. Protein release from these liquid injectable polymers occurred by convection driven by osmotic pressure through zones of excess hydration formed around the protein/trehalose particles.

3. It was demonstrated that copolymer of EKC with DLLA initiated with octan-1-ol was well tolerated after subcutaneous injection in rats for 18 weeks.

4. It was identified that a major factor influencing VEGF and HGF release by the osmotic pressure mechanism was their solubility in the concentrated trehalose solution.

Bibliography

(1) Messina, L. M.; Brevetti, L. S.; Chang, D. S.; Paek, R.; Sarkar, R. Therapeutic angiogenesis for critical limb ischemia: invited commentary. *J. Control. Release* **2002**, *78*, 285-294.

(2) Layman, H.; Spiga, M. G.; Brooks, T.; Pham, S.; Webster, K. A.; Andreopoulos, F. M. The effect of the controlled release of basic fibroblast growth factor from ionic gelatin-based hydrogels on angiogenesis in a murine critical limb ischemic model. *Biomaterials* **2007**, *28*, 2646-2654.

(3) Nikol, S.; Baumgartner, I.; Van Belle, E.; Diehm, C.; Visona, A.; Capogrossi, M. C.; Ferreira-Maldent, N.; Gallino, A.; Wyatt, M. G.; Wijesinghe, L. D.; Fusari, M.; Stephan, D.; Emmerich, J.; Pompilio, G.; Vermassen, F.; Pham, E.; Grek, V.; Coleman, M.; Meyer, F.; TALISMAN 201 investigators Therapeutic angiogenesis with intramuscular NV1FGF improves amputation-free survival in patients with critical limb ischemia. *Mol. Ther.* **2008**, *16*, 972-978.

(4) Novo, S.; Coppola, G.; Milio, G. Critical limb ischemia: definition and natural history. *Curr. Drug Targets Cardiovasc. Haematol. Disord.* **2004**, *4*, 219-225.

(5) Annex, B. H.; Simons, M. Growth factor-induced therapeutic angiogenesis in the heart: protein therapy. *Cardiovasc. Res.* **2005**, *65*, 649-655.

(6) Esaki, J.; Marui, A.; Tabata, Y.; Komeda, M. Controlled release systems of angiogenic growth factors for cardiovascular diseases. *Expert Opin. Drug Deliv.* **2007**, *4*, 635-649.

(7) Laham, R. J.; Sellke, F. W.; Edelman, E. R.; Pearlman, J. D.; Ware, J. A.; Brown, D. L.; Gold, J. P.; Simons, M. Local perivascular delivery of basic fibroblast growth factor in patients undergoing coronary bypass surgery: results of a phase I randomized, double-blind, placebo-controlled trial. *Circulation* **1999**, *100*, 1865-1871.

(8) Lara-Hernandez, R.; Lozano-Vilardell, P.; Blanes, P.; Torreguitart-Mirada, N.; Galmes, A.; Besalduch, J. Safety and efficacy of therapeutic angiogenesis as a novel treatment in patients with critical limb ischemia. *Ann. Vasc. Surg.* **2010**, *24*, 287-294.

(9) Lee, K. Y.; Peters, M. C.; Mooney, D. J. Comparison of vascular endothelial growth factor and basic fibroblast growth factor on angiogenesis in SCID mice. *J. Control. Release* **2003**, *87*, 49-56.

(10) Abramson, D.; Dobrin, P., Eds.; In *Blood vessels and Lymphatics in organ systems;* Academic press inc: orlando, Florida, 1984; , pp 771.

(11) Mohrman, D.; Heller, L., Eds.; In *Cardiovascular Physiology;* Lange Medical Books/(McGraw-Hill): United States of America, 2002; , pp 255.

(12) Shepherd, J. T.; Vanhoutte, P. M. In Raven Press: New York, United State of America, 1980; , pp 328.

(13) Lawall, H.; Bramlage, P.; Amann, B. Treatment of peripheral arterial disease using stem and progenitor cell therapy. *J. Vasc. Surg.* **2011**, *53*, 445-453.

(14) Torsney, E.; Xu, Q. Resident vascular progenitor cells. *J. Mol. Cell. Cardiol.* **2011**, *50*, 304-311.

(15) Hirschi, K. K.; DAmore, P. A. Pericytes in the microvasculature. *Cardiovasc. Res.* **1996**, *32*, 687-698.

(16) Hu, Y.; Xu, Q. Adventitial Biology Differentiation and Function. *Arteriosclerosis Thrombosis and Vascular Biology* **2011**, *31*, 1523-1529.

(17) Carmeliet, P.; Collen, D. Genetic analysis of blood vessel formation role of endothelial versus smooth muscle cells. *Trends Cardiovasc. Med.* **1997**, *7*, 271-281.

(18) Tomiyama, H.; Yamashina, A. Non-Invasive Vascular Function Tests: Their Pathophysiological Background and Clinical Application. *Circulation Journal* **2010**, *74*, 24-33.

(19) Sato, Y.; Rifkin, D. B. Inhibition of Endothelial-Cell Movement by Pericytes and Smooth-Muscle Cells - Activation of a Latent Transforming Growth Factor-Beta-1-Like Molecule by Plasmin during Co-Culture. *J. Cell Biol.* **1989**, *109*, 309-315.

(20) Verbeek, M. M.; Otteholler, I.; Wesseling, P.; Ruiter, D. J.; Dewaal, R. M. W. Induction of Alpha-Smooth Muscle Actin Expression in Cultured Human Brain Pericytes by Transforming Growth-Factor-Beta-1. *Am. J. Pathol.* **1994**, *144*, 372-382.

(21) stenmark, K. R. The Adventitia: Essential role in pulmonary vascular remodelling. *Comprehensive physiology* **2011**, *1*, 141-161.

(22) Lee, H.; Chung, H. J.; Park, T. G. Perspectives on: Local and sustained delivery of angiogenic growth factors. *J. Bioact. Compatible Polym.* **2007**, *22*, 89-114.

(23) Risau, W. Mechanisms of angiogenesis. *Nature* **1997**, *386*, 671-674.

(24) Semenza, G. L. Vasculogenesis, angiogenesis, and arteriogenesis: mechanisms of blood vessel formation and remodeling. *J. Cell. Biochem.* **2007**, *102*, 840-847.

(25) Wang, H. U.; Chen, Z. F.; Anderson, D. J. Molecular distinction and angiogenic interaction between embryonic arteries and veins revealed by ephrin-B2 and its receptor Eph-B4. *Cell* **1998**, *93*, 741-753.

(26) Heil, M.; Eitenmuller, I.; Schmitz-Rixen, T.; Schaper, W. Arteriogenesis versus angiogenesis: similarities and differences. *J. Cell. Mol. Med.* **2006**, *10*, 45-55.

(27) Papetti, M.; Herman, I. Mechanisms of normal and tumor-derived angiogenesis. *American Journal of Physiology-Cell Physiology* **2002**, *282*, C947-C970.

(28) Cai, W.; Schaper, W. Mechanisms of arteriogenesis. *Acta Biochimica Et Biophysica Sinica* **2008**, *40*, 681-692.

(29) Yancopoulos, G. D.; Davis, S.; Gale, N. W.; Rudge, J. S.; Wiegand, S. J.; Holash, J. Vascular-specific growth factors and blood vessel formation. *Nature* **2000**, *407*, 242-248.

(30) Amsden, B. G.; Timbart, L.; Marecak, D.; Chapanian, R.; Tse, M. Y.; Pang, S. C. VEGF-induced angiogenesis following localized delivery via injectable, low viscosity poly(trimethylene carbonate). *J. Control. Release* **2010**, *145*, 109-115.

(31) Chapanian, R.; Amsden, B. G. Combined and sequential delivery of bioactive VEGF165 and HGF from poly(trimethylene carbonate) based photo-cross-linked elastomers. *J. Control. Release* **2010**, *143*, 53-63.

(32) Sun, Q.; Chen, R. R.; Shen, Y.; Mooney, D. J.; Rajagopalan, S.; Grossman, P. M. Sustained vascular endothelial growth factor delivery enhances angiogenesis and perfusion in ischemic hind limb. *Pharm. Res.* **2005**, *22*, 1110-1116.

(33) Silva, E. A.; Mooney, D. J. Spatiotemporal control of vascular endothelial growth factor delivery from injectable hydrogels enhances angiogenesis. *J. Thromb. Haemost.* **2007**, *5*, 590-598.

(34) Marui, A.; Kanematsu, A.; Yamahara, K.; Doi, K.; Kushibiki, T.; Yamamoto, M.; Itoh, H.; Ikeda, T.; Tabata, Y.; Komeda, M. Simultaneous application of basic fibroblast growth factor and hepatocyte growth factor to enhance the blood vessels formation. *J. Vasc. Surg.* **2005**, *41*, 82-90.

(35) Ruvinov, E.; Leor, J.; Cohen, S. The effects of controlled HGF delivery from an affinity-binding alginate biomaterial on angiogenesis and blood perfusion in a hindlimb ischemia model. *Biomaterials* **2010**, *31*, 4573-4582.

(36) Ruvinov, E.; Leor, J.; Cohen, S. The promotion of myocardial repair by the sequential delivery of IGF-1 and HGF from an injectable alginate biomaterial in a model of acute myocardial infarction. *Biomaterials* **2011**, *32*, 565-578.

(37) Lazarous, D. F.; Shou, M.; Scheinowitz, M.; Hodge, E.; Thirumurti, V.; Kitsiou, A. N.; Stiber, J. A.; Lobo, A. D.; Hunsberger, S.; Guetta, E.; Epstein, S. E.; Unger, E. F. Comparative effects of basic fibroblast growth factor and vascular endothelial growth factor on coronary collateral development and the arterial response to injury. *Circulation* **1996**, *94*, 1074-1082.

(38) Roy, H.; Bhardwaj, S.; Yla-Herttuala, S. Biology of vascular endothelial growth factors. *FEBS Lett.* **2006**, *580*, 2879-2887.

(39) Ferrara, N.; Gerber, H. P.; LeCouter, J. The biology of VEGF and its receptors. *Nat. Med.* **2003**, *9*, 669-676.

(40) Xin, X.; Yang, S.; Ingle, G.; Zlot, C.; Rangell, L.; Kowalski, J.; Schwall, R.; Ferrara, N.; Gerritsen, M. E. Hepatocyte growth factor enhances vascular endothelial growth factor-induced angiogenesis in vitro and in vivo. *Am. J. Pathol.* **2001**, *158*, 1111-1120.

(41) Takeshita, S.; Zheng, L. P.; Brogi, E.; Kearney, M.; Pu, L. Q.; Bunting, S.; Ferrara, N.; Symes, J. F.; Isner, J. M. Therapeutic angiogenesis. A single intraarterial bolus of vascular endothelial growth factor augments revascularization in a rabbit ischemic hind limb model. *J. Clin. Invest.* **1994**, *93*, 662-670.

(42) Sulpice, E.; Ding, S.; Muscatelli-Groux, B.; Berge, M.; Han, Z. C.; Plouet, J.; Tobelem, G.; Merkulova-Rainon, T. Cross-talk between the VEGF-A and HGF signalling pathways in endothelial cells. *Biol. Cell.* **2009**, *101*, 525-539.

(43) Goolcharran, C.; Cleland, J.; Keck, R.; Jones, A.; Borchardt, R. Comparison of the rates of deamidation, diketopiperazine formation, and oxidation in recombinant human vascular endothelial growth factor and model peptides. *Aaps Pharmsci* **2000**, *2*, 5.

(44) Gu, F.; Amsden, B.; Neufeld, R. Sustained delivery of vascular endothelial growth factor with alginate beads. *J. Control. Release* **2004**, *96*, 463-472.

(45) Ferrara, N.; Houck, K.; Jakeman, L.; Leung, D. W. Molecular and biological properties of the vascular endothelial growth factor family of proteins. *Endocr. Rev.* **1992**, *13*, 18-32.

(46) Cleland, J. L.; Duenas, E. T.; Park, A.; Daugherty, A.; Kahn, J.; Kowalski, J.; Cuthbertson, A. Development of poly-(D,L-lactide--coglycolide) microsphere formulations containing recombinant human vascular endothelial growth factor to promote local angiogenesis. *J. Control. Release* **2001**, *72*, 13-24.

(47) Muller, Y.; Christinger, H.; Keyt, B.; deVos, A. The crystal structure of vascular endothelial growth factor (VEGF) refined to 1.93 angstrom resolution: multiple copy flexibility and receptor binding. *Structure* **1997**, *5*, 1325-1338.

(48) Dobaczewski, M.; Gonzalez-Quesada, C.; Frangogiannis, N. G. The extracellular matrix as a modulator of the inflammatory and reparative response following myocardial infarction. *J. Mol. Cell. Cardiol.* **2010**, *48*, 504-511.

(49) Gille, J.; Khalik, M.; Konig, V.; Kaufmann, R. Hepatocyte growth factor scatter factor (HGF/SF) induces vascular permeability factor (VPF/VEGF) expression by cultured keratinocytes. *J. Invest. Dermatol.* **1998**, *111*, 1160-1165.

(50) Wojta, J.; Kaun, C.; Breuss, J.; Koshelnick, Y.; Beckmann, R.; Hattey, E.; Mildner, M.; Weninger, W.; Nakamura, T.; Tschachler, E.; Binder, B. Hepatocyte growth factor increases expression of vascular endothelial growth factor and plasminogen activator inhibitor-1 in human keratinocytes and the vascular endothelial growth factor receptor flk-1 in human endothelial cells. *Laboratory Investigation* **1999**, *79*, 427-438.

(51) Amsden, B. G. Delivery approaches for angiogenic growth factors in the treatment of ischemic conditions. *Expert Opin. Drug Deliv.* **2011**, *8*, 873-890.

(52) Van Belle, E.; Witzenbichler, B.; Chen, D.; Silver, M.; Chang, L.; Schwall, R.; Isner, J. M. Potentiated angiogenic effect of scatter factor/hepatocyte growth factor via induction of vascular endothelial growth factor: the case for paracrine amplification of angiogenesis. *Circulation* **1998**, *97*, 381-390.

(53) Kawaida, K.; Matsumoto, K.; Shimazu, H.; Nakamura, T. Hepatocyte growth factor prevents acute renal failure and accelerates renal regeneration in mice. *Proc. Natl. Acad. Sci. U. S. A.* **1994**, *91*, 4357-4361.

(54) Gherardi, E.; Gray, J.; Stoker, M.; Perryman, M.; Furlong, R. Purification of scatter factor, a fibroblast-derived basic protein that modulates epithelial interactions and movement. *Proc. Natl. Acad. Sci. U. S. A.* **1989**, *86*, 5844-5848.

(55) Naldini, L.; Tamagnone, L.; Vigna, E.; Sachs, M.; Hartmann, G.; Birchmeier, W.; Daikuhara, Y.; Tsubouchi, H.; Blasi, F.; Comoglio, P. M. Extracellular Proteolytic Cleavage by Urokinase is Required for Activation of Hepatocyte Growth-Factor Scatter Factor. *EMBO J.* **1992**, *11*, 4825-4833.

(56) Stephens, P.; Hiscox, S.; Cook, H.; Jiang, W.; Wu, Z.; Thomas, D. Phenotypic variation in the production of bioactive hepatocyte growth factor/scatter factor by oral mucosal and skin fibroblasts RID B-1293-2010. *Wound Repair and Regeneration* **2001**, *9*, 34-43.

(57) Zhou, H.; Mazzulla, M.; Kaufman, J.; Stahl, S.; Wingfield, P.; Rubin, J.; Bottaro, D.; Byrd, R. The solution structure of the N-terminal domain of hepatocyte growth factor reveals a potential heparin-binding site RID F-8550-2010. *Structure* **1998**, *6*, 109-116.

(58) Nakamura, T. Structure and function of hepatocyte growth factor. *Progress in growth factor research* **1991**, *3*, 67-85.

(59) Ozeki, M.; Ishii, T.; Hirano, Y.; Tabata, Y. Controlled release of hepatocyte growth factor from gelatin hydrogels based on hydrogel degradation. *J. Drug Target.* **2001**, *9*, 461-471.

(60) Sun, Q.; Silva, E. A.; Wang, A.; Fritton, J. C.; Mooney, D. J.; Schaffler, M. B.; Grossman, P. M.; Rajagopalan, S. Sustained release of multiple growth factors from injectable polymeric system as a novel therapeutic approach towards angiogenesis. *Pharm. Res.* **2010**, *27*, 264-271.

(61) Sun, G.; Shen, Y. I.; Kusuma, S.; Fox-Talbot, K.; Steenbergen, C. J.; Gerecht, S. Functional neovascularization of biodegradable dextran hydrogels with multiple angiogenic growth factors. *Biomaterials* **2011**, *32*, 95-106.

(62) Richardson, T. P.; Peters, M. C.; Ennett, A. B.; Mooney, D. J. Polymeric system for dual growth factor delivery. *Nat. Biotechnol.* **2001**, *19*, 1029-1034.

(63) Layman, H.; Rahnemai-Azar, A.; Pham, S. M.; Tsechpenakis, G.; Andreopoulos, F. M. Synergistic angiogenic effect of codelivering fibroblast growth factor 2 and granulocyte-colony stimulating factor from fibrin scaffolds and bone marrow transplantation in critical limb ischemia. *Tissue Engineering - Part A* **2011**, *17*, 243-254.

(64) Davies, N.; Dobner, S.; Bezuidenhout, D.; Schmidt, C.; Beck, M.; Zisch, A. H.; Zilla, P. The dosage dependence of VEGF stimulation on scaffold neovascularisation. *Biomaterials* **2008**, *29*, 3531-3538.

(65) GRANT, D.; KLEINMAN, H.; GOLDBERG, I.; BHARGAVA, M.; NICKOLOFF, B.; KINSELLA, J.; POLVERINI, P.; ROSEN, E. Scatter Factor Induces Blood-Vessel Formation Invivo. *Proc. Natl. Acad. Sci. U. S. A.* **1993**, *90*, 1937-1941.

(66) Golocheikine, A.; Tiriveedhi, V.; Angaswamy, N.; Benshoff, N.; Sabarinathan, R.; Mohanakumar, T. Cooperative Signaling for Angiogenesis and Neovascularization by VEGF and HGF Following Islet Transplantation. *Transplantation* **2010**, *90*, 725-731.

(67) Bauters, C.; Asahara, T.; Zheng, L. P.; Takeshita, S.; Bunting, S.; Ferrara, N.; Symes, J. F.; Isner, J. M. Site-specific therapeutic angiogenesis after systemic administration of vascular endothelial growth factor. *J. Vasc. Surg.* **1995**, *21*, 314-24; discussion 324-5.

(68) Hariawala, M. D.; Horowitz, J. R.; Esakof, D.; Sheriff, D. D.; Walter, D. H.; Keyt, B.; Isner, J. M.; Symes, J. F. VEGF improves myocardial blood flow but produces EDRF-mediated hypotension in porcine hearts. *J. Surg. Res.* **1996**, *63*, 77-82.

(69) Henry, T. D.; Annex, B. H.; McKendall, G. R.; Azrin, M. A.; Lopez, J. J.; Giordano, F. J.; Shah, P. K.; Willerson, J. T.; Benza, R. L.; Berman, D. S.; Gibson, C. M.; Bajamonde, A.; Rundle, A. C.; Fine, J.; McCluskey, E. R.; VIVA Investigators The VIVA trial: Vascular endothelial growth factor in Ischemia for Vascular Angiogenesis. *Circulation* **2003**, *107*, 1359-1365.

(70) Marui, A.; Kanematsu, A.; Yamahara, K.; Doi, K.; Kushibiki, T.; Yamamoto, M.; Itoh, H.; Ikeda, T.; Tabata, Y.; Komeda, M. Simultaneous application of basic fibroblast growth factor and hcpatocyte growth factor to enhance the blood vessels formation. *Journal of Vascular Surgery* **2005**, *41*, 82-90.

(71) Cleland, J. L.; Powell, M. F.; Shire, S. J. The Development of Stable Protein Formulations - a Close Look at Protein Aggregation, Deamidation, and Oxidation. *Crit. Rev. Ther. Drug Carrier Syst.* **1993**, *10*, 307-377.

(72) Geiger, T.; Clarke, S. Deamidation, isomerization and recemization at asparaginyl and aspartyl residues in peptides. **1987**, *262*, 785.

(73) Duenas, E. T.; Keck, R.; De Vos, A. **Comparison between light induced and chemically induced oxidation of rhVEGF**. **2001**, *18*, 1455.

(74) Goolcharran, C.; Borchardt, R. Kinetics of diketopiperazine formation using model peptides. *J. Pharm. Sci.* **1998**, *87*, 283-288.

(75) Hirose, K.; Fujita, M.; Marui, A.; Arai, Y.; Sakaguchi, H.; Huang, Y.; Chandra, S.; Tabata, Y.; Komeda, M. Combined treatment of sustained-release basic fibroblast growth factor and sarpogrelate enhances collateral blood flow effectively in rabbit hindlimb ischemia. *Circulation Journal* **2006**, *70*, 1190-1194.

(76) Hao, X.; Silva, E. A.; Mansson-Broberg, A.; Grinnemo, K. H.; Siddiqui, A. J.; Dellgren, G.; Wardell, E.; Brodin, L. A.; Mooney, D. J.; Sylven, C. Angiogenic effects of sequential release of VEGF-A165 and PDGF-BB with alginate hydrogels after myocardial infarction. *Cardiovasc. Res.* **2007**, *75*, 178-185.

(77) Post, M. J.; Simons, M. Gene therapy versus protein-based therapy: a matter of pharmacokinetics. *Drug Discov. Today* **2001**, *6*, 769-770.

(78) Germani, A.; Di Campli, C.; Pompilio, G.; Biglioli, P.; Capogrossi, M. C. Regenerative Therapy in Peripheral Artery Disease. *Cardiovascular Therapeutics* **2009**, *27*, 289-304.

(79) Kang, S.; Lim, H.; Seo, S.; Jeon, O.; Lee, M.; Kim, B. Nano sphere-mediated deliver of vascular endothelial growth factor gene for therapeutic angiogenesis in mouse ischemic limbs RID B-3179-2008. *Biomaterials* **2008**, *29*, 1109-1117.

(80) Kusumanto, Y.; Van Weel, V.; Mulder, N.; Smit, A.; Van den Dungen, J.; Hooymans, J.; Sluiter, W.; Tio, R.; Quax, P.; Gans, R.; Dullaart, R.; Hospers, G. Treatment with intramuscular vascular endothelial growth factor gene compared with placebo for patients with diabetes mellitus and critical limb ischemia: A double-blind randomized trial. *Hum. Gene Ther.* **2006**, *17*, 683-691.

(81) Shintani, S.; Murohara, T.; Ikeda, H.; Ueno, T.; Sasaki, K.; Duan, J.; Imaizumi, T. Augmentation of postnatal neovascularization with autologous bone marrow transplantation. *Circulation* **2001**, *103*, 897-903.

(82) Kamihata, H.; Matsubara, H.; Nishiue, T.; Fujiyama, S.; Tsutsumi, Y.; Ozono, R.; Masaki, H.; Mori, Y.; Iba, O.; Tateishi, E.; Kosaki, A.; Shintani, S.; Murohara, T.; Imaizumi, T.; Iwasaka, T. Implantation of bone marrow mononuclear cells into ischemic myocardium enhances collateral perfusion and regional function via side supply of angioblasts, angiogenic ligands, and cytokines. *Circulation* **2001**, *104*, 1046-1052.

(83) Finney, M. R.; Greco, N. J.; Haynesworth, S. E.; Martin, J. M.; Hedrick, D. P.; Swan, J. Z.; Winter, D. G.; Kadereit, S.; Joseph, M. E.; Fu, P. F.; Pompili, V. J.; Laughlin, M. J. Direct comparison of umbilical cord blood versus bone marrow-derived endothelial precursor cells in mediating neovascularization in response to vascular ischemia. *Biology of Blood and Marrow Transplantation* **2006**, *12*, 585-593.

(84) Huang, P.; Chen, Y.; Wang, C.; Chen, J.; Tsai, H.; Lin, F.; Lo, W.; Wu, T.; Sata, M.; Chen, J.; Lin, S. Matrix Metalloproteinase-9 Is Essential for Ischemia-Induced Neovascularization by Modulating Bone Marrow-Derived Endothelial Progenitor Cells. *Arteriosclerosis Thrombosis and Vascular Biology* **2009**, *29*, 1179-U58.

(85) Bhang, S. H.; Cho, S.; Lim, J. M.; Kang, J. M.; Lee, T.; Yang, H. S.; Song, Y. S.; Park, M. H.; Kim, H.; Yoo, K.; Jang, Y.; Langer, R.; Anderson, D. G.; Kim, B. Locally Delivered Growth Factor Enhances the Angiogenic Efficacy of Adipose-Derived Stromal Cells Transplanted to Ischemic Limbs. *Stem Cells* **2009**, *27*, 1976-1986.

(86) Sneider, E. B.; Nowicki, P. T.; Messina, L. M. Regenerative Medicine in the Treatment of Peripheral Arterial Disease. *J. Cell. Biochem.* **2009**, *108*, 753-761.

(87) Sprengers, R. W.; Lips, D. J.; Moll, F. L.; Verhaar, M. C. Progenitor cell therapy in patients with critical limb ischemia without surgical options. *Ann. Surg.* **2008**, *247*, 411-420.

(88) van de Weert, M.; Hennink, W.; Jiskoot, W. Protein instability in poly(lactic-co-glycolic acid) microparticles. *Pharm. Res.* **2000**, *17*, 1159-1167.

(89) Takahata, H.; Lavelle, E.; Coombes, A.; Davis, S. The distribution of protein associated with poly(DL-lactide co-glycolide) microparticles and its degradation in simulated body fluids RID A-1716-2008. *J. Controlled Release* **1998**, *50*, 237-246.

(90) von Degenfeld, G.; Banfi, A.; Springer, M. L.; Wagner, R. A.; Jacobi, J.; Ozawa, C. R.; Merchant, M. J.; Cooke, J. P.; Blau, H. M. Microenvironmental VEGF distribution is critical for stable and functional vessel growth in ischemia. *Faseb Journal* **2006**, *20*, 2657-+.

(91) Qiu, B.; Stefanos, S.; Ma, J.; Lalloo, A.; Perry, B. A.; Leibowitz, M. J.; Sinko, P. J.; Stein, S. A hydrogel prepared by in situ cross-linking of a thiol-containing poly(ethylene glycol)-based copolymer: a new biomaterial for protein drug delivery. *Biomaterials* **2003**, *24*, 11-18.

(92) Fujita, M.; Ishihara, M.; Simizu, M.; Obara, K.; Ishizuka, T.; Saito, Y.; Yura, H.; Morimoto, Y.; Takase, B.; Matsui, T.; Kikuchi, M.; Maehara, T. Vascularization in vivo caused by the controlled release of fibroblast growth factor-2 from an injectable chitosan/non-anticoagulant heparin hydrogel. *Biomaterials* **2004**, *25*, 699-706.

(93) Bouhadir, K.; Lee, K.; Alsberg, E.; Damm, K.; Anderson, K.; Mooney, D. Degradation of partially oxidized alginate and its potential application for tissue engineering. *Biotechnol. Prog.* **2001**, *17*, 945-950.

(94) ALSHAMKHANI, A.; DUNCAN, R. Radioiodination of Alginate Via Covalently-Bound Tyrosinamide Allows Monitoring of its Fate In-Vivo. *J. Bioact. Compatible Polym.* **1995**, *10*, 4-13.

(95) Kanematsu, A.; Yamamoto, S.; Ozeki, M.; Noguchi, T.; Kanatani, I.; Ogawa, O.; Tabata, Y. Collagenous matrices as release carriers of exogenous growth factors. *Biomaterials* **2004**, *25*, 4513-4520.

(96) Young, S.; Wong, M.; Tabata, Y.; Mikos, A. G. Gelatin as a delivery vehicle for the controlled release of bioactive molecules. *J. Controlled Release* **2005**, *109*, 256-274.

(97) Yamamoto, M.; Tabata, Y.; Ikada, Y. Growth factor release from gelatin hydrogel for tissue engineering. *J. Bioact. Compatible Polym.* **1999**, *14*, 474-489.

(98) Patel, Z. S.; Ueda, H.; Yamamoto, M.; Tabata, Y.; Mikos, A. G. In vitro and in vivo release of vascular endothelial growth factor from gelatin microparticles and biodegradable composite scaffolds. *Pharm. Res.* **2008**, *25*, 2370-2378.

(99) Ueno, H.; Yamada, H.; Tanaka, I.; Kaba, N.; Matsuura, M.; Okumura, M.; Kadosawa, T.; Fujinaga, T. Accelerating effects of chitosan for healing at early phase of experimental open wound in dogs. *Biomaterials* **1999**, *20*, 1407-1414.

(100) Adekogbe, I.; Ghanem, A. Fabrication and characterization of DTBP-crosslinked chitosan scaffolds for skin tissue engineering. *Biomaterials* **2005**, *26*, 7241-7250.

(101) Bae, K.; Jun, E. J.; Lee, S. M.; Paik, D. I.; Kim, J. B. Effect of water-soluble reduced chitosan on Streptococcus mutans, plaque regrowth and biofilm vitality. *Clin. Oral Investig.* **2006**, *10*, 102-107.

(102) Ono, K.; Saito, Y.; Yura, H.; Ishikawa, K.; Kurita, A.; Akaike, T.; Ishihara, M. Photocrosslinkable chitosan as a biological adhesive. *J. Biomed. Mater. Res.* **2000**, *49*, 289-295.

(103) Ishihara, M.; Obara, K.; Ishizuka, T.; Fujita, M.; Sato, M.; Masuoka, K.; Saito, Y.; Yura, H.; Matsui, T.; Hattori, H.; Kikuchi, M.; Kurita, A. Controlled release of fibroblast growth factors and heparin from photocrosslinked chitosan hydrogels and subsequent effect on in vivo vascularization. *Journal of Biomedical Materials Research Part a* **2003**, *64A*, 551-559.

(104) Yeo, Y.; Geng, W.; Ito, T.; Kohane, D. S.; Burdick, J. A.; Radisic, M. Photocrosslinkable hydrogel for myocyte cell culture and injection. *Journal of Biomedical Materials Research Part B-Applied Biomaterials* **2007**, *81B*, 312-322.

(105) Jeon, O.; Kang, S.; Lim, H.; Hyung Chung, J.; Kim, B. Long-term and zero-order release of basic fibroblast growth factor from heparin-conjugated poly(L-lactide-co-glycolide) nanospheres and fibrin gel. *Biomaterials* **2006**, *27*, 1598-1607.

(106) Formiga, F. R.; Pelacho, B.; Garbayo, E.; Abizanda, G.; Gavira, J. J.; Simon-Yarza, T.; Mazo, M.; Tamayo, E.; Jauquicoa, C.; Ortiz-de-Solorzano, C.; Prosper, F.; Blanco-Prieto, M. Sustained release of VEGF through PLGA microparticles improves vasculogenesis and tissue remodeling in an acute myocardial ischemia-reperfusion model. *J. Controlled Release* **2010**, *147*, 30-37.

(107) Zhu, X. H.; Wang, C. H.; Tong, Y. W. In vitro characterization of hepatocyte growth factor release from PHBV/PLGA microsphere scaffold. *J. Biomed. Mater. Res. A.* **2009**, *89*, 411-423.

(108) Quaglia, F.; Ostacolo, L.; Nese, G.; De Rosa, G.; La Rotonda, M.; Palumbo, R.; Maglio, G. Microspheres made of poly (epsilon-caprolactone)-based amphiphilic copolymers: Potential in sustained delivery of proteins. *Macromolecular Bioscience* **2005**, *5*, 945-954.

(109) Zambaux, M.; Bonneaux, F.; Gref, R.; Dellacherie, E.; Vigneron, C. Preparation and characterization of protein C-loaded PLA nanoparticles RID F-1487-2011. *J. Controlled Release* **1999**, *60*, 179-188.

(110) Kim, T. K.; Burgess, D. J. Pharmacokinetic characterization of 14C-vascular endothelial growth factor controlled release microspheres using a rat model. *J. Pharm. Pharmacol.* **2002**, *54*, 897-905.

(111) Fu, K.; Pack, D.; Klibanov, A.; Langer, R. Visual evidence of acidic environment within degrading poly(lactic-co-glycolic acid) (PLGA) microspheres. *Pharm. Res.* **2000**, *17*, 100-106.

(112) Cromwell, M. E. M.; Hilario, E.; Jacobson, F. Protein aggregation and bioprocessing. *Aaps Journal* **2006**, *8*, E572-E579.

(113) Chen, R. R.; Silva, E. A.; Yuen, W. W.; Mooney, D. J. Spatio-temporal VEGF and PDGF delivery patterns blood vessel formation and maturation. *Pharm. Res.* **2007**, *24*, 258-264.

(114) Ward, W. K.; Slobodzian, E. P.; Tiekotter, K. L.; Wood, M. D. The effect of microgeometry, implant thickness and polyurethane chemistry on the foreign body response to subcutaneous implants. *Biomaterials* **2002**, *23*, 4185-4192.

(115) Yoon, J. J.; Chung, H. J.; Lee, H. J.; Park, T. G. Heparin-immobilized biodegradable scaffolds for local and sustained release of angiogenic growth factor. *Journal of Biomedical Materials Research Part a* **2006**, *79A*, 934-942.

(116) Ziegler, J.; Mayr-Wohlfart, U.; Kessler, S.; Breitig, D.; Gunther, K. Adsorption and release properties of growth factors from biodegradable implants. *J. Biomed. Mater. Res.* **2002**, *59*, 422-428.

(117) Sheridan, M.; Shea, L.; Peters, M.; Mooney, D. Bioadsorbable polymer scaffolds for tissue engineering capable of sustained growth factor delivery RID B-7615-2009. *J. Controlled Release* **2000**, *64*, 91-102.

(118) Ennett, A. B.; Kaigler, D.; Mooney, D. J. Temporally regulated delivery of VEGF in vitro and in vivo. *Journal of Biomedical Materials Research Part a* **2006**, *79A*, 176-184.

(119) Smith, M.; Riddle, K.; Mooney, D. Delivery of hepatotrophic factors fails to enhance longer-term survival of subcutaneously transplanted hepatocytes. *Tissue Eng.* **2006**, *12*, 235-244.

(120) Riggs, P. D.; Kinchesh, P.; Braden, M.; Patel, M. P. Nuclear magnetic imaging of an osmotic water uptake and delivery process. *Biomaterials* **2001**, *22*, 419-427.

(121) Fedors, R. F. OSMOTIC EFFECTS IN WATER ABSORPTION BY POLYMERS. *Polymer* **1980**, *21*, 207-212.

(122) Amsden, B. Review of osmotic pressure driven release of proteins from monolithic devices. *J. Pharm. Pharm. Sci.* **2007**, *10*, 129-143.

(123) Amsden, B. G.; Cheng, Y. Enhanced fraction releasable above percolation threshold from monoliths containing osmotic excipients. *J. Controlled Release* **1994**, *31*, 21-32.

(124) GOLOMB, G.; FISHER, P.; RAHAMIM, E. The Relationship between Drug Release Rate, Particle-Size and Swelling of Silicone Matrices. *J. Controlled Release* **1990**, *12*, 121-132.

(125) Gu, F.; Neufeld, R.; Amsden, B. Sustained release of bioactive therapeutic proteins from a biodegradable elastomeric device. *J. Controlled Release* **2007**, *117*, 80-89.

(126) Amsden, B.; Cheng, Y. -. A generic protein delivery system based on osmotically rupturable monoliths. *J. Controlled Release* **1995**, *33*, 99-99.

(127) Gu, F.; Neufeld, R.; Amsden, B. Sustained release of bioactive therapeutic proteins from a biodegradable elastomeric device RID C-5187-2008. *J. Controlled Release* **2007**, *117*, 80-89.

(128) Gu, F.; Neufeld, R.; Amsden, B. Sustained release of bioactive therapeutic proteins from a biodegradable elastomeric device. *J. Controlled Release* **2007**, *117*, 80-89.

(129) Amsden, B. G.; Timbart, L.; Marecak, D.; Chapanian, R.; Tse, M. Y.; Pang, S. C. VEGF-induced angiogenesis following localized delivery via injectable, low viscosity poly(trimethylene carbonate). *J. Control. Release* **2010**, *145*, 109-115.

(130) Babasola, O. I.; Amsden, B. G. Surface Eroding, Liquid Injectable Polymers Based on 5-Ethylene Ketal epsilon-Caprolactone. *Biomacromolecules* **2011**.

(131) Heller, J.; Barr, J.; Ng, S.; Shen, H. R.; Gurny, R.; Schwach-Abdelaoui, K.; Rothen-Weinhold, A.; van de Weert, M. Development of poly(ortho esters) and their application for bovine serum albumin and bupivacaine delivery. *J. Control. Release* **2002**, *78*, 133-141.

(132) van de Weert, M.; van Steenbergen, M. J.; Cleland, J. L.; Heller, J.; Hennink, W. E.; Crommelin, D. J. Semisolid, self-catalyzed poly(ortho ester)s as controlled-release systems: protein release and protein stability issues. *J. Pharm. Sci.* **2002**, *91*, 1065-1074.

(133) van de Weert, M.; van Steenbergen, M. J.; Cleland, J. L.; Heller, J.; Hennink, W. E.; Crommelin, D. J. Semisolid, self-catalyzed poly(ortho ester)s as controlled-release systems: protein release and protein stability issues. *J. Pharm. Sci.* **2002**, *91*, 1065-1074.

(134) Luttikhuizen, D. T.; Harmsen, M. C.; Van Luyn, M. J. Cellular and molecular dynamics in the foreign body reaction. *Tissue Eng.* **2006**, *12*, 1955-1970.

(135) WILLIAMS, D. Tissue - Biomaterial Interactions. *J. Mater. Sci.* **1987**, *22*, 3421-3445.

(136) Anderson, J. M.; Rodriguez, A.; Chang, D. T. Foreign body reaction to biomaterials. *Semin. Immunol.* **2008**, *20*, 86-100.

(137) Broughton, G.; Janis, J. E.; Attinger, C. E. The basic science of wound healing. *Plast. Reconstr. Surg.* **2006**, *117*, 12S-34S.

(138) Anderson, J. M.; McNally, A. K. Biocompatibility of implants: lymphocyte/macrophage interactions. *Seminars in Immunopathology* **2011**, *33*, 221-233.

(139) Tang, Y.; Singh, J. Thermosensitive Drug Delivery System of Salmon Calcitonin: In Vitro Release, In Vivo Absorption, Bioactivity and Therapeutic Efficacies. *Pharm. Res.* **2010**, *27*, 272-284.

(140) Fournier, E.; Passirani, C.; Montero-Menei, C.; Benoit, J. Biocompatibility of implantable synthetic polymeric drug carriers: focus on brain biocompatibility. *Biomaterials* **2003**, *24*, 3311-3331.

(141) Zdolsek, J.; Eaton, J. W.; Tang, L. Histamine release and fibrinogen adsorption mediate acute inflammatory responses to biomaterial implants in humans. *Journal of Translational Medicine* **2007**, *5*, 31.

(142) Bergsma, J. E.; de Bruijn, W. C.; Rozema, F. R.; Bos, R. R.; Boering, G. Late degradation tissue response to poly(L-lactide) bone plates and screws. *Biomaterials* **1995**, *16*, 25-31.

(143) Bergsma, J. E.; Rozema, F. R.; Bos, R. R.; Boering, G.; de Bruijn, W. C.; Pennings, A. J. In vivo degradation and biocompatibility study of in vitro pre-degraded as-polymerized polyactide particles. *Biomaterials* **1995**, *16*, 267-274.

(144) Guan, J.; Stankus, J. J.; Wagner, W. R. Biodegradable elastomeric scaffolds with basic fibroblast growth factor release. *J. Controlled Release* **2007**, *120*, 70-78.

(145) Tian, D.; Dubois, P.; Jerome, R. Macromolecular engineering of polylactones and polylactides .23. Synthesis and characterization of biodegradable and biocompatible homopolymers and block copolymers based on 1,4,8-trioxa[4.6]spiro-9-undecanone RID B-9983-2008. *Macromolecules* **1997**, *30*, 1947-1954.

(146) Bergsma, J. E.; de Bruijn, W. C.; Rozema, F. R.; Bos, R. R.; Boering, G. Late degradation tissue response to poly(L-lactide) bone plates and screws. *Biomaterials* **1995**, *16*, 25-31.

(147) Sharifpoor, S.; Amsden, B. In vitro release of a water-soluble agent from low viscosity biodegradable, injectable oligomers. *Eur. J. Pharm. Biopharm.* **2007**, *65*, 336-345.

(148) Tian, D.; Dubois, P.; Jerome, R. Macromolecular engineering of polylactones and polylactides. 22. Copolymerization of e-caprolactone and 1,4,8-trioxaspiro[4.6]-9-undecanone initiated by aluminum isopropoxide. *Macromolecules* **1997**, *30*, 2575-2581.

(149) Kumar, T. R.; Soppimath, K.; Nachaegari, S. K. Novel delivery technologies for protein and peptide therapeutics. *Curr. Pharm. Biotechnol.* **2006**, *7*, 261-276.

(150) Lee, J. Y.; Kim, K. S.; Kang, Y. M.; Kim, E. S.; Hwang, S. J.; Lee, H. B.; Min, B. H.; Kim, J. H.; Kim, M. S. In vivo efficacy of paclitaxel-loaded injectable in situ-forming gel against subcutaneous tumor growth. *Int. J. Pharm.* **2010**, *392*, 51-56.

(151) Amsden, B. G. Liquid, injectable, hydrophobic and biodegradable polymers as drug delivery vehicles. *Macromol. Biosci.* **2010**, *10*, 825-835.

(152) Schwach-Abdellaoui, K.; Gurny, R.; Heller, J.; Barr, J. Control of molecular weight for auto-catalyzed poly(ortho ester) obtained by polycondensation reaction. *Int. J. Polym. Anal. Charact.* **2002**, *7*, 145-161.

(153) Schwach-Abdellaoui, K.; Heller, J.; Gurny, R. Hydrolysis and erosion studies of autocatalyzed poly(ortho esters) containing lactoyl-lactyl acid dimers. *Macromolecules* **1999**, *32*, 301-307.

(154) Schwach-Abdellaoui, K.; Loup, P. J.; Vivien-Castioni, N.; Mombelli, A.; Baehni, P.; Barr, J.; Heller, J.; Gurny, R. Bioerodible injectable poly(ortho ester) for tetracycline controlled delivery to periodontal pockets: preliminary trial in humans. *AAPS PharmSci* **2002**, *4*, E20.

(155) Schwach-Abdellaoui, K.; Monti, A.; Barr, J.; Heller, J.; Gurny, R. Optimization of a novel bioerodible device based on auto-catalyzed poly(ortho esters) for controlled delivery of tetracycline to periodontal pocket. *Biomaterials* **2001**, *22*, 1659-1666.

(156) Hatefi, A.; Knight, D.; Amsden, B. A biodegradable injectable thermoplastic for localized camptothecin delivery. *J. Pharm. Sci.* **2004**, *93*, 1195-1204.

(157) Sokolsky-Papkov, M.; Domb, A. J. Stereoisomeric effect on in vitro drug release from injectable poly(lactic acid co castor oil) polyesters. *Polym. Adv. Technol.* **2008**, *19*, 671-679.

(158) Scopelianos, A. G.; Bezwada, R. S.; Arnold, S. C.; Huxel, S. T. Reg.Pat.Tr.Des.States: Designated States R: DE, FR, GB, IT.; Patent Application Country: Application: EP; Patent Country: EP; Priority Application Country: US Patent 711794, 1996.

(159) Trimaille, T.; Gurny, R.; Moller, M. Poly(hexyl-substituted lactides): novel injectable hydrophobic drug delivery systems. *J. Biomed. Mater. Res. A.* **2007**, *80*, 55-65.

(160) Timbart, L.; Tse, M. Y.; Pang, S. C.; Babasola, O.; Amsden, B. G. Low viscosity poly(trimethylene carbonate) for localized drug delivery: rheological properties and in vivo degradation. *Macromol. Biosci.* **2009**, *9*, 786-794.

(161) Nathan, A. Reg.Pat.Tr.Des.States: Designated States R: AT, BE, CH, DE, DK, ES, FR, GB, GR, IT, LI, LU, NL, SE, MC, PT, IE, SI, LT, LV, FI, RO, MK, CY, AL, TR, BG, CZ, EE, HU, SK.; Patent Application Country: Application: EP; Patent Country: EP; Priority Ap(TRUNCATED) Patent 1369136, 2003.

(162) Nathan, A.; Melican, M.; Brown, K.; Zimmerman, M. Reg.Pat.Tr.Des.States: Designated States R: AT, BE, CH, DE, DK, ES, FR, GB, GR, IT, LI, LU, NL, SE, MC, PT, IE, SI, LT, LV, FI, RO, MK, CY, AL, TR, BG, CZ, EE, HU, SK.; Patent Application Country: Application: EP; Patent Country: EP; Priority Ap(TRUNCATED) Patent 1348450, 2003.

(163) Bezwada, R. S.; Arnold, S. C.; Shalaby, S. W.; Williams, B. L. Reg.Pat.Tr.Des.States: Designated States R: FR, GB.; Patent Application Country: Application: EP; Patent Country: EP; Priority Application Country: US Patent 635272, 1995.

(164) Amsden, B.; Hatefi, A.; Knight, D.; Bravo-Grimaldo, E. Development of biodegradable injectable thermoplastic oligomers. *Biomacromolecules* **2004**, *5*, 637-642.

(165) Tian, D.; Dubois, P.; Jerome, R. Macromolecular Engineering of Polylactones and Polylactides. 23. Synthesis and Characterization of Biodegradable and Biocompatible Homopolymers and Block Copolymers Based on 1,4,8-Trioxa[4.6]spiro-9-undecanone. *Macromolecules* **1997**, *30*, 1947-1954.

(166) Tian, D.; Dubois, P.; Grandfils, C.; Jerome, R. Ring-Opening Polymerization of 1,4,8-Trioxaspiro[4.6]-9-undecanone: A New Route to Aliphatic Polyesters Bearing Functional Pendent Groups. *Macromolecules* **1997**, *30*, 406-409.

(167) Lima, R.; do Espirito Santo Pereira, A.; Porto, R.; Fraceto, L. Evaluation of Cyto- and Genotoxicity of Poly(lactide-co-glycolide) Nanoparticles. *J Polym Environ* **2011**, *19*, 196-202.

(168) Grijpma, D. W.; Pennings, A. J. Polymerization temperature effects on the properties of L-lactide and e-caprolactone copolymers. *Polym. Bull. (Berlin)* **1991**, *25*, 335-341.

(169) Dwan'Isa, J. L.; Lecomte, P.; Dubois, P.; Jerome, R. Hydrolytic and thermal degradation of random copolyesters of e-caprolactone and 2-oxepane-1,5-dione. *Macromol. Chem. Phys.* **2003**, *204*, 1191-1201.

(170) Timbart, L.; Amsden, B. G. Functionalizable biodegradable photocrosslinked elastomers based on 2-oxepane-1,5-dione. *J. Polym. Sci. , Part A: Polym. Chem.* **2008**, *46*, 8191-8199.

(171) Brode, G. L.; Koleske, J. V. Lactone polymerization and polymer properties. *J. Macromol. Sci. , Chem.* **1972**, *6*, 1109-1144.

(172) Domb, A. J.; Elmalak, O.; Shastri, V. R.; Ta-Shma, Z.; Masters, D. M.; Ringel, I.; Teomim, D.; Langer, R. Polyanhydrides. *Drug Targeting Delivery* **1997**, *7*, 135-159.

(173) Ferry, J. D. Viscoelastic Properties of Polymers. 3rd Ed. **1980**, 641.

(174) Pitt, C. G.; Gratzl, M. M.; Kimmel, G. L.; Surles, J.; Schindler, A. Aliphatic polyesters II. The degradation of poly (DL-lactide), poly (epsilon-caprolactone), and their copolymers in vivo. *Biomaterials* **1981**, *2*, 215-220.

(175) Burkersroda, F. v.; Schedl, L.; Göpferich, A. Why degradable polymers undergo surface erosion or bulk erosion. *Biomaterials* **2002**, *23*, 4221-4231.

(176) Szlachcic, A.; Zakrzewska, M.; Otlewski, J. Longer action means better drug: Tuning up protein therapeutics. *Biotechnol. Adv.* **2011**, *29*, 436-441.

(177) Asmus, L. R.; Gurny, R.; Moeller, M. Solutions as solutions - Synthesis and use of a liquid polyester excipient to dissolve lipophilic drugs and formulate sustained-release parenterals. *European Journal of Pharmaceutics and Biopharmaceutics* **2011**, *79*, 584-591.

(178) Vilker, V. L.; Colton, C. K.; Smith, K. A.; Green, D. L. The osmotic pressure of concentrated protein and lipoprotein and its significance to ultrafiltration. *J. Membr. Sci.* **1984**, *20*, 63-77.

(179) Sukarto, A.; Amsden, B. G. Low melting point amphiphilic microspheres for delivery of bone morphogenetic protein-6 and transforming growth factor-β3 in a hydrogel matrix. *J. Control. Release* **2011**.

(180) Papadokostaki, K. G.; Amarantos, S. G.; Petropoulos, J. H. Kinetics of release of particulate solutes incorporated in cellulosic polymer matrices as a function of solute solubility and polymer swellability. II. Highly soluble solute. *J Appl Polym Sci* **1998**, *69*, 1275-1290.

(181) BRESLER, E.; GROOME, L. On Equations for Combined Convective and Diffusive Transport of Neutral Solute Across Porous Membranes. *Am. J. Physiol.* **1981**, *241*, F469-F476.

(182) Jiang, Y.; Mao, K.; Cai, X.; Lai, S.; Chen, X. Poly(ethyl glycol) Assisting Water Sorption Enhancement of Poly(epsilon-caprolactone) Blend for Drug Delivery. *J Appl Polym Sci* **2011**, *122*, 2309-2316.

(183) Yu, Z. J.; Liu, L. J. Microwave-assisted synthesis of poly(epsilon-caprolactone)poly(ethylene glycol)-poly(epsilon-caprolactone) tri-block co-polymers and use as matrices for sustained delivery of ibuprofen taken as model drug. *Journal of Biomaterials Science-Polymer Edition* **2005**, *16*, 957-971.

(184) Siegel, R. A.; Kost, J.; Langer, R. Mechanistic studies of macromolecular drug release from macroporous polymers. I. Experiments and preliminary theory concerning completeness of drug release. *J. Controlled Release* **1989**, *8*, 223-236.

(185) Hatefi, A.; Knight, D.; Amsden, B. A biodegradable injectable thermoplastic for localized camptothecin delivery. *J. Pharm. Sci.* **2004**, *93*, 1195-1204.

(186) Scopelianos, A. G.; Bezwada, R. S.; Arnold, S. C.; Huxel, S. T. Reg.Pat.Tr.Des.States: Designated States R: DE, FR, GB, IT.; Patent Application Country: Application: EP; Patent Country: EP; Priority Application Country: US Patent 711794, 1996.

(187) Trimaille, T.; Gurny, R.; Moeller, M. Poly(hexyl-substituted lactides): Novel injectable hydrophobic drug delivery systems. *Journal of Biomedical Materials Research Part a* **2007**, *80A*, 55-65.

(188) Trimaille, T.; Mondon, K.; Gurny, R.; Moeller, M. Novel polymeric micelles for hydrophobic drug delivery based on biodegradable poly#hexyl-substituted lactides#. *Int. J. Pharm.* **2006**, *319*, 147-154.

(189) Trimaille, T.; Moller, M.; Gurny, R. Synthesis and ring-opening polymerization of new monoalkyl-substituted lactides. *Journal of Polymer Science Part A-Polymer Chemistry* **2004**, *42*, 4379-4391.

(190) Trimaille, T.; Gurny, R.; Moller, M. Synthesis and properties of novel poly(hexyl-substituted lactides) for pharmaceutical applications. *Chimia* **2005**, *59*, 348-352.

(191) MATSUSUE, Y.; HANAFUSA, S.; YAMAMURO, T.; SHIKINAMI, Y.; IKADA, Y. Tissue Reaction of Bioabsorbable Ultra-High Strength Poly(l-Lactide) Rod - a Long-Term Study in Rabbits. *Clin. Orthop.* **1995**, 246-253.

(192) Wang, Y.; Ameer, G.; Sheppard, B.; Langer, R. A tough biodegradable elastomer RID B-6765-2009. *Nat. Biotechnol.* **2002**, *20*, 602-606.

(193) da, S.,Rosangeta P.; Gordon, S. Phagocytosis stimulates alternative glycosylation of macrosialin (mouse CD68), a macrophage-specific endosomal protein. *Biochem. J.* **1999**, *338*, 687-694.

(194) De Jong, W. H.; Eelco Bergsma, J.; Robinson, J. E.; Bos, R. R. Tissue response to partially in vitro predegraded poly-L-lactide implants. *Biomaterials* **2005**, *26*, 1781-1791.

(195) Pego, A.; Van Luyn, M.; Brouwer, L.; van Wachem, P.; Poot, A.; Grijpma, D.; Feijen, J. In vivo behavior of poly(1,3-trimethylene carbonate) and copolymers of 1,3-trimethylene carbonate with D,L-lactide or epsilon-caprolactone: Degradation and tissue response. *Journal of Biomedical Materials Research Part a* **2003**, *67A*, 1044-1054.

(196) Pulavendran, S.; Rose, C.; Mandal, A. B. Hepatocyte growth factor incorporated chitosan nanoparticles augment the differentiation of stem cell into hepatocytes for the recovery of liver cirrhosis in mice. *Journal of Nanobiotechnology* **2011**, *9*.

(197) Amsden, B. G.; Sukarto, A.; Knight, D. K.; Shapka, S. N. Methacrylated glycol chitosan as a photopolymerizable biomaterial. *Biomacromolecules* **2007**, *8*, 3758-3766.

(198) Freeman, I.; Cohen, S. The influence of the sequential delivery of angiogenic factors from affinity-binding alginate scaffolds on vascularization. *Biomaterials* **2009**, *30*, 2122-2131.

(199) Patil, S. D.; Papadmitrakopoulos, F.; Burgess, D. J. Concurrent delivery of dexamethasone and VEGF for localized inflammation control and angiogenesis. *J. Controlled Release* **2007**, *117*, 68-79.

Appendix A

^{1}H-NMR spectrum of the PEKC polymerized at 120ºC for 24 hours, showing evidence of degradation due to pyrolysis in the way of peaks in the alkene region at 5.7 ppm, 5.9 ppm, 6.3 ppm, which indicate the unsaturated end group formed, and at 12 ppm, corresponding to the carboxylic acid formed, as a result of pyrolysis.

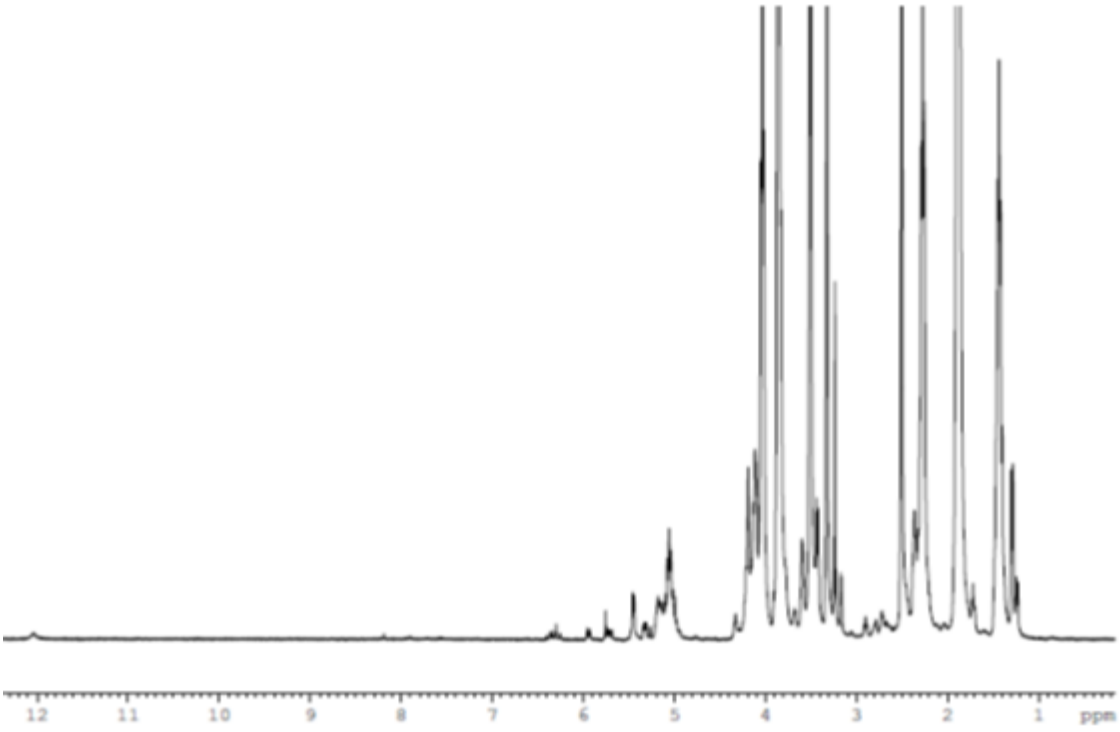

Appendix B

Photograph of the polymers in buffer at 3 weeks showing the opaque colour of the layer of polymer directly in contact with the buffer and the yellow and clear colour of the layer of polymer not directly in contact with the buffer.

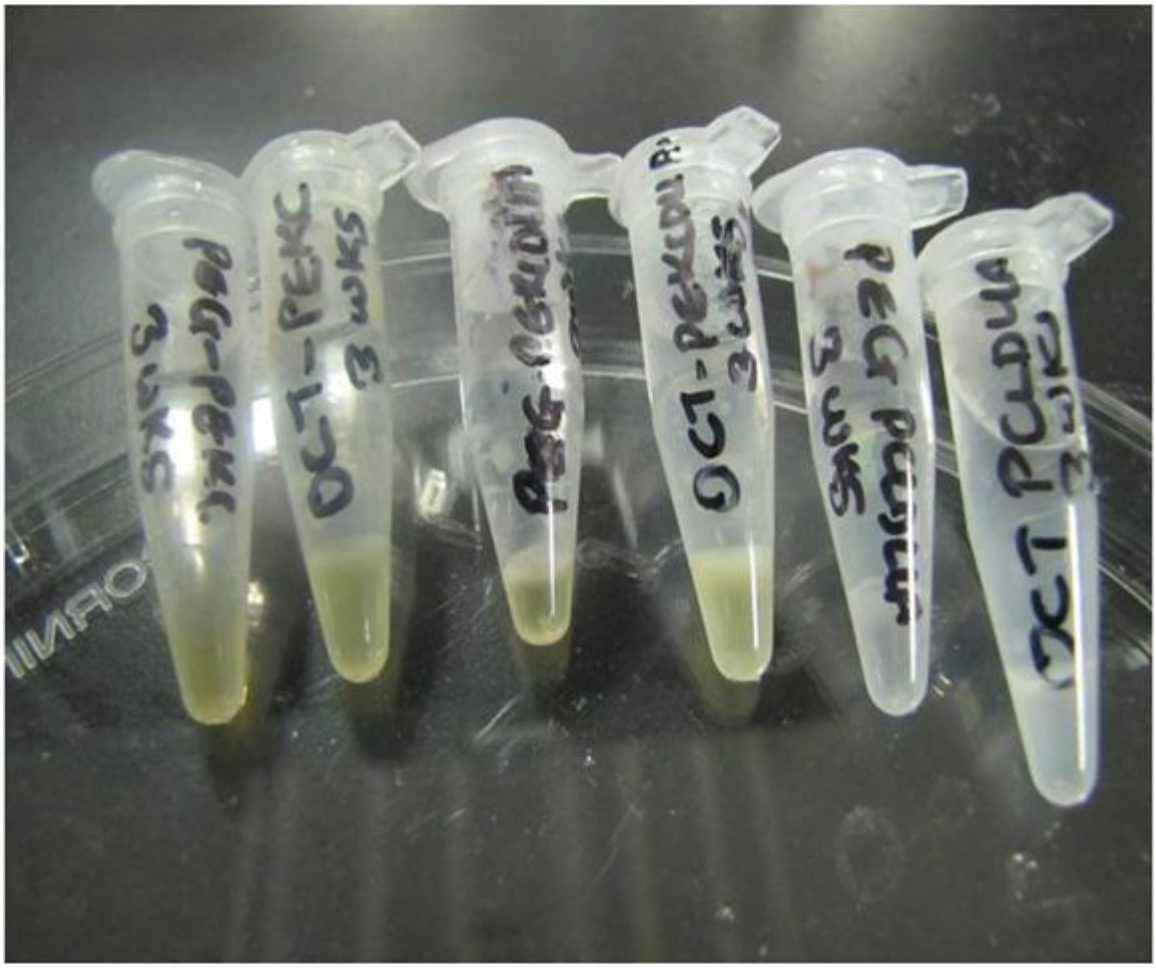

Appendix C

[1]HNMR spectrum of purified PEG-PEKCDLLA, PEG-PEKC and MPEG 350 in DMSO showing evidence of the absence of unreacted monomer and initiator.

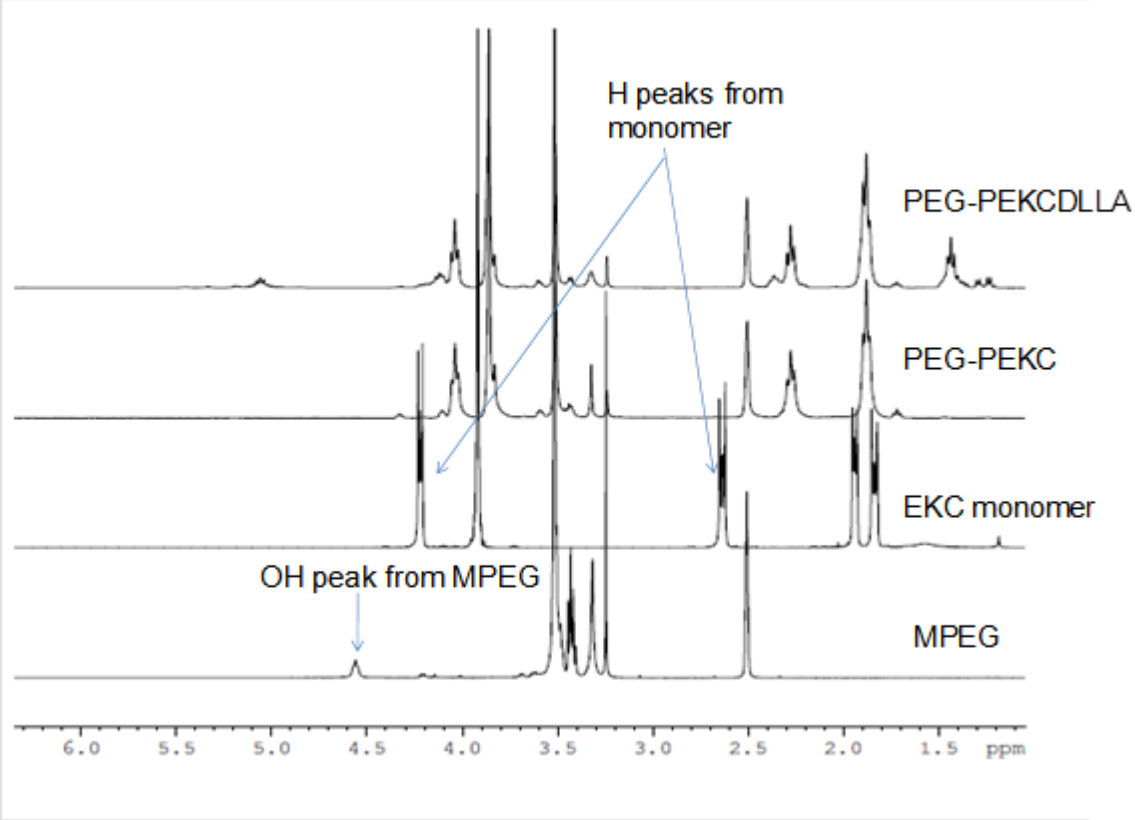

Appendix D

^{1}H-NMR spectra of PEG-PCLDLLA during *in vitro* degradation for 24 weeks. The spectra show the gradual loss of the MPEG portion of the polymers by hydrolysis, indicated by the decrease in the methyl peak of the MPEG at 3.23 pm.

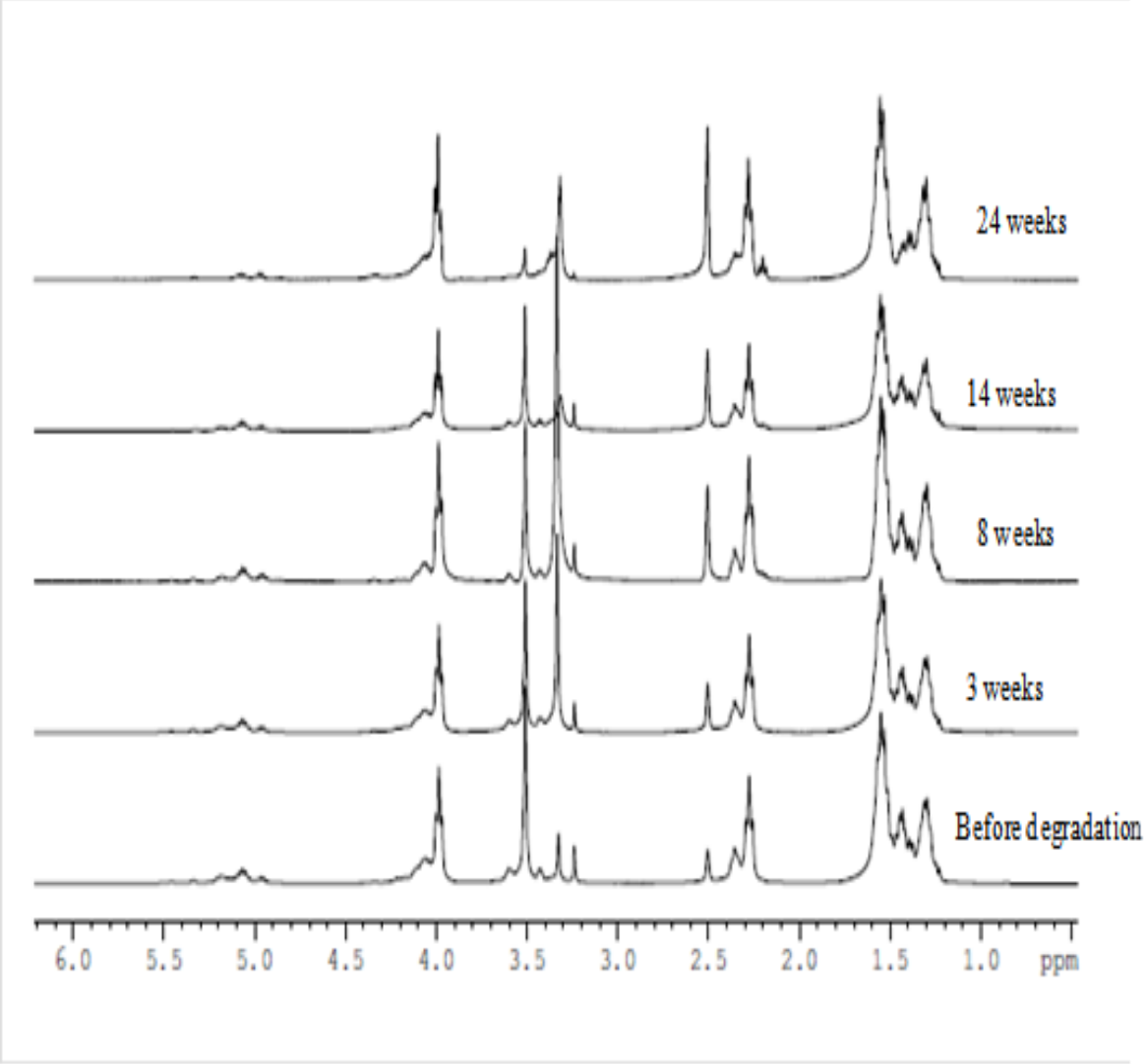

Appendix E

^{1}H-NMR spectra of PEG-PEKCDLLA during *in vitro* degradation for 24 weeks. The spectra show the gradual loss of the MPEG portion of the polymers by hydrolysis, indicated by the decrease in the methyl peak of the MPEG at 3.23 pm.

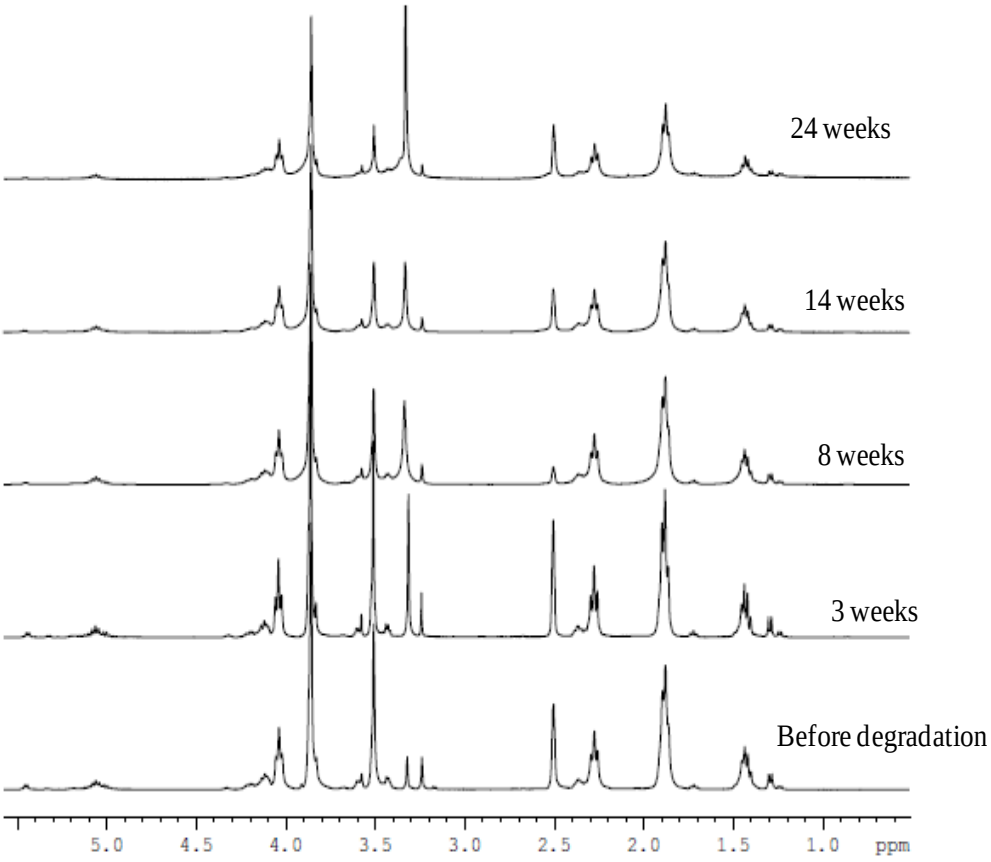

Appendix F

Wet and dry glass transition temperatures (ºC) of the EKC containing polymers during degradation.

Time	OCT-PEKC		PEG-PEKC		OCT-PEKCDLLA		PEG-PEKCDLLA	
(week)	wet	dry	wet	dry	wet	dry	wet	dry
3	-34	-30	-35	-32	-29	-24	-27	-21
8	-34	-29	-34	-30	-33	-24	-27	-21
14	-35	-30	-34	-30	-31	-26	-24	-19
24	-35	-31	-35	-30	-29	-26	-25	-20

Appendix G

Wet and dry glass transition temperatures (ºC) of the CL containing polymers during degradation.

Time	OCT-PCLDLLA		PEG-PCLDLLA	
(week)	wet	dry	wet	dry
3	-56	-53	-55	-53
8	-57	-55	-56	-55
14	-61	-55	-57	-54
24	-67	-65	-63	-58